PORINS OF
LYME DISEASE AND RELAPSING FEVER
SPIROCHETES

Dissertation

zur Erlangung des naturwissenschaftlichen Doktorgrades

der Fakultät für Biologie

an der Bayerischen Julius-Maximilians-Universität Würzburg

vorgelegt von

Marcus Thein

aus Würzburg

Würzburg, 2009

Eingereicht am: ……………………………………..

Mitglieder der Promotionskommission: Vorsitzender: Prof. Dr. ………………….

1. Gutachter: Prof. Dr. Dr. h.c. Roland Benz

2. Gutachter: Prof. Dr. Sven Bergström

Tag des Promotionskolloquiums: ……………………………………..

Doktorurkunde ausgehändigt am: ……………………………………..

Diese Dissertation wurde von mir selbständig und nur mit den
angegebenen Quellen und Hilfsmitteln angefertigt.

Die von mir vorgelegte Dissertation hat noch in keinem früheren
Prüfungsverfahren in ähnlicher oder gleicher Form vorgelegen.

Ich habe zu keinem früheren Zeitpunkt versucht,
einen akademischen Grad zu erwerben.

Würzburg, ……………..   ……………………………

"Natürlicher Verstand kann fast jeden Grad von Bildung ersetzen,
aber keine Bildung den natürlichen Verstand."

Arthur Schopenhauer

Publications

Pinne M., Thein M., Denker K., Benz R., Coburn J. and Bergström S. (2007). Elimination of channel-forming activity by insertional inactivation of the p66 gene in *Borrelia burgdorferi*. *FEMS Microbiol Lett* **266**:241-9.

Thein M., Bunikis I., Denker K., Larsson C., Cutler S., Drancourt M., Schwan T. G., Mentele R., Lottspeich F., Bergström S. and Benz R. (2008). Oms38 is the first identified pore-forming protein in the outer membrane of relapsing fever spirochetes. *J Bacteriol* **190**(21):7035-42.

Thein M., Bonde M., Bunikis I., Denker K., Sickmann A., Bergström S. and Benz, R. (2008). DipA, a pore-forming protein in the outer membrane of Lyme disease *Borrelia* exhibits specificity for the permeation of dicarboxylates. *Manuscript*.

Thein M., Bárcena-Uribarri I., Sacher A., Bunikis I., Bergström S. and Benz R. (2008). The P66 porin is present in both Lyme disease and relapsing fever species: a comparison of the biophysical properties of six P66 species. *Manuscript*.

Thein M., Bárcena-Uribarri I., Maier E., Bonde M., Bergström S. and Benz R. (2008). The use of nonelectrolytes as molecular tools reveals the channel size and the oligomeric constitution of the *Borrelia burgdorferi* porin P66. *Manuscript*.

Table of contents

SUMMARY

Summary

The genus ***Borrelia*** belongs to the spirochete phylum, an ancient evolutionary branch of the domain bacteria that is only afar related to Gram-negative bacteria. All *Borrelia* species are obligate parasites and have a biphasic life cycle in common alternating between vertebrate hosts, usually rodents, deer, bird and human, and their arthropod vectors, such as ticks and lice. Borreliae can be subdivided into the agents of the two borrelian-caused human diseases, Lyme disease and relapsing fever. Both disease patterns are closely related to the peculiar biology of *Borrelia* species and exhibit a wide spectrum of diverse clinical manifestations. The first, **Lyme disease**, is a systemic disorder and manifested in a series of different symptoms which are classified according to the infection stage as early localized, disseminated or chronic. A typical etiopathology can comprise amongst others skin-rash, neuroborreliosis, Lyme arthritis and meningitis. The latter, **relapsing fever,** is according to its name clinically manifested in recurring high fever peaks and can be accompanied by malaise and general ache, often myalgica, headache and also nausea.

Due to the small 0.91 Mb chromosome, borreliae have a lack of biosynthetic capacity and limited metabolic pathways. Thus, all *Borrelia* species are highly dependent on nutrients provided by their hosts. The transport of nutrients and other molecules across the outer membrane of Gram-negative bacteria, such as *Borrelia* species, is enabled by pore-forming proteins, so-called porins. **Porins** are water-filled channels and can be subdivided into two different classes, general diffusion pores and substrate-specific porins. General diffusion pores sort mainly according to the molecular mass of the solutes and show a linear relation between translocation rate and solute concentration gradient. Specific porins with a substrate-binding site inside the channel exhibit Michaelis-Menten kinetics for the transport of certain solutes and are responsible for the rapid uptake of different classes of solutes.

In terms of the Lyme disease agent *Borrelia burgdorferi*, three putative porins were characterized in previous studies: P13, Oms28 and P66. In contrast to Lyme disease species, the porin knowledge of relapsing fever *Borrelia* is low, which means that not any porin has actually

been described for representatives of these agents. Thus, the general aim of this thesis was to provide insight into the porin content of both, Lyme disease and relapsing fever spirochetes. This aim could be achieved by isolating and identifying porins from *Borrelia* outer membranes and by biophysically characterizing their properties in artificial lipid membranes.

In one chapter of this study, the first identification and characterization of a relapsing fever porin is presented. The pore-forming protein was isolated from outer membranes of *Borrelia duttonii*, *Borrelia hermsii* and *Borrelia recurrentis* and designated **Oms38**, for "**o**uter **m**embrane-**s**panning protein of **38** kDa". Biophysical characterization of Oms38 was achieved by using the black lipid bilayer method and demonstrated that Oms38 forms small, water-filled channels with a single-channel conductance of 80 pS in 1 M KCl. The Oms38 channel did not exhibit voltage-dependent closure and is slightly selective for anions with a permeability ratio of cations over anions of 0.41 in KCl. Analysis of the deduced amino acid sequence demonstrated that Oms38 contains an N-terminal signal sequence which is processed under *in vivo* conditions.

Subsequently, a protein homologous to Oms38 was identified in the Lyme disease agents *Borrelia burgdorferi*, *Borrelia garinii* and *Borrelia afzelii*. The pore-forming protein of these species exhibits high sequence homology to Oms38 and similar biophysical properties, i.e. it forms pores of 50 pS in 1 M KCl. Interestingly, titration experiments revealed that this pore could be partly blocked by dicarboxylic anions, which means that this protein does not form a general diffusion pore but a channel with a binding-site specific for those compounds. Consequently, this porin was termed **DipA**, for "**di**carboxylate-specific **p**orin **A**". Additionally, polyserum against DipA was produced and allowed further analyses.

In another set of experiments, it was shown that the porin **P66 is present in both Lyme disease and relapsing fever species**. Therefor, the outer membranes of the Lyme disease species *Borrelia burgdorferi*, *Borrelia afzelii*, *Borrelia garinii* and the relapsing fever species *Borrelia duttonii*, *Borrelia recurrentis* and *Borrelia hermsii* were closer investigated. Except of the P66 homologue of *Borrelia hermsii* P66 of all species was highly active in artificial lipid membranes, forming pores with huge single-channel conductances between 9 and 11 nS in 1 M KCl. The particular biophysical properties of the homologues were compared by reconstitution experiments using black lipid bilayer membranes.

Moreover, the **channel diameter and the constitution of *Borrelia burgdorferi* P66** were investigated in detail. Therefor, the P66 single-channel conductance in the presence of different nonelectrolytes with known hydrodynamic radii was analyzed in black lipid bilayers. The effective diameter of the P66 channel lumen was determined to be ~1.9 nm. Furthermore, as derived from multi-channel experiments the P66-induced membrane conductance could be blocked by certain nonelectrolytes, such as PEG 400, PEG 600 and maltohexaose. The blockage

of the channel after addition of these molecules in the low millimolar range could also be used for the study of the current noise through the P66 channel and revealed $1/f$-noise for both open and closed channels. Additional blocking experiments on the single-channel level revealed seven subconducting states and indicated a heptameric constitution of the P66 channel. This indication could be confirmed by Blue native PAGE and immunoblot analysis which demonstrated that P66 units form a complex with a corresponding mass of approximately 440 kDa.

Taking together, this thesis describes detailed biochemical and biophysical investigations of both Lyme disease and relapsing fever *Borrelia* porins and represents an important step forward in understanding the outer membrane pathways for nutrient uptake of these strictly host-dependent, pathogenic spirochetes. Furthermore, it provides some knowledge of the outer-membrane protein composition of *Borrelia* spirochetes. Anyway, further studies, including genetic manipulations, growth experiments and X-ray analyses of protein crystals, remain to be done to understand the structure and functionality of *Borrelia* porins in detail. A profound knowledge of surface-exposed proteins, such as porins, is one precondition for the production of a successful vaccine and the drug design against the two borrelian-caused diseases.

Zusammenfassung

Die Gattung ***Borrelia*** gehört zur Abteilung der Spirochäten, einem alten Zweig der Bakteriendomäne, der nur entfernt mit Gram-negativen Bakterien verwandt ist. Sämtliche Arten dieser Gattung sind obligate Parasiten. Sie durchlaufen einen zweiphasigen Lebenszyklus, der zwischen Vertebratenwirten wie Nagetieren, Wild, Vögeln und dem Menschen und ihren Arthropodenüberträgern wie Zecken und Läusen alterniert. Borrelien können in die Erreger zweier humaner Krankheiten eingeteilt werden: die Lyme-Borreliose und das Rückfallfieber. Beide Krankheitsmuster sind eng geknüpft an die eigentümliche Biologie von Borrelien und geprägt durch ein weites Spektrum an verschiedenen klinischen Manifestationen. Erstere, die **Lyme-Borreliose**, ist eine systemische Erkrankung, die durch eine Reihe verschiedenartigster Symptome gekennzeichnet ist und mehrere Infektionsstadien durchlaufen kann, von lokal begrenzt über disseminiert bis chronisch. Letztere, das **Rückfallfieber**, wird gemäß seinem Namen klinisch an wiederkehrenden hohen Fieberschüben manifestiert, die von Übelkeit, allgemeinen Schmerzen, Kopfschmerzen und sogar Erbrechen begleitet werden können.

Borrelien besitzen mit 0.91 Mb ein sehr kleines Chromosom und sind daher in ihren biosynthetischen und metabolischen Fähigkeiten stark eingeschränkt. Folglich ist das Überleben sämtlicher Borrelienarten absolut abhängig von Nährstoffen, die von ihren Wirten bereitgestellt werden. Der Transport dieser Nährstoffe und anderer Moleküle über die äußere Membran von Gram-negativen Bakterien wie den Borrelien wird durch porenformende Proteine, so genannte Porine ermöglicht. **Porine** sind wassergefüllte Kanäle, die in zwei Klassen unterteilt werden können: allgemeine Diffusionsporen und substratspezifische Porine. Allgemeine Diffusionsporen filtern entsprechend der molekularen Masse der gelösten Substrate und weisen ein lineares Verhältnis zwischen Translokationsrate und Substratkonzentrationsgradient auf. Dagegen kann der Transport bestimmter Substanzen durch spezifische Porine mit einer Substrat-Bindestelle im Kanal durch die Michalis-Menten Kinetik beschrieben werden. Diese Kanäle ermöglichen den schnellen Influx bestimmter Klassen von Substraten.

Aus dem Lyme-Borreliose Erreger *Borrelia burgdorferi* wurden bisher drei mutmaßliche Porine charakterisiert und beschrieben: P13, Oms28 und P66. Demgegenüber sind die Kenntnisse über Porine in Rückfallfieberarten rudimentär und es wurde bisher noch kein einziges Porin für Vertreter dieser Krankheit identifiziert. Unter Berücksichtigung dieses Hintergrunds war die allgemeine Zielsetzung dieser Arbeit, einen Einblick in die Porinzusammensetzung von sowohl Lyme Borreliose- als auch Rückfallfieber-Spirochäten zu erlangen. Dieses Ziel konnte erreicht werden, indem Porine aus den Außenmembranen von Borrelien isoliert und identifiziert

wurden und anschließend ihre Eigenschaften biophysikalisch in künstlichen Lipidmembranen charakterisiert wurden.

Ein Kapitel dieser Arbeit beschreibt die Identifizierung und Charakterisierung des ersten Porins aus Rückfallfiebererregern. Das porenformende Protein wurde aus den Außenmembranen von *Borrelia duttonii*, *Borrelia hermsii* und *Borrelia recurrentis* isoliert und **Oms38** genannt, für „**o**uter **m**embrane-**s**panning protein of **38** kDa". Die biophysikalische Charakterisierung mit der „black lipid bilayer" Methode zeigte, dass Oms38 kleine, wassergefüllte Kanäle mit einer Einzelkanalleitfähigkeit von 80 pS in 1 M KCl bildet. Diese Kanäle sind nicht spannungsabhängig und leicht selektiv für Anionen mit einem Permeabilitätsverhältnis von Kationen zu Anionen von 0,41 in KCl. Eine genaue Betrachtung der Aminosäuresequenz zeigte, dass Oms38 eine N-terminale Signalsequenz besitzt, die *in vivo* abgespalten wird.

Ein homologes Protein zu Oms38 wurde in den Lyme Borreliose Erregern *Borrelia burgdorferi*, *Borrelia garinii* und *Borrelia afzelii* identifiziert. Das porenformende Protein dieser Arten weist eine hohe Sequenzhomologie zu Oms38 auf und zeigt ähnliche biophysikalische Eigenschaften, das heißt es formt Poren von 50 pS in 1 M KCl. Durch Titrationsexperimente konnte gezeigt werden, dass die Pore teilweise durch Dicarboxylate blockiert werden kann. Eine Auswertung dieser Versuche legte nahe, dass dieses Protein keine allgemeine Diffusionspore darstellt, sondern einen Kanal mit einer spezifischen Bindestelle für diese Komponenten. Daher wurde dieses Porin **DipA** genannt, was für „**di**carboxylate-specific **p**orin **A**" steht. Polyserum gegen DipA wurde hergestellt und ermöglichte die Durchführung weiterer Untersuchungen.

In einer anderen Versuchsreihe wurde gezeigt, dass das **Porin P66 sowohl in Lyme Borreliose Erregern als auch in Rückfallfieberarten** vorhanden ist. Hierfür wurden die Außenmembranen der Lyme Borreliose Erreger *Borrelia burgdorferi*, *Borrelia afzelii* und *Borrelia garinii* und der Rückfallfieberarten *Borrelia duttonii*, *Borrelia recurrentis* und *Borrelia hermsii* genauer untersucht. Mit Ausnahme des P66 Homologs von *Borrelia hermsii* rekonstituierten P66 Proteine aus allen Arten sehr aktiv in künstliche Membranen und formten Poren zwischen 9 und 11 nS in 1 M KCl. Die biophysikalischen Eigenschaften der Homologe wurden in Experimenten mit „black lipid bilayer" Membranen ausführlich verglichen.

Des Weiteren wurden **Porendurchmesser und Konstitution des *Borrelia burgdorferi* Porins P66** genau untersucht. Hierfür wurde die P66 Einzelkanalleitfähigkeit in Anwesenheit von verschiedenen Nichtelektrolyten in künstlichen Lipidmembranen analysiert. Der effektive Durchmesser des P66 Wasserlumens wurde auf ~1.9 nm bestimmt. Darüber hinaus konnte P66 mit bestimmten Nichtelektrolyten wie PEG 400, PEG 600 und Maltohexaose blockiert werden. Diese Blockierung konnte benutzt werden um das Stromrauschen durch P66 zu untersuchen, welches durch ein $1/f$ Rauschen sowohl für offene als auch geschlossene Kanäle beschrieben

werden kann. Weitere Blockierungsexperimente auf Einzelkanalebene deckten sieben Unterzustände von P66 auf, die stark auf ein P66 Heptamer schließen ließen. Dieser heptamere Charakter konnte durch Blue native PAGE und Immunblotanalysen bestätigt werden. Diese zeigten, dass P66 einen Komplex mit einer Masse von ungefähr 440 kDa bildet.

Zusammenfassend beschreibt diese Dissertation detaillierte biochemische und biophysikalische Untersuchungen von Porinen aus sowohl Lyme Borreliose- als auch Rückfallfieber-Borrelien. Erkenntnisse aus dieser Arbeit bringen das Verstehen der Nährstoffaufnahme über Außenmembranen dieser streng wirtsabhängigen, pathogenen Spirochäten einen großen Schritt vorwärts. Dennoch müssen weitere Untersuchungen wie genetische Manipulationen, Wachstumsanalysen und Röntgenstrukturauflösungen von Proteinkristallen durchgeführt werden, um die Strukturen und die Funktionalitäten von *Borrelia* Porinen in allen Einzelheiten zu verstehen. Ein fundiertes Wissen über oberflächenexponierte Proteine wie Porine ist Vorraussetzung für die Herstellung erfolgreicher Impfstoffe und Therapeutika gegen die von Borrelien verursachten Krankheiten.

<div align="right">

Chapter 1

</div>

INTRODUCTION

Infectious diseases transmitted by vectors play a major role in human history and have a tremendous impact on human health and mortality throughout the world. One of the most striking examples is the pest which killed more than 25 per centum of the European population in medieval times. And even in the twenty-first century, over one million people fall victim to a disease such as malaria per year. Beside these historical diseases which acted as selective factors in human evolution, there appeared recently other severe bacterial diseases on the stage of scientific interest. Two of those are the vector-borne Lyme disease and relapsing fever. Both disease patterns are caused by bacteria of the genus *Borrelia*. Because of the peculiar characteristics of these agents and the resulting complex pathogenesis, *Borrelia* species are items of an intensive research during the last decades.

1.1. The bacterial genus *Borrelia*

1.1.1. Classification

The genus *Borrelia* belongs to the spirochete phylum, an ancient evolutionary branch of bacteria and only afar related to Gram-negative bacteria (Woese 1987). Spirochetes are subdivided into three families, *Brachyspiraceae*, *Leptospiraceae* and *Spirochetacea*, which are all part of the order *Spirochetales*. Disease-causing members of this phylum include inter alia other important pathogens, such as *Treponema pallidum*, causing syphilis, *Treponema denticola*, causing periodontal disease, *Leptospira interrogans*, causing leptospirosis and *Brachyspira hyodysenteriae*, causing swine dysentery. The genus *Borrelia* contains agents of two human diseases: Lyme disease and relapsing fever. The Lyme disease causative agents include at least 12 different species all belonging to the *Borrelia burgdorferi* sensu lato complex, such as the well-studied *Borrelia burgdorferi*, *Borrelia afzelii*, *Borrelia garinii* (Baranton *et al.* 1992; Marconi *et al.* 1992; Canica *et al.* 1993) as well as the recently discovered *Borrelia spielmani* (Richter *et al.* 2004). Approximately 20 other *Borrelia* species are known as relapsing fever agents, such as the widespread *Borrelia recurrentis*, *Borrelia duttonii*, *Borrelia hermsii* and *Borrelia turicatae* (Bryceson *et al.* 1970; Goubau 1984; Dworkin *et al.* 2002; Schwan *et al.* 2005; Schwan *et al.* 2007).

1.1.2. General characteristics

Borrelia are elongated (10-30 µm in length), thin (approximately 0.3 µm in diameter) and helically shaped bacteria (Fig. 1.1). The length is variable, especially during *in vitro* cultivation. It differs in relation to growth rate but also between single bacteria, while the diameter is fairly constant within one strain (Barbour *et al.* 1986; Goldstein *et al.* 1996). The spirochetes are very motile by virtue of 7 – 11 bipolar endoflagella situated in the periplasmic space between the cytoplasmic and the outer membrane and anchored on both poles of the bacterial cell. By rotating the flagella clockwise or counter-clockwise, directional screw-like motion is achieved (Barbour *et al.* 1986; Charon *et al.* 1992; Goldstein *et al.* 1996; Motaleb *et al.* 2000). *Borrelia* are classified as Gram-negative, as their cell envelope consists of an outer and an inner membrane, but they have many properties in common with Gram-positive bacteria. For
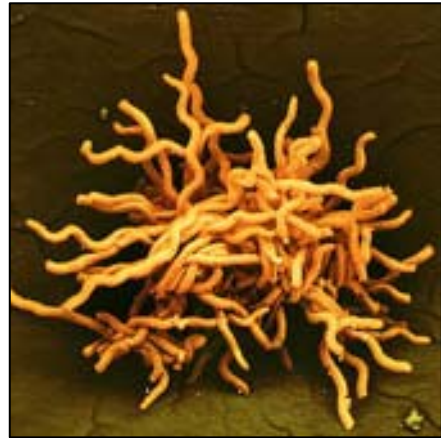
Fig. 1.1. *Borrelia burgdorferi* cells;

(picture taken from http://www.freeinfosociety.com/site.php?postnum=436)

example, the genomic guanine-cytosine content is very low (28.9%) and the inner membrane is closely associated with a peptidoglycan cell wall. In contrast to Gram-negative bacteria, the outer membrane of *Borrelia* is fluid, consists of 45-62% protein, 23-50% lipid and 3-4% carbohydrate (Barbour *et al.* 1986) and lacks lipopolysaccharides (LPS) (Takayama *et al.* 1987).

     Borrelia have an exceptionally organized genome. The *B. burgdorferi* genome consists of a 0.91 Mb linear chromosome and 21 plasmids (12 linear and 9 circular) which comprise additional 0.61 Mb. The *B. burgdorferi* chromosome contains 853 genes encoding a basis set for DNA replication, transcription, translation, solute transport and energy metabolism and there are 430 additional genes on the plasmids, most of them of unknown function, but even several essential genes are located on plasmids (Barbour 1993; Fraser *et al.* 1997; Casjens *et al.* 2000). Interestingly, *Borrelia* plasmids are associated with pathogenicity, as *Borrelia* loses virulence in about 10-15 passages of *in vitro* growth due to a loss of plasmids (Schwan *et al.* 1988). The small chromosome causes a lack of biosynthetic capacity and limited metabolic pathways and therefore, *Borrelia* are highly dependent on nutrients provided by their host. In consequence, *Borrelia* are obligate parasites and not able to survive outside their hosts. Probably, the spirochetal organisms compensate for their restricted coding potential by proteins which can import a wide variety of solutes. This is important because *Borrelia* is unable to synthesize any amino acids *de novo* (Fraser *et al.* 1997). Thus, they have complex life cycles involving arthropod and mammalian reservoir hosts, in general ticks and rodents (Burgdorfer 1984; Schwan 1996). To ensure the survival in this

enzootic life cycle, the microaerophilic spirochetes have to adapt to a range of diverse host environments and nutrient availability (de Silva *et al.* 1997; Steere *et al.* 2004).

1.1.3. Vectors, hosts and life cycle

All *Borrelia* have a biphasic life cycle in common which alternates between vertebrate hosts and their arthropod vectors. For most *Borrelia* species, the vertebrate reservoir is a small rodent or deer, but the importance of birds in the enzootic life cycle is undoubted (Barbour *et al.* 1986; Humair 2002). The cycle of *Borrelia* through animals is dependent on the transmission by their arthropod vectors, ticks and lice (Fig. 1.2.). Arthropod vectors usually are infected by feeding upon a spirochetemic vertebrate. Vectors vary between Lyme disease and relapsing fever strains and are often species specific. Thus, Lyme disease causative *Borrelia* are preferentially present in hard-bodied ticks of the *Ixodidae* family (Burgdorfer *et al.* 1982), while most of relapsing fever causing agents are transmitted by soft-bodied ticks belonging to the *Argasidae* family (Felsenfeld 1965). *Argasidae* comprises 5 genera of which *Ornithodoros* is the largest with around 100 species. In contrast to *Ixodes* ticks, which attach to their hosts for days, *Ornithodoros* ticks feed very quickly, completing their blood meal in about 30 minutes (Sonenshine 1997). Ticks have three developmental stages: larva, nymph and adult. They feed only once before they molt and reach the next stage. Prevalences of *Borrelia*-infected ticks are regionally varying and partly quite high. In central Europe at least 11% of the ticks are infected (Hildebrandt *et al.* 2003).

Fig. 1.2. Typical *Borrelia* vectors.
(**A**) tick *Ixodes ricinus*, nymph, larva and adult;
(**B**) tick *Ornithodoros moubata*;
(**C**) louse *Pediculus humanus humanus*;

(pictures taken from
(**A**) http://www.bag.admin.ch/themen/medizin/
00682/00684/01017/index.html?lang=de
(**B**) http://www.afpmb.org/pubs/Field_Guide/
Images/originals/Fig.%2061.jpg
(**C**) http://www.utah.edu/unews/releases/04/
oct/licemen.html)

Interestingly, the human body louse *Pediculus humanus humanus* is the only non-tick *Borrelia* vector. It is the vector of *B. recurrentis* which is able to cause massive epidemics of the louse-borne relapsing fever (Bryceson *et al.* 1970; Cutler 2006). Compared to the well-elaborated relationship between *Ornithodoros* ticks and relapsing fever species, it is mysterious to understand the outbreak of global epidemics caused by the less adapted louse-borne relapsing fever. Lice only feed on human blood and they are dependent on sucking blood daily (Raoult *et al.* 1999). Every

blood meal consists of only about 1 µl and consequently the probability of infecting the louse with *Borrelia* is only given at a relatively high spirochetemia of the human.

The cycle of all *Borrelia* species between their arthropod vector and their vertebrate reservoir is accompanied by many changes in environmental factors including temperature, pH, osmolarity, nutrient availability and immune system barriers, which evolved advanced strategies to sense and to survive in these natural habitats and to deploy their pathogenic potential (Thomas *et al.* 2001; Hefty *et al.* 2002; Tokarz *et al.* 2004).

1.1.4. *Borrelia* and pathogenicity

The two *Borrelia*-caused human diseases, Lyme disease and relapsing fever are spread throughout the world with partly high prevalences depending on the regional distribution of their causative species. While Lyme disease is emerging during the last decades, relapsing fever was already known to the physicians of the ancient Greece and provoking extensive epidemics in the ensuing centuries (Felsenfeld 1971; Barbour *et al.* 1986). The two disease patterns are closely related to the peculiar biology of *Borrelia* species and therefore exhibiting a wide spectrum of diverse clinical manifestations.

Lyme disease is a systemic disorder manifested in a series of different symptoms which are classified according to the infection stage – early localized, disseminated or chronic. The typical manifestation of an early localized infection is a skin-rash around the tick bite termed *Erythema migrans* (EM). During this stage of infection, *Borrelia* are susceptible to antibiotics and a treatment is promising. When left untreated, more severe symptoms can occur with the common clinical manifestations of an early disseminated infection, neuroborreliosis and Lyme arthritis. Manifestations of chronic (persistent) Lyme disease can involve *Acrodermatitis chronica atrophicans* (ACA), meningitis and rarely Lyme meningoencephalitis (Asbrink *et al.* 1984; Steere 1989; Nadelman *et al.* 1998; Orloski *et al.* 2000). It is noteworthy that the distribution patterns of *Borrelia* may account for variable frequency of Lyme disease depending on the causing species (Wang *et al.* 1999).

Relapsing fever, the second *Borrelia*-caused human disease, is according to its name clinically manifested in recurring high fever peaks with high densities of *Borrelia* in the blood (spirochetemia) (Southern *et al.* 1969; Felsenfeld 1971; Goubau 1984). It can be accompanied by malaise and general ache, often myalgica and headache and also nausea occurs frequently. Cutaneous symptoms such as petechial and hemorrhagic skin rashes are common (Bryceson *et al.* 1970; Butler *et al.* 1979). Even various neurological symptoms may appear of which meningitis and facial palsy are the most frequent (Cadavid *et al.* 1998). During pregnancy relapsing fever can

involve complications such as spontaneous abortion and perinatal death (Fuchs *et al.* 1969; Guggenheim *et al.* 2005). Furthermore, relapsing fever *Borrelia* are able to persist silently in host niches like capillaries, but also in the brain and even other organs, and further tissues can not be excluded to be harbors of persistent, residual *Borrelia* infections (Larsson *et al.* 2006). Human relapsing fever is most prevalent in endemic areas of Africa where people live in close proximity to burrows of host animals with incidences up to 11 per 100 person-years in West Africa (Vial *et al.* 2006). Relapsing fever *Borrelia* are very sensitive to antibiotics and often a single dose is recommended (Perine *et al.* 1974; Cook 2003).

1.1.5. Species included in this work

Several Lyme disease and relapsing fever agents have been selected for these studies (Tab. 1.1). The chosen species represent the main causing species of the respective human disease and represent the worldwide distribution of these bacteria belonging to the spirochetal genus *Borrelia*.

Tab. 1.1. Overview of different Lyme disease and relapsing fever *Borrelia* species included in this work.

Species	Vector	Geographical distribution	Host range	References
Lyme disease agents				
B. burgdorferi	*Ixodides spp.*	North America, Europe	Mammals, birds	(Burgdorfer 1991; Baranton *et al.* 1998; Wang *et al.* 1999)
B. garinii	*Ixodides spp.*	Eurasia	Mammals, birds	(Baranton *et al.* 1998; Wang *et al.* 1999)
B. afzelii	*Ixodides spp.*	Eurasia	Mammals, birds	(Baranton *et al.* 1998; Wang *et al.* 1999)
Relapsing fever agents				
B. duttonii	*Ornithodoros moubata moubata*	Sub-Saharan Africa	Humans	(Goubau 1984)
B. hermsii	*Ornithodoros hermsi*	North America	Mammals, birds	(Dworkin *et al.* 2002; Schwan *et al.* 2007)
B. recurrentis	*Pediculus humanus humanus*	Ethiopia, Sudan, potentially worldwide	Humans	(Bryceson *et al.* 1970)
B. turicatae	*Ornithodoros turicatae*	North America	Mammals	(Schwan *et al.* 2005)

1.2. The Gram-negative cell-envelope

The cell envelope plays various major roles in the biology of bacteria. Because of the concentration of dissolved solutes inside the bacterial cell, a considerable turgor pressure develops, estimated 3.5 bar in a bacterium like *Escherichia coli*. To withstand these pressures, bacteria contain cell envelopes, which function to provide rigidity and shape to the cell. In addition, it serves as important physical barrier between the cytoplasm and the external medium and fulfills crucial tasks in production of energy, proliferation, cell division and import and export of substrates and metabolites. (Beveridge 1981; Madigan *et al.* 2000). Thus, the evolved bacterial cell envelope has to solve the problem to be both stable and multifunctional at the same time.
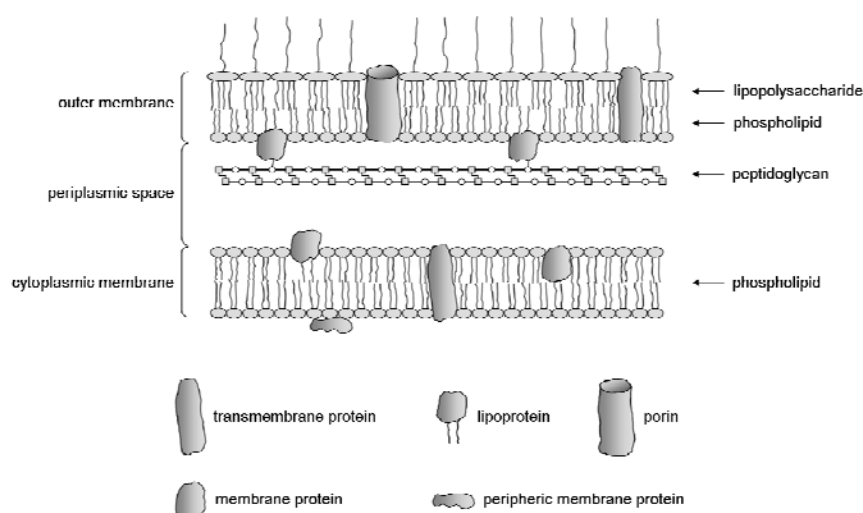
Fig. 1.3. Schematic illustration of a typical Gram-negative cell envelope, based on figures in (Penel *et al.* 1998; Madigan *et al.* 2000).

The characteristic of Gram-negative bacteria is their cell envelope which is composed of two membranes enclosing the peptidoglycan-containing periplasmic space (Fig. 1.3). The cytoplasmic membrane is a phospholipid bilayer, whereas the outer membrane is an asymmetrical bilayer containing phospholipids in its inner and lipopolysaccharides in its outer leaflet. Both cytoplasmic and outer membranes include proteins that are attached, inserted or anchored in the lipid bilayers. These proteins are all synthesized in the cytoplasm and are guided towards the cell envelope. There, many of them have to cross the cytoplasmic membrane. At their designated location, the proteins fulfill different functions. Lipoproteins are acylated and anchored in the cytoplasmic or outer membrane via an amino-terminal N-acyl-diacylglyceryl-cysteine (Ichihara *et al.* 1981). Integral membrane proteins are inserted in the lipid bilayer and display characteristical structures. The membrane-spanning domains of cytoplasmic membrane proteins are composed of α-helices, while the ones of outer membrane proteins are containing β-strands, forming a cylindrical β-barrel with a hydrophobic outer surface (Nikaido *et al.* 1985; Wimley 2003).

1.2.1. General features of pore-forming outer-membrane proteins (Porins)

One type of fundamental outer membrane proteins are pore-forming proteins, so-called porins. Porins are water-filled channels and enable the solute and nutrient influx from the environment into the bacterial cell. (Benz 1994b; Achouak *et al.* 2001) and can be subdivided in two different classes: (1) general diffusion pores and (2) substrate-specific porins.

  General diffusion pores, such as OmpF of *Escherichia coli* (Benz 1994b; Benz 2001) (Fig. 1.4), sort mainly according to the molecular mass of the solutes and show linear relation between translocation rate and solute concentration gradient. **Specific porins**, such as LamB of *Escherichia coli* (Benz *et al.* 1986), with a substrate-binding site inside the channel exhibit Michaelis-Menten kinetics for the transport of certain solutes and are responsible for the rapid uptake of classes of solutes such as carbohydrates (Ferenci *et al.* 1980; Benz *et al.* 1986), nucleosides (Benz *et al.* 1988b) or phosphate (Hancock *et al.* 1986).
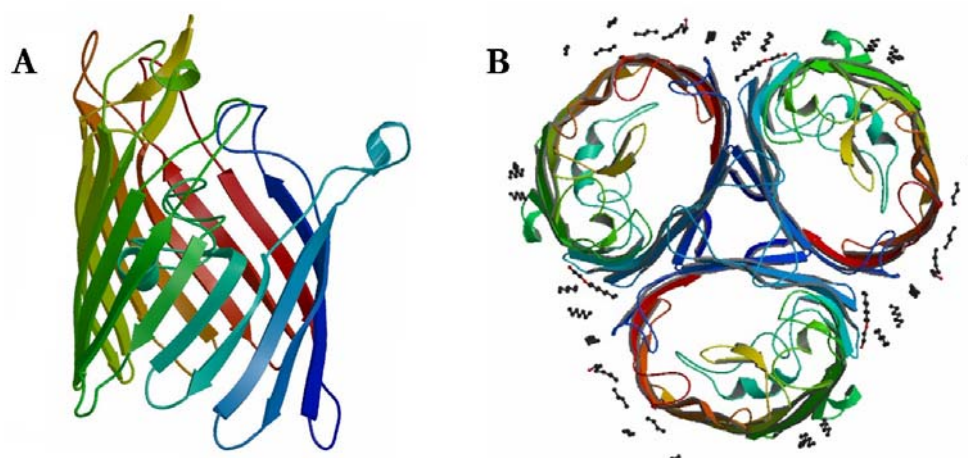
Fig. 1.4. The crystal structure of the general, trimeric porin OmpF from *Escherichia coli* (Lou *et al.* 1996; Penel *et al.* 1998; Schirmer 1998). **(A)** General fold of a porin monomer. The hollow β-barrel structure is formed by antiparallel arrangement of 16 β-strands. The strands are connected by turns or loops on the periplasmic side (bottom), whereas long, irregular loops face the cell exterior (top). **(B)** Schematic representation of an OmpF trimer. The view is from the extracellular space along the molecular threefold symmetry axis. The three pores have the size of about 7 x 11 Å.

(Pictures taken from http://www.pdb.org/)

  The architecture of a typical porin monomer, such as *Escherichia coli* OmpF, is quite simple (Fig. 1.4.A). The polypeptide of about 300 to 420 amino acids is folded into a 16- or 18-stranded antiparallel β-barrel. Three such barrels form stable trimeric molecules (Fig. 1.4.B) that can be dissociated only upon denaturation. The trimer is encircled by a hydrophobic band that facilitates the insertion of the molecule into the core of the outer membrane. In all porins with known 3D structure the transmembrane pore, which is formed by the large, hollow barrel, is constricted by a

loop (Fig 1.4) that folds inwardly and is attached to the inner side of the barrel wall. This internal loop constricts the internal diameter of the pore and stabilizes the porin β-barrel. On the periplasmic side the β-strands are connected by short loops and on the extracellular side by long irregular loops (Schirmer 1998). These loops show very high sequence variation and can be surface-exposed. Porins can show very low sequence homology, but the similarity in topology and charge distribution is striking (Schirmer 1998). For instance, the C-terminus contains an aromatic amino acid (usually phenylalanine), which is absolutely conserved in classical porins of *Enterobacteriaceae* (Struyve *et al.* 1991).

Beside the solute influx, porins can have additional functions. Porins are able to insert into eukaryotic cell membranes (Rudel *et al.* 1996), activate complement (Alberti *et al.* 1996; Merino *et al.* 1998), act as receptors for bacteriophages (Yu *et al.* 1998) and are potential targets of bactericidal compounds (Sallmann *et al.* 1999). Furthermore, surface-exposed porin domains are capable of adhering to cellular receptors, an aptitude observed for a couple of proteins, such as *Campylobacter jejuni* MOMP (Moser *et al.* 1997), *Shigella flexneri* OmpC (Bernardini *et al.* 1993), *Treponema denticola* Msp (Weinberg *et al.* 1991; Haapasalo *et al.* 1992; Fenno *et al.* 1996) and *Borrelia burgdorferi* P66 (Coburn *et al.* 2003).

1.3. The *Borrelia* cell-envelope

Although *Borrelia* are counted among the Gram-negative bacteria, because they have both cytoplasmic and outer membrane, the *Borrelia* cell envelope and membrane composition exhibits major differences compared to those of other Gram-negative bacteria (Fig. 1.5).
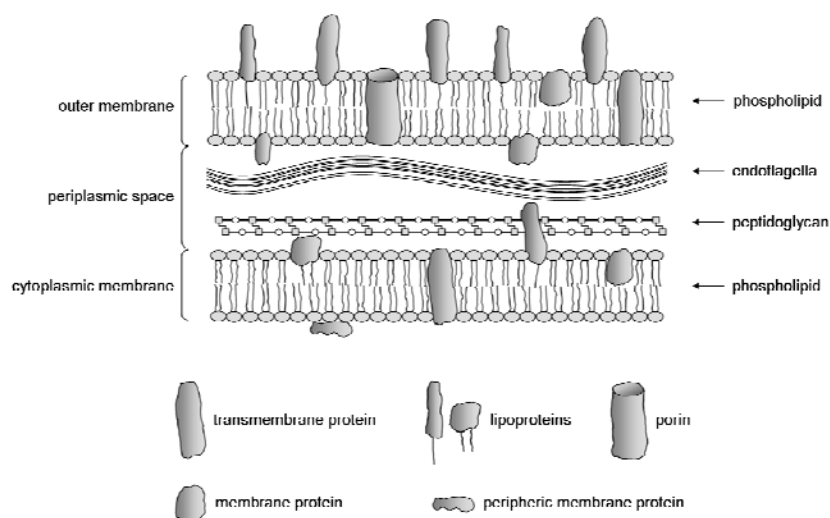
Fig. 1.5. Schematic illustration of the *Borrelia* cell envelope, based on figures in (Rosa *et al.* 2005).

One characteristic are the mentioned endoflagella located in the periplasmic space and responsible for the motility and helical shape of *Borrelia* (Barbour *et al.* 1986). And interestingly,

the peptidoglycan cell wall is closely associated with the cytoplasmic membrane. Furthermore, unlike Gram-negative bacteria, the outer membrane is very fluid and consisting of 45-62% protein, 23-50% lipid and 3-4% carbohydrate. The labile outer membrane often excretes extracellular vesicles or blebs during *in vitro* growth (Barbour *et al.* 1986; Radolf *et al.* 1994). Strikingly, the outer leaflet of the outer membrane does not contain any lipopolysaccharide and phosphatidylethanolamine, but includes other glycolipids instead (Takayama *et al.* 1987; Eiffert *et al.* 1991; Wheeler *et al.* 1993; Belisle *et al.* 1994). In addition, the outer membrane has a low density of integral, membrane-spanning proteins (Walker *et al.* 1991; Radolf *et al.* 1994) and comprises an enormously high abundance of lipoproteins. More than 8% of *B. burgdorferi* coding sequences are predicted to encode around 105 lipoproteins in total, the highest frequency among all sequenced bacterial genomes (Brandt *et al.* 1990; Fraser *et al.* 1997).

1.3.1. Biogenesis and structure of spirochetal outer membrane proteins

Spirochetes are known to contain at least three types of outer membrane proteins (OMPs): (1) lipoproteins tethered to either side of the membrane via lipids, (2) transmembrane proteins that span the whole membrane and (3) peripheral OMPs.

The structures of several *B. burgdorferi* outer membrane lipoproteins have been solved (Fig 1.6). OspA consists of four β-sheets, formed by 21 antiparallel β-strands and a C-terminal α-helix (Makabe *et al.* 2006) (Fig. 1.6.A). In contrast, the three-dimensional structure of another borrelian lipoprotein, OspC, revealed a dimer of two molecules each comprising five parallel α-helices and two short β-strands (Eicken *et al.* 2001; Kumaran *et al.* 2001) (Fig. 1.6.B). The preponderance of helical content in OspC is striking in comparison to OspA. Interestingly, the structure of VlsE, a further *B. burgdorferi* lipoprotein, that undergoes antigenic variation, was different again from the other structurally characterized lipoproteins, containing eleven α-helices and four short β-strands (Fig. 1.6.C). But it is notably that OspC exhibits sequence heterogeneity in a surface-exposed region distal to the membrane, a property that is in common with the VlsE protein (Eicken *et al.* 2002).
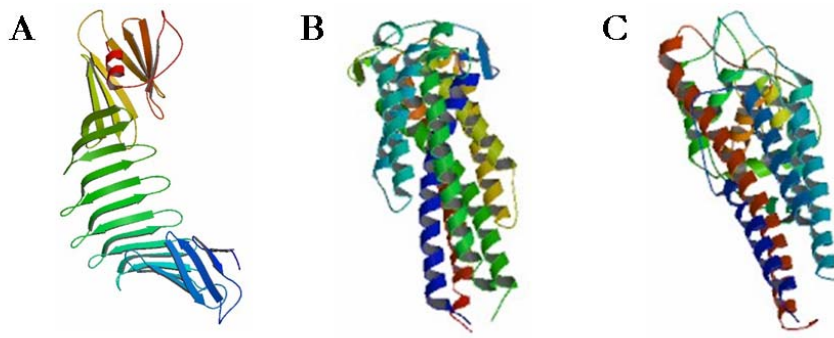
Fig. 1.6. The crystal structures of three *B. burgdorferi* outer membrane lipoproteins. **(A)** OspA (Makabe *et al.* 2006), **(B)** OspC (Eicken *et al.* 2001; Kumaran *et al.* 2001) and **(C)** VlsE (Eicken *et al.* 2002).

(Pictures taken from http://www.pdb.org/)

1.3.2. Outer surface lipoproteins of *Borrelia*

The protein content of the *Borrelia* outer membrane is represented by a huge quantity of lipoproteins. As an indication of their importance in *Borrelia*, lipoproteins are the most abundant proteins in these species (Haake 2000). These proteins are situated on the surface of the bacterial cell and anchored in the outer leaflet of the outer membrane. Borrelian lipoproteins play a major role in the activation of the innate immune response and in adaptive responses and pathogenicity of *Borrelia* spirochetes. Thus, this class of proteins is responsible for the activation of host inflammatory response as tissue inflammation is a unifying feature during the manifestation of Lyme disease. Lipoproteins dominate pathogenic mechanisms exploited by *B. burgdorferi*, including such as antigenic variation (Zhang *et al.* 1997; Zhang *et al.* 1998), evasion of complement killing (Kraiczy *et al.* 2001; Alitalo *et al.* 2002; Stevenson *et al.* 2002) and adhesion mechanisms (Coburn *et al.* 2005).

The most abundant and best described outer membrane lipoproteins in the Lyme disease species *B. burgdorferi* are the so-called outer surface proteins (Osps). The most prominent lipoprotein species is OspA (see also figure 1.6.A). Immunization with OspA protects against subsequent *B. burgdorferi* infection (Wallich *et al.* 1996). Nevertheless it is unsuitable as a vaccine because of detrimental side effects (Lathrop *et al.* 2002). OspC, another well-studied *B. burgdorferi* lipoprotein (see also figure 1.6.B), is homologous to variable small proteins (Vsps) of relapsing fever *Borrelia* (Carter *et al.* 1994). Strikingly, the OspA/B and OspC expression is reciprocally regulated and undergoing a switch during spirochete transition from the tick vector to the mammalian host. Thus, the OspA expression is upregulated in ticks while OspC is expressed in high amounts in the mammalian host. Beside the Osps, there is a wide variety of lipoproteins

with different functionalities present in *B. burgdorferi*, such as the multicopy lipoproteins Mlps (Caimano *et al.* 2000), Lp6.6, a small lipoprotein of 6.6 kDa (Lahdenne *et al.* 1997), the decorin-binding proteins DbpA/B (Guo *et al.* 1995), the glycosaminoglycan-binding protein Bgp (Parveen *et al.* 2000), P35 comprising two lipoproteins (Fikrig *et al.* 2000), the Vmp-like-sequence Vls (Barbour 1990), the Bmp family (Aron *et al.* 1994), P22 (Lam *et al.* 1994), the OspE/F related proteins Erps (Akins *et al.* 1999), the Elps containing OspE/F-like leader peptides (Akins *et al.* 1999) and the complement regulator acquiring surface proteins CRASPs (Kraiczy *et al.* 2001).

In contrast to Lyme disease species, the most abundant proteins in the relapsing fever species' outer membrane are the variable major proteins Vmps, lipoproteins that are expressed with different surface epitopes through antigenic variation (Stoenner *et al.* 1982; Barbour 2002; Barbour *et al.* 2006; Tabuchi *et al.* 2006). The lipoproteins of relapsing fever agents are subdivided into two families: the variable large proteins (Vlps) and the variable small proteins (Vsps) (Hinnebusch *et al.* 1998; Haake 2000; Cullen *et al.* 2004). Interestingly, the expression of the single Vsp species is correlated to the pattern and the state of the disease. Vsps undergo antigenic variation and at least three mechanisms for this surface alteration of relapsing fever lipoproteins are known (Kehl *et al.* 1986).

1.3.3. Pore-forming proteins in the outer membrane of *Borrelia burgdorferi*

Integral outer membrane proteins fulfill several tasks such as maintaining the bacterial cell structure, binding to different substances and transport of nutrients, bactericidal and toxic agents (Achouak *et al.* 2001). In comparison to other Gram-negative bacteria, *Borrelia* species contain very low amounts of those integral membrane proteins (Walker *et al.* 1991; Radolf *et al.* 1994). These few-membrane-spanning proteins in *Borrelia* are therefore likely to act as pore-forming components. Borrelian pore-forming proteins are mainly described for *B. burgdorferi*, and to date, five of this species are identified and characterized (see Tab. 1.2):

(1) P13 is an unusual pore-forming protein with a single-channel conductance of 3.5 nS in 1 M KCl and is predicted to insert in the outer membrane by amphipathic α-helices (Nilsson *et al.* 2002; Östberg *et al.* 2002). It is N- and C-terminally processed (Östberg *et al.* 2004) and interestingly the 28 amino acid long C-terminus is also capable of pore-formation (unpublished data). To date, the structure and the exact function of P13 are not yet defined. (2) Oms28 exhibits a single-channel conductance of 0.6 nS in 1 M KCl (Skare *et al.* 1996), but its porin-like properties have recently been questioned (Mulay *et al.* 2007). (3) P66 is a protein with dual functions. It acts as adhesin (Coburn *et al.* 1999; Coburn *et al.* 2003; Coburn *et al.* 2005) and as porin with the atypical large single-channel conductance of 11 nS (Thein *et al.* 2008a). Studies of

P66 in Lyme disease and relapsing fever species are presented in chapter 4 and 5. (4) DipA is a 36 kDa porin with a single-channel conductance of 50 pS in 1 M KCl. Its identification and characterization as a porin specific for dicarboxylates is described in chapter 3. A homologue of DipA is present in relapsing fever agents and termed Oms38. It exhibits a single-channel conductance of 80 pS in 1 M KCl and is described in chapter 2. And (5) BesC is a channel-tunnel with homology to *E. coli* TolC and thus part of the *Borrelia* efflux system. Together with BesA and BesC the systems spans the cytoplasmic membrane, the periplasmic space and the outer membrane and plays an important role in the drug efflux (Bunikis *et al.* 2008).

In contrast to LD species, the porin knowledge in terms of relapsing fever *Borrelia* is rather stinted. Beside the identification of the mentioned Oms38 (see chapter 2), there are indications of several pore-forming activities in outer membrane preparations of RF spirochetes (Shang *et al.* 1998; Thein *et al.* 2008b) and genes with a high homology to *B. burgdorferi p13*, *oms28* and *p66* can be found in the published genomes of the RF agents *B. duttonii*, *B. recurrentis* and *B. hermsii*.

All *Borrelia* porins contain N-terminal extensions that are responsible for the transport across the cytoplasmic membrane. After the translocation these N-terminal leader peptides are cleaved (Cullen *et al.* 2004). Porins of typical Gram-negative bacteria such as *E. coli* contain a determined pattern of aromatic amino acids including phenylalanine and tryptophane on the C-terminus. This pattern is recognized by the Omp85 machinery and essential for the accurate folding, the insertion in the outer membrane and functionality (Bos *et al.* 2007). Yet, this is not the case for the mentioned spirochetal porins (Nikaido 2003) and could be one reason for the difficulties and the loss of pore-forming capability after producing *Borrelia* porins recombinant in *E. coli* (author's observation).

Tab. 1.2. Pore-forming outer membrane proteins of *B. burgdorferi*.

Protein	M.W. [kDa]	Conductance [nS] in 1 M KCl	Selectivity	Voltage-dependence	Function
P13	13	3.5	for cations	yes	porin?
Oms28	28	0.6	*n.d.*	no	porin-like properties?
P66	66	11.0	not selective	yes	adhesin, porin
DipA	36	0.05	for anions	no	dicarboxylate-specificity
BesC	48	0.3	not selective	*n.d.*	part of efflux-system

M.W. means molecular weight; *n.d.* means not determined; conductance means single-channel conductance measured in 1 M KCl.

1.4. Aims of this work

The general aim of this thesis was to provide insight into the porin content of both Lyme disease and relapsing fever spirochetes. This aim should be achieved by isolating and identifying porins from *Borrelia* outer membranes and by biophysically characterizing their properties in artificial lipid membranes. Within the *Borrelia* genus, the knowledge of the porin content is divergent comparing the agents of the two borrelian-caused diseases, Lyme disease species and relapsing fever species. In terms of the Lyme disease agent *Borrelia burgdorferi*, three putative porins were characterized in previous studies: P13, Oms28 and P66. In contrast to Lyme disease species, the porin knowledge of relapsing fever *Borrelia* is low, which means that not any porin has actually been described for representatives of these agents.

Thus, one major aim focused on the identification and the characterization of porins of relapsing fever species. Chapter 2 describes the first identification and characterization of a porin in those species. Besides, also chapter 4 focuses on that aim and deals with the investigation of homologous proteins to the *Borrelia burgdorferi* porin P66 in relapsing fever *Borrelia*.

A second major aim was to closer investigate porins of Lyme disease agents with regard to their functionality. In chapter 3, the identification of a new Lyme disease *Borrelia* porin together with the determination of its biological function is presented. Also chapter 5 focuses on Lyme disease porins and describes studies concerning channel sizing and revealing the constitution of the *B. burgdorferi* porin P66.

Chapter 2

OMS38 IS THE FIRST IDENTIFIED
PORE-FORMING PROTEIN IN THE OUTER MEMBRANE
OF RELAPSING FEVER SPIROCHETES

2.1. Summary

Relapsing fever is a worldwide, endemic disease caused by several spirochetal species belonging to the genus *Borrelia*. During the recurring fever peaks borreliae proliferate remarkably fast compared to the slow dissemination of Lyme disease *Borrelia* and therefore require an efficient nutrient uptake from the blood of their hosts. This study describes the identification and characterization of the first relapsing fever porin, which is present in the outer membranes of *B. duttonii*, *B. hermsii*, *B. recurrentis* and *B. turicatae*. The pore-forming protein was purified by hydroxyapatite chromatography and designated Oms38, for outer membrane spanning protein of 38 kDa. Biophysical characterization of Oms38 was obtained by using the black lipid bilayer method demonstrating that Oms38 forms small, water-filled channels of 80 pS in 1 M KCl that did not exhibit voltage-dependent closure. The Oms38 channel is slightly selective for anions and shows a ratio of the permeability for cations over anions of 0.41 in KCl. Analysis of the deduced amino acid sequences demonstrated that Oms38 contains an N-terminal signal sequence which is processed under *in vivo* conditions. Oms38 is highly conserved within the four studied relapsing fever species, sharing an overall amino acid identity of 58% with a strong indication for the presence of amphipathic β-sheets.

2.2. Introduction

Relapsing fever (RF) is caused by spirochetes of the genus *Borrelia*, which also includes species responsible for Lyme disease. RF occurs worldwide - often endemically in temperate to tropical and subtropical regions and in some African communities the incidence is highest of any bacterial diseases reported (Vial *et al.* 2006). The main clinical manifestations are, according to the name, recurring high fever peaks with high densities of *Borrelia* in the blood (Southern *et al.* 1969; Felsenfeld 1971; Goubau 1984), which may be accompanied with complications such as spontaneous abortion and perinatal death (Fuchs *et al.* 1969; Brasseur 1985; van Holten *et al.* 1997; Guggenheim *et al.* 2005).

RF is caused by approximately 20 species of *Borrelia* distributed nearly world wide and is transmitted by hematophagous ticks and lice (Southern *et al.* 1969; Bryceson *et al.* 1970; Felsenfeld 1971). Four species of spirochetes representing the wide distribution of different RF species are considered as the main cause of RF: (1) *B. duttonii* is present in sub-Saharan Africa and transmitted by the soft-body tick *Ornithodoros moubata moubata*; this species likely causes more RF cases than anywhere else in the world (Goubau 1984). (2) *B. hermsii* is the most common RF-causing pathogen in North America, transmitted by the tick *Ornithodoros hermsi* (Dworkin *et al.* 2002; Schwan *et al.* 2007) and has been the focus of antigenic variation research (Stoenner *et al.* 1982; Barbour *et al.* 2006). (3) *B. recurrentis* occurs endemically in the highlands of Ethiopia with sporadic cases in Sudan and is transmitted by the human body louse *Pediculus humanus humanus* (Bryceson *et al.* 1970). (4) *B. turicatae* has been sporadically isolated in Texas, Kansas and Florida from the tick vector *Ornithodoros turicata* and dogs, while its exact geographic distribution is not defined (Schwan *et al.* 2005); *B. turicatae* is used to study neuroborreliosis (Cadavid *et al.* 1997). These four species were chosen for the study of outer membrane porins.

Borrelia are limited in their metabolic and biosynthetic capacities and therefore highly dependent on nutrients provided by their hosts (Fraser *et al.* 1997). Consequently, these parasites need to have an efficient regulation of the nutrient uptake across the cell envelope. The *Borrelia* cell envelope structure and membrane composition shows major differences compared to those of other Gram-negative bacteria (Johnson 1977; Takayama *et al.* 1987; Walker *et al.* 1991; Belisle *et al.* 1994; Radolf *et al.* 1995; Cox *et al.* 1996; Cox *et al.* 2001). Few membrane-spanning proteins are located in the outer membrane (Radolf *et al.* 1994; Fraser *et al.* 1997). The most abundant proteins in the RF outer membrane are the variable major proteins Vmp, lipoproteins that are expressed with different surface epitopes through antigenic variation (Stoenner *et al.* 1982; Barbour 2002; Barbour *et al.* 2006; Tabuchi *et al.* 2006).

In Lyme borreliosis, bacteria slowly disseminate from the infection site with symptoms often arising weeks or months after the tick bite. In contrast, RF borreliae grow rapidly, reaching high cell densities in the blood in only a few days. To maintain this rapid growth, the bacteria need, in part, to have an extraordinarily efficient nutrient uptake from the plasma. The transport of nutrients and other molecules across the outer membrane is performed by pore-forming proteins, so-called porins. These are integral membrane proteins which form large water-filled pores in the outer membrane of Gram-negative bacteria (Benz 1994b) to enable the influx of nutrients and other substances from the environment into the bacterial cell. Porins can be subdivided into two classes: (i) general diffusion pores, such as OmpF of *E. coli* K12 (Benz 1994b; Benz 2001), which sort mainly according to the molecular mass of the solutes, and (ii) pores with a substrate-binding site inside the channel (Ferenci *et al.* 1980; Hancock *et al.* 1986; Benz *et al.* 1987; Benz *et al.* 1988b; Charbit 2003). Furthermore, surface-exposed porin loops are potential targets in interaction with other cells (Bernardini *et al.* 1993), bacteriophages (Yu *et al.* 1998) and bactericidal compounds (Sallmann *et al.* 1999) and are therefore putative candidates for vaccine development.

Several outer membrane porins such as P66 (Skare *et al.* 1997), Oms28 (Skare *et al.* 1996) and P13 (Nilsson *et al.* 2002; Östberg *et al.* 2002) were identified recently in the Lyme disease agent *B. burgdorferi*. Intriguingly, no RF porin – although there are indications of their presence (Shang *et al.* 1998) – has been described in the literature to date. Nevertheless, the analysis of RF porins is of high importance to understand the spirochetes' nutrient uptake in the blood during their exceptionally fast growth during the fever peaks.

Here, we describe the identification of the first RF porin present in outer membrane fractions of *B. duttonii*, *B. hermsii* and *B. recurrentis*. The pore-forming proteins were purified by hydroxyapatite chromatography to homogeneity and designated Oms38. Biophysical characterizations of the porins were achieved by using the black lipid bilayer method. They demonstrated that Oms38 porins form water-filled pores of small conductance (80 pS in 1 M KCl) and are selective for anions. Partial sequencing of the protein and searches of genomic DNA sequences from ongoing projects revealed sequences of *oms38* in *B. duttonii*, *B. hermsii*, *B. recurrentis* and *B. turicatae*. Alignments demonstrated that the deduced amino acid sequences of the different Oms38 are highly conserved among the studied RF species and contain β-strands.

2.3. Materials and Methods

2.3.1. Bacterial strains and growth conditions

The relapsing fever species used in this study were *B. duttonii* 1120K3, *B. hermsii* HS1 and *B. recurrentis* A1. Bacteria were grown in BSKII medium (Barbour 1984) supplemented with 10% rabbit serum and 1.4% gelatine at 37°C until cell densities reached approximately 10^7-10^8 cells ml^{-1} and harvested by centrifugation.

2.3.2. Isolation of outer membrane proteins and purification of the 38 kDa protein

Outer membrane fractions (OMFs) of the three *Borrelia* species used in this study were prepared as described previously (Magnarelli *et al.* 1989). Purification of the native 38 kDa protein was performed by using a hydroxyapatite Bio-gel (Bio-Rad) column as it has been used previously for the purification of mitochondrial porins (Freitag *et al.* 1982; Benz 1994a). 100 µl of OMF (approx. 100 ng proteins) were diluted in 400 µl 2% Genapol (Roth) and applied to a hydroxyapatite column made from 0.3 g hydroxyapatite in an Econo-Column (Bio-Rad) with the dimensions of 0.5 x 5 cm and a column volume of 2 ml. The column was washed with six column volumes of a buffer containing 2% Genapol, 10 mM Tris-HCl (pH 8.0). For protein elution, four column volumes of buffer containing 2% Genapol, 250 mM KCl and 10 mM Tris-HCl (pH 8.0) were passed through the column; fractions of 2.0 ml volume were collected.

2.3.3. Protein electrophoresis

Sodium dodecyl sulfate-polyacrylamide gel electrophoresis (SDS-PAGE) was performed according to the Laemmli gel system (Laemmli 1970). 100 µl of protein samples eluted by hydroxyapatite-chromatography were precipitated by the protocol of Wessel and Flügge (Wessel *et al.* 1984). Proteins were separated by 12% SDS-PAGE under denatured conditions (boiled for 5 min in 4x SDS sample buffer before loading the gel) by using a Bio-Rad electrophoresis system. The gels were stained with silver (Blum *et al.* 1987).

2.3.4. Protein sequencing

For N-terminal sequence analysis, proteins were blotted onto a PVDF-membrane after 12% SDS-PAGE. Microsequencing was performed using a gas-phase sequenator Procise 492 cLC (Applied Biosystems GmbH) using the instructions of the manufacturer (Eckerskorn *et al.* 1993).

2.3.5. Planar lipid bilayer assays

The methods used for black lipid bilayer experiments have been described previously (Benz *et al.* 1978). The instrumentation consisted of a Teflon chamber with two compartments separated by a thin wall and connected by a small circular hole with an area of 0.4 mm^2. The membranes were formed by a 1% (w/v) solution of diphytanoyl phosphatidylcholine (Avanti Polar Lipids, Alabaster, AL) in *n*-decane. The porin-containing fractions were diluted 1:100 in 1% Genapol (Roth) and added to the aqueous phase after the membrane had turned black. The membrane current was measured with a pair of Ag/AgCl electrodes with salt bridges switched in series with a voltage source and a highly sensitive current amplifier (Keithley 427) while kept at 20°C throughout.

Voltage-dependence of the pores was checked as described elsewhere (Mirzabekov *et al.* 1996) using membrane potentials as high as -200 to +200 mV. Zero-current membrane potential measurements were performed by establishing a salt gradient across membranes containing approximately 100 reconstituted channels as described earlier (Benz *et al.* 1979; Ludwig *et al.* 1986). The zero-current membrane potentials were measured with a high impedance electrometer (Keithley 617).

2.4. Results

2.4.1. Pore-forming activities in the outer membrane fractions of *B. duttonii*, *B. hermsii* and *B. recurrentis*

Outer membrane fractions (OMFs) isolated from the three RF *Borrelia* species contained numerous proteins as shown by SDS-PAGE (Fig. 2.1, left panel). Several differences in the outer membrane bands between *B. duttonii*, *B. hermsii* and *B. recurrentis* are obvious. *B. duttonii* OMF exhibits major protein bands at a molecular weight of around 28 kDa, whereas major bands of *B. hermsii* and *B. recurrentis* OMFs corresponded to a molecular weight of around 40 kDa. These findings are supposedly due to differences in expression and antigenic variation of the numerous variable major proteins known to be present in the outer membrane of relapsing fever spirochetes (Saint Girons *et al.* 1991; Carter *et al.* 1994; Tabuchi *et al.* 2006).
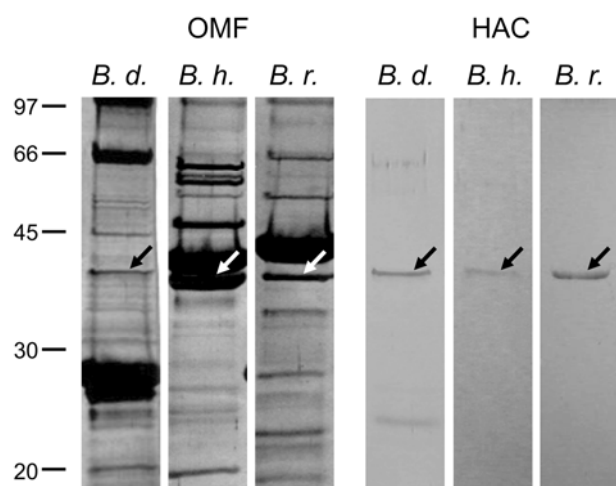
Figure 2.1. SDS-PAGE analysis of outer membrane fractions and the purified 38 kDa pore of *B. duttonii*, *B. hermsii* and *B. recurrentis*. Approximately 1-10 ng of outer membrane fractions (OMF) of *B. duttonii* (*B. d.*), *B. hermsii* (*B. h.*) and *B. recurrentis* (*B. r.*) (left panel) or 100 µl hydroxyapatite chromatography-fractions (HAC) containing the purified 38 kDa protein (right panel) were separated by 12% SDS-PAGE and silver-stained. The positions of molecular mass standards in kDa are shown at the left.

For investigations in the black lipid bilayer OMFs were highly diluted in 1% Genapol. All OMFs exhibited a broad range of different pore-forming activities (Fig. 2.2) ranging from 0.1 to 11 nS caused by different pore-forming proteins reconstituted into the lipid bilayer. A similar broad distribution of channels has been found for detergent-treated OMF of *Borrelia burgdorferi* (Östberg *et al.* 2002). A particular high pore-forming activity was observed within the conductance range from about 10 pS to 0.75 nS for experiments with detergent-treated OMFs of all three RF species. However, the full conductance fluctuation patterns of the single RF species exhibited several remarkable differences.
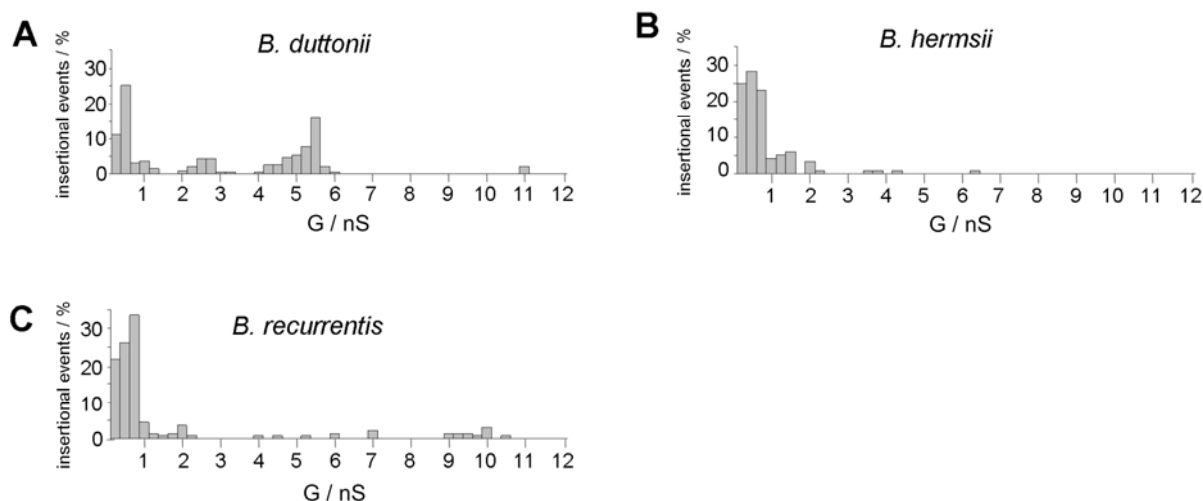
Figure 2.2. Pore-forming activities in the outer membrane fractions of *B. duttonii*, *B. hermsii* and *B. recurrentis*. The histograms of the single-channel conductance (G) distributions were derived from at least 100 individual single channel on-steps derived from at least 4 different membranes. Highly diluted OMFs treated with 1% Genapol were added to a diphytanoyl phosphatidylcholine/*n*-decane membrane using 1 M KCl as electrolyte. The applied voltage was 20 mV and the temperature was 20°C throughout.

The OMF of *B. duttonii* (Fig. 2.2.A) contained pores with maxima within the histogram of the single-channel conductance centered on 0.5 nS, 2.5 nS, 5.5 nS and 11 nS. For *B. hermsii* (Fig. 2.2.B), the highest maximum of the single-channel conductance distribution was about 6.25 nS. Our histogram agrees with the one previously reported (Shang *et al.* 1998). The histogram derived from conductance fluctuations observed with the *B. recurrentis* OMF (Fig. 2.2.C) was similar to those of *B. duttonii* and *B. hermsii*, which also had high pore-forming activity of about 2 nS and contained maxima within the histogram around 7 nS and 10 nS.

2.4.2. Purification and identification of a 38 kDa, pore-forming protein in the outer membranes of *B. duttonii*, *B. hermsii* and *B. recurrentis*

To identify proteins that are responsible for a defined pore-forming activity in the OMFs, about 100 ng of *Borrelia* OMF were diluted in 400 μl 2% Genapol, 10 mM Tris-HCl (pH 8.0). This sample was applied to a dry hydroxyapatite column, which has been used successfully for the purification of mitochondrial porins (Freitag *et al.* 1982; Benz 1994a). After wash of the column with six column volumes of a buffer containing 2% Genapol, 10 mM Tris-HCl (pH 8.0), the pore-forming protein was eluted using different protocols. The most efficient one was the addition of 250 mM KCl to the buffer thus increasing its ionic strength. Some of the fractions (fractions 1 and 2) eluted from the column showed a high pore-forming activity (see below). To check the purity of the proteins from the pore-forming protein fractions, 100 μl were precipitated

by the protocol of Wessel and Flügge (Wessel *et al.* 1984) and subjected to a 12% SDS-PAGE. Pore-formation was found exclusively in fractions exhibiting a band that corresponded to a molecular mass of 38 kDa (Fig. 2.1, right panel). The fractions derived from the OMFs of *B. hermsii* and *B. recurrentis* contained exclusively the 38 kDa protein. The fractions derived from the OMF of *B. duttonii* contained the 38 kDa protein and a second band visible through all fractions, which corresponded to a molecular mass of 27 kDa. Amino acid sequencing identified this band as member of the Vsp lipoprotein family with similarity to the *B. burgdorferi* OspC (Schwan *et al.* 1998; Barbour *et al.* 2000) (data not shown). The protein was abundant in the OMF of *B. duttonii* (Fig. 2.1, left panel); secondary-structure analysis, comparisons with other pore-forming lipoproteins and the fact that fractions exclusively containing this 27 kDa band did not exhibit pore-forming activity suggested that Vsp is not a pore-forming component. Thus, the 38 kDa protein component was claimed to be a putative porin within the fractions.

To identify the gene encoding the 38 kDa protein, we performed partial amino acid sequencing of the protein fractions that contained only the corresponding protein band. 200 µl of the hydroxyapatite chromatography fraction 1 derived from the *B. duttonii* OMF were separated by 12% SDS-PAGE and blotted onto a PVDF-membrane. N-terminal sequencing provided the first 19 N-terminal amino acids of the native 38 kDa protein of *B. duttonii*: EEETKQKLETKENSTTKEN. Using this sequence we searched in the genome sequences of current work in progress with several relapsing fever spirochetes.

The chromosome sequence of *B. duttonii* revealed the gene coding for the 38 kDa protein and its complete amino acid sequence (GenBank accession number CP000976) (Fig. 2.3). According to its molecular mass the protein was designated as Oms38, for outer membrane spanning protein of 38 kDa. Further analyses identified homologues of *oms38* in the chromosome of *B. hermsii* (GenBank accession number EU660961), *B. recurrentis* (GenBank accession number CP000993) and *B. turicatae* (GenBank accession number EU660962).

2.4.3. Analysis of the amino acid sequences of Oms38 of *B. duttonii, B. hermsii, B. recurrentis* and *B. turicatae*

Figure 2.3 shows an alignment of the deduced amino acid sequences of Oms38 of *B. duttonii, B. hermsii, B. recurrentis* and *B. turicatae* (Chenna *et al.* 2003). The identity of Oms38 of the four species was 58%. *B. duttonii* and *B. recurrentis* derived Oms38 shared the highest amino acid identity of 98%, *B. hermsii* and *B. turicatae* Oms38 were 83% identical, and *B. duttonii* and *B. hermsii* Oms38 were 67% identical. The main discrepancies were located in the N-terminus while the remaining parts of the sequences were highly similar. N-terminal sequencing of the native *B. duttonii* Oms38

identified the amino acids 20 to 38 of the full length protein (Fig. 2.3). Consequently, the first N-terminal amino acids are removed under *in vivo* conditions being the putative signal peptide (Fig. 2.3) as is known for other spirochetal outer membrane proteins and porins (Cullen *et al.* 2004). The putative N-terminal cleavage sites of *B. recurrentis*, *B. hermsii* and *B. turicatae* Oms38 are marked in Figure 2.3 (Bendtsen *et al.* 2004).
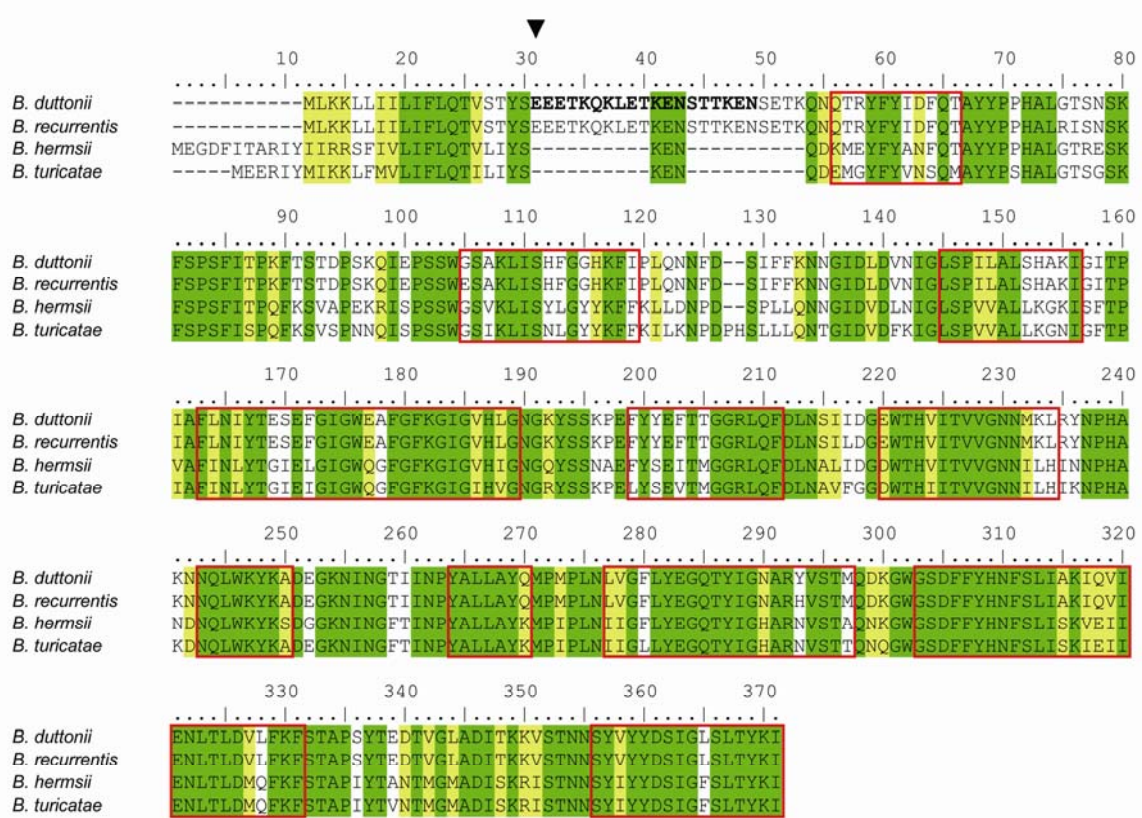
Figure 2.3. Amino acid sequence alignment of Oms38 of *B. duttonii, B. hermsii, B. recurrentis* and *B. turicatae* (Chenna *et al.* 2003). Amino acids identical in all four strains are shaded in green, similar amino acids are highlighted in yellow. The sequences of *B. duttonii, B. hermsii, B. recurrentis* and *B. turicatae* Oms38 share an amino acid identity of 58%. *B. duttonii* and *B. recurrentis* Oms38 are identical in 98% of their amino acid sequence, *B. hermsii* and *B. turicatae* Oms38 in 83% and *B. duttonii* and *B. hermsii* in 67%. The putative N-terminal cleavage site of all four species Oms38 is marked by an arrow (Bendtsen *et al.* 2004). The 19 amino acid sequence derived from the partial sequencing of the native *B. duttonii* protein is in bold. Predicted ß-sheet transmembrane domains concordant in the four proteins are framed in red (Bagos *et al.* 2004; Gromiha *et al.* 2004).

Computational analyses (Bagos *et al.* 2004; Gromiha *et al.* 2004) revealed putative beta-sheet stretches in the secondary structure of Oms38 (red boxes in Fig 2.3). The predicted beta-sheet regions allow structural conceptions of a protein containing 12-14 beta-sheets forming a beta-barrel pore as is known for other well-studied porins (Saier 2000; Delcour 2002; Charbit 2003).

2.4.4. Single-channel measurements of Oms38

The pores formed by Oms38 were studied in more detail by adding small amounts of Oms38 to black lipid bilayer membranes. The reconstitution of the protein into the membrane caused a substantial conductance increase over several orders of magnitude due to the formation of small ion-permeable channels similar to that caused by other bacterial porins (Benz 1994b). Under conditions of appropriate amplification and low protein concentration, the records of single reconstitution events into the membranes could be resolved as conductance steps with an average single-channel conductance of 80 pS in 1 M KCl (Fig. 2.4).
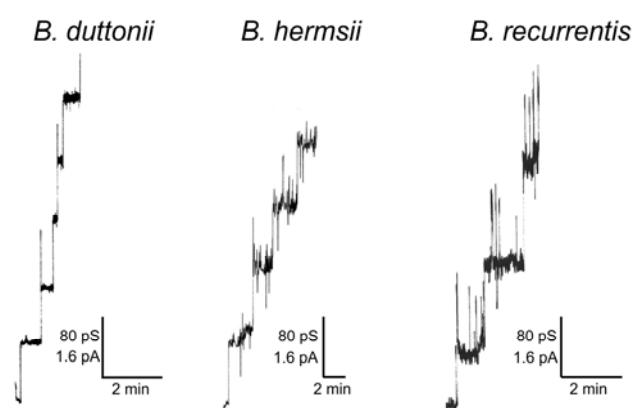
Figure 2.4. Pore-forming activity associated with purified *B. duttonii*, *B. hermsii* and *B. recurrentis* Oms38. Single-channel insertional events observed for *B. duttonii*, *B. hermsii* and *B. recurrentis* Oms38 in a diphytanoyl phosphatidyl-choline/*n*-decane membrane. Highly diluted, purified Oms38 at a concentration of about 10 ng ml⁻¹ was added to the membrane and bathed in 1 M KCl. The applied voltage was 20 mV and the temperature was 20°C throughout.

Some single-channel events showed initial sharp spikes during their reconstitution which immediately switched to the stable 80-pS level. This stable level was defined as single-channel conductance of Oms38. By statistical analysis of at least 50 of these conductance steps, the single-channel conductance of Oms38 was measured as a function of different electrolytes and different concentrations. Fig. 2.5 shows histograms of all current fluctuations observed for *B. duttonii*, *B. hermsii* and *B. recurrentis* Oms38 in 1 M KCl. The data demonstrate that Oms38 of all three studied RF species consistently exhibited the small average single-channel conductance of 80 pS in 1 M KCl, which is not surprising, given the close identity of all three Oms38 proteins. The measurement of Oms38 pores from *B. duttonii* in different KCl concentrations from 0.1 to 3 M demonstrated that the channel conductance was an almost linear function of the electrolyte concentration (Table 2.1).

To obtain further information on the properties of the pores formed by Oms38, single-channel experiments were also performed with electrolytes other than KCl. The results are summarized in Table 2.1 and suggested an anion-selectivity of the pore, as being derived from single-channel experiments in KCH₃COO and LiCl. Replacement of chloride with the large and less mobile acetate resulted in a substantial influence on the single-channel conductance (30 pS

for *B. duttonii*, 65 pS for *B. hermsii* and 50 pS for *B. recurrentis* in 1 M KCH$_3$COO, pH 7), whereas the replacement of potassium by lithium led to a lower influence on the conductance (50 pS for *B. duttonii*, 75 pS for *B. hermsii* and 60 pS for *B. recurrentis* in 1 M LiCl).
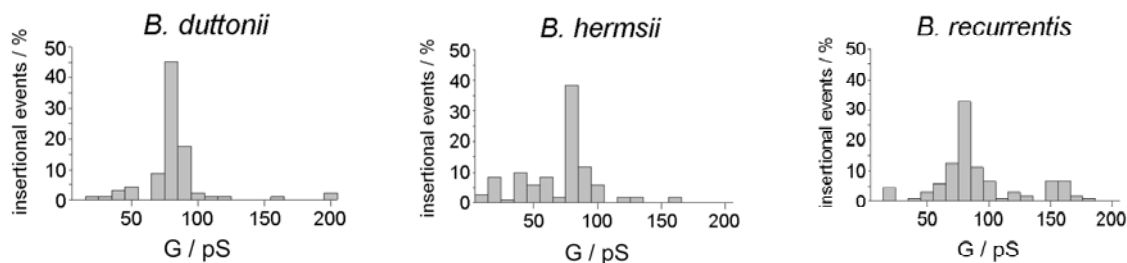
Figure 2.5. Histograms of individual single-channel events observed for purified Oms38 of *B. duttonii*, *B. hermsii* and *B. recurrentis*. For each histogram a total number of at least 50 insertional events of Oms38 into a diphytanoyl phosphatidylcholine/*n*-decane membrane were evaluated. The average single-channel conductance (G) for at least 50 on-steps was 80 pS for Oms38 derived from *B. duttonii*, *B. hermsii* and *B. recurrentis* OMFs. The aqueous phase contained 1 M KCl; the applied voltage was 20 mV and the temperature was 20°C throughout.

Table 2.1. Average single-channel conductances (*G*) of Oms38 of *B. duttonii*, *B. hermsii* and *B. recurrentis* in different electrolyte solutions.

Electrolyte	Concentration (*M*)	*B. duttonii*	*B. hermsii*	*B. recurrentis*
			G (*pS*)	
KCl	3	275	*n.m.*	*n.m.*
	1	80	80	80
	0.3	30	*n.m.*	*n.m.*
	0.1	15	*n.m.*	*n.m.*
LiCl	1	50	75	60
KCH$_3$COO (pH 7)	1	30	65	50

The membranes were formed from diphytanoyl phosphatidylcholine dissolved in *n*-decane. The single-channel conductance was measured in unbuffered electrolyte solutions (approx. pH 6) unless otherwise indicated at 20 mV applied voltage and 20°C. The average single-channel conductance, G, was calculated from at least 50 single events of Oms38. *n.m.* means not measured.

Strikingly, the single-channel conductance of 80 pS in 1 M KCl of *B. duttonii* Oms38 and its homologues in *B. hermsii* and *B. recurrentis* were identical, whereas the measured conductance in LiCl and KCH₃COO differed slightly when comparing Oms38 of the three species. A possible explanation could be different stability states of the proteins derived from different species after the OMF preparation and purification procedure. While *B. duttonii* Oms38 formed well-defined pores throughout, the channels formed by *B. hermsii* and *B. recurrentis* Oms38 were accompanied by flickering and noise, and were scarcely measurable after about 10 single-channel events. Thus, the purification resulted in a observable percentage of flickering pores in the bilayer and therefore gave a less precise evaluation of the *B. hermsii* and *B. recurrentis* pores compared to the *B. duttonii* Oms38. It is noteworthy, however, that channel flicker was not a purification artefact because different purification protocols of Oms38 from *B. hermsii* and *B. recurrentis* resulted in the same flickering indicating that the flicker represents an intrinsic property of the channels. Interestingly, Oms38 homologues of all three species agreed in the trend of single-channel results with LiCl and KCH₃COO in which the change of the anion in the electrolyte had a higher influence on the conductance than the change of the cation, indicating anion-selectivity.

2.4.5. Voltage dependence

Certain bacterial porins exhibit voltage-dependent closure at high voltages despite the fact that no voltage-dependent closure has been observed so far in *in vivo* experiments (Sen *et al.* 1988; Lakey *et al.* 1989; Benz 1994b). To check if Oms38 is voltage-dependent, a multi-channel experiment with approximately 100 reconstituted pores was performed. The application of membrane potentials ranging from -200 mV to +200 mV showed no influence on conductance, revealing that Oms38 did not exhibit voltage-dependent closure (data not shown).

2.4.6. Selectivity measurements

Selectivity measurements allow a quantification of the permeability of the Oms38 pore for anions relative to cations. The selectivity of *B. duttonii*-derived Oms38 was investigated by multi-channel experiments under zero-current conditions in KCl, LiCl and KCH₃COO. Membranes were formed in 100 mM salt solution and purified Oms38 was added to the aqueous phase when the membranes were in the black state. After the incorporation of approximately 100 pores into the membrane, five-fold salt gradients were established by the addition of small amounts of 3 M salt solution to one side of the membrane. The permeability ratios for cations over anions through Oms38 were calculated using the Goldman-Hodgkin-Katz equation (Benz *et al.* 1979) and are

listed in Table 2.2 together with the zero-current membrane potentials. These data support the idea that Oms38 is indeed selective for anions.

The potential on the more diluted side of the membrane was negative throughout the experiments for KCl (-14.0 mV), LiCl (-22.4 mV) and KCH$_3$COO (-8.6 mV), suggesting preferential movement of anions through the Oms38 pore. Nevertheless, cations may pass the Oms38 pore because the ratios of the permeability coefficients P$_{cation}$/P$_{anion}$ were 0.41 (in KCl), 0.24 (in LiCl) and 0.58 (in KCH$_3$COO). These data demonstrate also that the selectivity follows the mobility sequence of the ions because the decrease in mobility of the anions (KCH$_3$COO) resulted in a decrease of the anion selectivity. Similarly, the cations had a smaller influence on the selectivity because the replacement of K$^+$ by the less mobile Li$^+$ had a smaller influence on the permeability ratio. The results of the selectivity measurements are in agreement with the single-channel measurements because they also suggested anion selectivity for the Oms38 pore.

Table 2.2 Zero-current membrane potentials (V_m) of diphytanoyl phosphatidylcholine/*n*-decane membranes in the presence of *B. duttonii* Oms38 measured for a five-fold concentration gradient of different electrolytes.

Electrolyte	V_m (*mV*)	P_c/P_a
KCl	-14.0	0.41
LiCl	-22.4	0.24
KCH$_3$COO (pH 7)	-8.6	0.58

V_m is defined as the difference between the potential at the diluted side (100 mM) and the potential at the concentrated side (500 mM). The aqueous electrolyte solutions were buffered with 10 mM Tris-HCl (pH 7.5); temperature = 20°C; The permeability ratio P_c/P_a was calculated using the Goldman-Hodgkin-Katz equation (Benz *et al.* 1979) from at least two individual experiments.

2.5. Discussion

2.5.1. Lipid bilayer experiments with outer membrane fractions (OMFs) of RF species suggest the presence of porins

In this study we demonstrated that outer membrane fractions of the RF species *B. duttonii*, *B. recurrentis* and *B. hermsii* contained channel-forming proteins, with properties similar to those of porins from other Gram-negative bacteria (Skare *et al.* 1996; Skare *et al.* 1997; Benz 2001; Nilsson *et al.* 2002; Östberg *et al.* 2002; Nikaido 2003). The conductance of these putative porins reconstituted into lipid bilayer membranes was spread over a considerable range with an obvious accumulation of pores in the low conductance range from about 10 pS to 0.75 nS. The histogram observed with OMF of *B. hermsii* agrees with previously reported data, which revealed a similar distribution of conductance (Shang *et al.* 1998). The distribution in all three histograms appears to be similar to that observed with OMF of *B. burgdorferi* (Östberg *et al.* 2002): detergent-treated outer membranes of this Lyme disease-causing species form channels in lipid bilayer membranes that are also spread across a considerable range in terms of conductance. This may indicate that its outer membrane contains a variety of channels (Mirzabekov *et al.* 1996; Skare *et al.* 1996; Skare *et al.* 1997; Östberg *et al.* 2002; Bunikis *et al.* 2008). From this organism P13, P66, Oms28 and a TolC analogous outer membrane channel were identified and characterized in lipid bilayer experiments. All these porins form channels with a conductance in 1 M KCl that is greater than that observed for the channel-forming activity in this study. A channel-forming protein with a molecular mass of about 38 kDa was identified in the RF species, purified to homogeneity and termed Oms38 in accordance with the nomenclature used for the outer membrane spanning Oms28. This protein is also a porin, although its pore function has recently been questioned by analysis of its secondary structure, by the observation that Oms28 is not surface-exposed and by Triton X-114 extraction of outer membrane vesicles (Skare *et al.* 1996; Mulay *et al.* 2007). The Oms38 channels have a single-channel conductance of about 80 pS in 1 M KCl, which is considerably lower than the conductance of all porins that were identified to date in Lyme disease-causing *B. burgdorferi*.

2.5.2. Purification and identification of Oms38 of *B. duttonii*, *B. hermsii* and *B. recurrentis*

Oms38, the first porin identified in any RF *Borrelia* species, was purified to homogeneity using hydroxyapatite chromatography across a dry hydroxyapatite column. The features responsible for

protein purification using this column material are not well understood but it has been used with great success for the purification of mitochondrial porin and mitochondrial carriers (Palmieri *et al.* 1993; Benz 2004). These proteins are deeply buried in the mitochondrial membranes and probably also in the detergent micelles after membrane digestion using detergent treatment. We assume that Oms38 is similarly deeply buried in the outer membrane because of its function as an outer membrane channel. Using the same purification procedure, Oms38 was purified from the OMFs of all three studied RF species. SDS-PAGE revealed a high degree of purity of Oms38 of *B. hermsii* and *B. recurrentis*, even under sensitive conditions of silver-staining of the proteins separated by SDS-PAGE. The additional, weak 27 kDa protein band visible on the SDS-PAGE gel of the *B. duttonii* fraction after purification across the hydroxyapatite column could not be responsible for pore-formation because fractions exclusively containing this 27 kDa band did not exhibit pore-forming activity. Mass spectrometry identified this protein as member of the Vsp lipoprotein family, with similarity to OspC of *B. burgdorferi* (Schwan *et al.* 1998; Barbour *et al.* 2000). Additional secondary-structure analysis and comparison with other pore-forming lipoproteins supported the view that it is not a channel-forming component.

2.5.3. Deduced amino acid sequences of Oms38 of *B. duttonii*, *B. hermsii*, *B. recurrentis* and *B. turicatae*

Partial sequencing of the purified Oms38 of *B. duttonii* allowed the identification of its gene within the genomes of the three other RF species *B. hermsii*, *B. recurrentis* and *B. turicatae*. Interestingly, a gene homologous to *oms38* is also present in the well-studied Lyme disease agent *B. burgdorferi* (as "hypothetical protein" *bb0418*). The function of this gene has not yet been defined, but its presence may indicate the existence of a protein in *B. burgdorferi* with similar properties as Oms38 of RF *Borrelia*.

The deduced amino acid sequences of the four RF species Oms38 showed an overall identity of 58%, indicating that the identities between the Oms38 homologues in *B. duttonii*, *B. hermsii*, *B. recurrentis* and *B. turicatae* are rather high. *B. duttonii* and *B. recurrentis* Oms38 shared an identity of 98% while *B. hermsii* and *B. turicatae* shared an identity of 83%. The high identity of the primary structure is in good agreement with the biophysical results, demonstrating that the Oms38 homologues of *B. duttonii*, *B. hermsii* and *B. recurrentis* exhibited identical biochemical and biophysical properties (see below). From this point of view we assume that structure and function of the Oms38 homologues are identical under *in vivo* conditions. The N-terminus of Oms38 of *B. duttonii* starts with three glutamic acids. This means that this protein contains a 19 amino-acid long, N-terminal signal peptide with a putative recognition sequence for the leader

peptidase similar to those of other spirochetal outer membrane proteins (Cullen *et al.* 2004). The deduced amino acid sequences of all Oms38 proteins may contain similar N-terminal extensions that are responsible for their transport into the periplasm as is known for porins of *B. burgdorferi* (Cullen *et al.* 2004). The signal peptides are cleaved during the *sec*-dependent export process and the protein is able to insert into the outer membrane. Computational analyses predicted several putative beta-sheets in the primary sequences of the different Oms38. This suggests that the protein may form a beta-barrel in the outer membrane as like most Gram-negative bacterial porins (Benz 1994b; Saier 2000; Delcour 2002; Charbit 2003). However, structural predictions for *Borrelia* porins have to be considered with caution, because of the possible presence of alpha-helices in some borrelian porins as shown by computational analysis for P13 and P66 and circular dichroism spectroscopy for Oms28 (Bunikis *et al.* 1995; Noppa *et al.* 2001; Mulay *et al.* 2007). This means that their definitive structure can only be deduced from X-ray analysis of protein crystals.

2.5.4. Biophysical properties of Oms38

Pure Oms38 were obtained by affinity chromatography across a hydroxyapatite column using increasing ionic strength in the elution buffer. The results of lipid bilayer experiments revealed that all Oms38 studied here form channels with the small single-channel conductance of 80 pS in 1 M KCl. To date, a similar pore-forming activity is not known from *B. burgdorferi* OMF studies and the value of 80 pS differs clearly from the comparatively huge single-channel conductance of 600 pS (Skare *et al.* 1996), 3.5 nS (Östberg *et al.* 2002) and 9.6 nS (Skare *et al.* 1997) associated with well-characterized *B. burgdorferi* porins. However, Oms38 forms pores with a single-channel conductance in the range of certain outer membrane porins of *E. coli* that have a lower conductance such as the nucleotide-specific Tsx (10 pS) (Maier *et al.* 1988) and the sugar-specific LamB (160 pS) (Benz *et al.* 1986). These *E. coli* channels with comparable single channel conductance are substrate-specific channels, which means that further investigations have to be done to determine if Oms38 functions as general diffusion pore or as substrate-specific channel.

Interestingly, we observed in some experiments with Oms38 of *B. duttonii* initial sharp peaks (see Fig. 2.4), which could be interpreted as additional transient states of the Oms38 channels. These transient states were difficult to resolve fully in some cases; in others they had approximately the same conductance as the stable state. In experiments with Oms38 from *B. hermsii* and *B. recurrentis* the additional state with a conductance of about 80 pS occurred more frequently and not only during the reconstitution of the channels into the membrane but also as a superposition to the stable 80 pS state (see Fig. 2.4). These results suggest that Oms38 could have at least two states one transient and one stable. The trigger for the opening of the transient state

is not clear but it was definitely not caused by the purification procedure. In addition, it was also not caused by voltage-dependent gating. In general, no indication for voltage-dependent gating of the Oms38 channels was observed.

Experiments with salts other than KCl demonstrated that the conductance of the Oms38 channels was dependent on the aqueous mobility of the ions (Table 2.1). Nevertheless, the effect of the anions on the single-channel conductance was more substantial indicating anion selectivity of the Oms38 channels (Table 2.1). This is supported by the results of the zero-current potential measurements (see below). The single-channel conductance of the Oms38 channel of *B. duttonii* was an almost linear function of the KCl concentration. This suggests that the channel does not contain a binding site for the ions used in this study. In addition, the channel probably does not contain net charges that could result in charge effects. The possible anion-selectivity of the Oms38 channels was confirmed by selectivity measurements with Oms38 of *B. duttonii*. For all three salts employed in this study, the more dilute side of the membrane became negative due to the preferential movement of anions over cations (Table 2.2). This indicates preferential diffusion of anions through the pore.

Taken together, we have identified, purified and characterized the first putative porin in the outer membrane of the RF species *B. duttonii*, *B. hermsii* and *B. recurrentis*. While detailed structure-function analyses of Oms38 and further RF outer membrane investigations remain to be done, this work represents an important step forward in understanding the outer membrane pathways for nutrient uptake of these strictly host-dependent, pathogenic spirochetes. Furthermore, it provides some knowledge of the outer-membrane protein composition and surface-exposed protein domains of RF spirochetes. This could lead to a basis for a successful drug design. Further characterization of RF *Borrelia* porins could also provide information concerning the physiology of these spirochetes and discover a surface-exposed protein that could function as a potential vaccine candidate.

DIP A, A PORE-FORMING PROTEIN IN THE OUTER MEMBRANE OF LYME DISEASE SPIROCHETES EXHIBITS SPECIFICITY FOR THE PERMEATION OF DICARBOXYLATES

3.1. Summary

The Lyme disease causative agent *Borrelia burgdorferi* is due to its small genome metabolically and biosynthetically deficient, thereby making it highly dependent on nutrients provided by their hosts. Considering that the uptake of nutrients by the *Borrelia* cell is not yet completely understood, this study describes the purification and characterization of a 36 kDa protein that functions as putative dicarboxylate-specific porin in the outer membrane of Lyme disease *Borrelia*. The protein was purified from outer membranes of *B. burgdorferi* by hydroxyapatite chromatography and designated as DipA, for dicarboxylate-specific porin A. DipA was partially sequenced, and based on the resulting amino acid sequence, the corresponding gene *dipA* was identified in the published genome sequences of *B. burgdorferi* B31, *B. garinii* PBi and *B. afzelii* PKo. Strikingly, the DipA sequence exhibits high homology to the Oms38 porin of relapsing fever *Borrelia*. *B. burgdorferi* DipA was biophysically characterized using the black lipid bilayer assay. The protein has an average single-channel conductance of 50 pS in 1 M KCl. DipA is selective for anions with a ratio of permeability for cations over anions of 0.57 in KCl and did not show voltage-dependent closure. The permeation of KCl through the channel could be partly blocked by titration of the DipA-mediated membrane conductance with increasing concentrations of different di- and tricarboxylic organic anions. Particular high stability constants up to about 28,000 l/mol (in 0.1 M KCl) were obtained among the 11 tested anions, such as oxaloacetate, 2-oxoglutarate and citrate. The obtained results imply that DipA does not form a general diffusion pore, but a porin with a binding site specific for dicarboxylates which play an important key role in the deficient metabolic and biosynthetic pathways of *Borrelia* species.

3.2. Introduction

Lyme disease is a systemic disorder manifested in a wide spectrum of different symptoms such as a circular skin rash around a tick bite and arthritis up to paralysis appearances and other neurological effects (Nadelman *et al.* 1998; Orloski *et al.* 2000). It is caused by infection with *Borrelia* spirochetes (Benach *et al.* 1983; Steere *et al.* 1983), which include inter alia the main European Lyme disease causing species *B. burgdorferi* s.s., *B. garinii* and *B. afzelii* (Wilske 2003). Borreliae are obligate parasites and have complex life cycles involving arthropod and mammalian reservoir hosts, usually ticks and rodents (Burgdorfer 1984; Schwan 1996). To ensure the survival in this enzootic life cycle, the spirochetes must adapt to a range of diverse host environments and nutrient availability (de Silva *et al.* 1997; Steere *et al.* 2004). Thus, these parasites need to have an efficient control of the nutrient uptake system across the cell envelope.

The *B. burgdorferi* cell envelope structure and membrane composition exhibit major differences compared to those of other Gram-negative bacteria (Johnson 1977; Walker *et al.* 1991; Belisle *et al.* 1994; Radolf *et al.* 1995; Cox *et al.* 1996; Cox *et al.* 2001). For example, *B. burgdorferi* is known to lack lipopolysaccharides (Takayama *et al.* 1987) and the flagella are localized in the periplasmic space (Barbour *et al.* 1986). In addition, the outer membrane has a low ratio of protein to lipid and a lower density than the inner membrane (Walker *et al.* 1991; Radolf *et al.* 1994). To date, a few integral membrane proteins have been identified and characterized in *B. burgdorferi* (Bunikis *et al.* 1995; Probert *et al.* 1995; Skare *et al.* 1997; Noppa *et al.* 2001). Thereof proteins associated with the *Borrelia* outer membrane are mostly lipoproteins (Radolf *et al.* 1994; Shang *et al.* 1998). The few integral membrane proteins present in the *B. burgdorferi* outer membrane are therefore likely to act as pore-forming proteins.

Pore-forming proteins, so-called porins, are integral membrane proteins which form large, water-filled pores in the outer membrane of Gram-negative bacteria (Benz 1994b) in order to enable the influx of nutrients and other substances from the environment into the bacterial cell. Porins can be subdivided into two classes: (1) general diffusion pores, such as OmpF of *E. coli* K12 (Benz 1994b; Benz 2001) which sort mainly according to the molecular mass of the solutes and (2) pores with a binding site inside the channel. The latter porins are responsible for the rapid uptake of classes of solutes such as carbohydrates (Ferenci *et al.* 1980; Benz *et al.* 1986), nucleosides (Benz *et al.* 1988b) or phosphate (Hancock *et al.* 1986). Surface-exposed porin loops are potential targets for adhesion to other cells (Bernardini *et al.* 1993) as well as bacteriophages (Yu *et al.* 1998) and bactericidal compounds (Sallmann *et al.* 1999) and are therefore putative vaccine candidates.

Borrelia burgdorferi has a relative small chromosome of 0.91 Mb which code only for a few metabolic pathways and cause a lack of biosynthetic capacity. The bacteria are therefore highly dependent on nutrients provided by their hosts (Fraser *et al.* 1997). The important first step for the uptake of those nutrients into the bacterial cell is mainly limited by porins in the outer membrane. To date, three putative porins of *B. burgdorferi* were characterized: P13 (Nilsson *et al.* 2002; Östberg *et al.* 2002), Oms 28 (Skare *et al.* 1996), which has recently been questioned to have porin-like properties (Mulay *et al.* 2007) and P66 (Skare *et al.* 1997) with single-channel conductances of 3.5 nS, 0.6 nS and 9.6 nS in 1 M KCl, respectively. Recently, the channel-tunnel BesC, a component of the *Borrelia* multi-drug-efflux system, was identified in the outer membrane, forming channels of 300 pS in 1 M KCl (Bunikis *et al.* 2008).

In this study, we report the purification and biophysical characterization of a dicarboxylate-specific porin in the outer membrane of *B. burgdorferi*, a homologue of the Oms38 porin of relapsing fever spirochetes (Thein *et al.* 2008b). Subsequently homologous proteins of this newly identified porin are present in the Lyme disease agents *B. garinii* and *B. afzelii*, sharing a high amino acid homology of 88%. The pore-forming protein was purified by hydroxyapatite chromatography and designated as DipA, for dicarboxylate-specific porin A. Biophysical characterization by the black lipid bilayer method revealed anion selectivity of the small channel of 50 pS conductance (in 1 M KCl). DipA is the first identified solute-specific porin in *Borrelia*. It contains at least one binding site with a high affinity for dicarboxylic anions and related compounds and is therefore suggested to play a major role in the metabolic pathway for the uptake of those chemicals.

3.3. Materials and Methods

3.3.1. Bacterial strains and growth conditions

The Lyme disease strain used in this study was *B. burgdorferi* Δp66, a *p66* knock-out strain of *B. burgdorferi* B31-A (Pinne *et al.* 2007). Bacteria were grown in Barbour-Stoenner-Kelly-II (BSKII) medium (Barbour 1984) supplemented with 10% rabbit serum and 1.4% gelatine at 37°C until cell density reached approximately 10^7-10^8 cells ml^{-1} followed by harvesting the cells by centrifugation.

3.3.2. Isolation of outer membrane proteins and purification of the 36 kDa protein

Outer membrane fractions (OMFs) of *B. burgdorferi* Δp66 used in this study were prepared as described elsewhere (Magnarelli *et al.* 1989). Purification of the native porin was performed by using a hydroxyapatite Bio-gel (Bio-Rad) column as it has been used previously for the purification of mitochondrial porins (Freitag *et al.* 1982; Benz 1994a) and the porin Oms38 of relapsing fever spirochetes (Thein *et al.* 2008b). 100 μl of OMF (approx. 100 ng proteins) were diluted in 400 μl 2% Genapol (Roth). The mixture was applied to a hydroxyapatite column made from 0.3 g hydroxyapatite in an Econo-Column (Bio-Rad) with the dimensions of 0.5 x 5 cm and a column volume of 2 ml. The column was washed with six column volumes of a buffer containing 2% Genapol, 10 mM Tris-HCl (pH 8.0). For protein elution four column volumes of a buffer containing 2% Genapol, 250 mM KCl and 10 mM Tris-HCl (pH 8.0) were passed through the column. Fractions of 2.0 ml volume were collected.

3.3.3. SDS-PAGE and Immunoblotting

Sodium dodecyl sulfate-polyacrylamide gel electrophoresis (SDS-PAGE) was performed according to the Laemmli gel system (Laemmli 1970). 100 μl of hydroxyapatite-chromatography fractions were precipitated by the protocol of Wessel and Flügge (Wessel *et al.* 1984). Proteins were separated by 12% SDS-PAGE under denatured conditions (boiled for 5 min in 4x SDS sample buffer before loading the gel) by using a Bio-Rad electrophoresis system. The gels were silver-stained (Blum *et al.* 1987). For immunoblots, a tank blot system (Amersham Biosciences) was used as previously described (Towbin *et al.* 1979). Bound antibodies were detected using peroxidase-conjugated anti-rabbit or anti-mouse antibodies (DAKO A/S) and enhanced

chemiluminescence reagents according to the manufacturer's instructions (Amersham Biosciences).

3.3.4. Overexpression of a recombinant fragment of DipA

A fragment of DipA representing the 90 C-terminal amino acids was produced in *E. coli* Rosetta™ 2 (DE3) (Novagen), using expression vector pET 15b (Novagen) containing N-terminal His-Tag. The gene fragment of 285 bp was amplified by PCR using following oligonucleotides: rbb0418_f (5'-CTG**CATATG**GAAGGAAAAACACAAATTGG-3') containing NdeI restriction site and rbb0418_r (5'-GACTTTA**GGATCC**TTAAGTTATA GACATTCC-3') containing BamHI restriction site. After restriction enzyme digestion, the PCR product was ligated into the plasmid pET-15b. The *E. coli* cells carrying expression plasmids were grown at 37°C to $OD_{600} = 0.6$ in LB medium containing 50 µg of carbecillin per ml and protein expression was induced by addition of isopropyl-β-d-thiogalactopyranoside (IPTG) to a final concentration of 1 mM. The culture was further grown for 4 h, and cells were collected by centrifugation at 6,000 x *g* for 15 min. The cells were lysed using BugBuster 10X Protein Extraction Reagent (Novagen) according to manufacturer's instructions. Recombinant fragment containing N-terminal His-Tag was purified using Ni-NTA Spin Columns (Qiagen) following manufacturer's recommendations. Elution fractions were combined and proteins were precipitated using trichloroacetic acid (TCA). Briefly, to protein solution TCA was added to a final concentration of 10%, samples were incubated on ice for 30 min., pelleted by centrifugation, washed with cold acetone, pelleted and resuspended in NuPAGE® LDS Sample Buffer (Invitrogen).

3.3.5. Antiserum

Polyclonal antiserum was raised against the recombinant fragment of DipA produced as described above. Precipitated elution fractions were separated by SDS-PAGE electrophoresis. Recombinant protein fragment was excised from the gel and approximately 100 µg of protein was used for rabbit immunization and subsequent boosts (Agrisera AB, Sweden).

3.3.6. Mass spectrometry

The hydroxyapatite fractions showing pore-forming activity were subjected to SDS-PAGE followed by silver-staining (Blum *et al.* 1987). The two bands were analyzed by mass spectrometry (nano LC-MS/MS) as described elsewhere (Schindler *et al.* 2008). Data of the MS/MS datasets were evaluated by Mascot algorithm (Perkins *et al.* 1999). In detail, mass spectrometric analysis was performed on a Qtrap4000 linear ion trap system (Applied Biosystems, Darmstadt, Germany). Mass spectra obtained by LC-MS/MS analysis were used to identify the corresponding peptides with the MascotTM (version 2.1.6) (Perkins *et al.* 1999). The algorithm searched in the Uniprot *Borrelia* FASTA database (April, 2007) with the following parameter set: (a) fixed modification: carbamidomethyl (C); (b) variable modification: oxidation (M); (c) peptide and MS/MS tolerance: +/- 0.4 Da; (d) ion score cut-off: 30.

3.3.7. Planar lipid bilayer assays

The methods used for black lipid bilayer experiments have been described previously (Benz *et al.* 1978). The instrumentation consisted of a Teflon chamber with two compartments separated by a thin wall and connected by a small circular hole with an area of about 0.4 mm^2. The membranes were formed from a 1% (w/v) solution of diphytanoyl phosphatidylcholine (PC) (Avanti Polar Lipids, Alabaster, AL) in *n*-decane. The porin-containing protein fractions were 1:100 diluted in 1% Genapol (Roth) and added to the aqueous phase after the membrane had turned black. The membrane current was measured with a pair of Ag/AgCl electrodes with salt bridges switched in series with a voltage source and a highly sensitive current amplifier (Keithley 427). The temperature was kept at 20°C throughout. To analyze the effect of DipA-specific antibodies on channel-forming abilities of DipA, preincubation with antibodies was performed as previously described (Paschen *et al.* 2005). Briefly, approximately 100 ng of purified DipA was incubated with polyclonal antiserum against DipA in a ratio of 1:3, incubated for 1 h at room temperature, and investigated in the planar lipid bilayer assay.

Zero-current membrane potential measurements were performed by establishing a salt gradient across membranes containing approximately 100 pore-forming proteins as it has been described earlier (Benz *et al.* 1979; Ludwig *et al.* 1986). The zero-current membrane potentials were measured with a high impedance electrometer (Keithley 617). Voltage-dependence of the porin channels was checked following the method described elsewhere (Mirzabekov *et al.* 1996), using membrane potentials as high as -120 to +120 mV.

Binding of dicarboxylates to DipA was investigated in the same way as the binding of malto-oligosaccharides to carbohydrate-specific porins (Benz *et al.* 1986; Benz *et al.* 1987). Binding of the substrate to a binding site inside the channel could be detected by a reduced ion flux through the channel. These measurements were performed with multi-channel experiments under stationary conditions. The protein was added to black diphytanoyl phosphatidylcholine/*n*-decane membranes. The membrane conductance increased upon reconstitution of channels. After about 90 minutes the conductance was stationary. At that point of time dicarboxylates were added in defined concentrations to both sides of the membrane while stirring continuously to allow equilibration. Bound compounds to the DipA channel resulted in a dose-dependent decrease of the membrane conductance as result of the restricted ion flux. The conductance data of the titration experiments were analyzed using the following equations (Benz *et al.* 1987). The conductance, $G_{(c)}$, of a DipA channel in the presence of dicarboxylates with the stability constant K (half saturation constant K_s) and the dicarboxylate concentration, c, is given by the maximum conductance (without dicarboxylates), G_{max}, times the probability that the binding site is free:

$$G_{(c)} = \frac{G_{max}}{(1 + K \cdot c)} \qquad \text{(Eq. 3.1)}$$

Equation 3.1 may also be written as

$$\frac{G_{max} - G_{(c)}}{G_{max}} = \frac{K \cdot c}{K \cdot c + 1} \qquad \text{(Eq. 3.2)}$$

which means that the conductance as a function of the dicarboxylate concentration can be analyzed using Lineweaver-Burk plots.

Equation 3.2 did not provide a satisfactory fit in these experiments, a fact which could be explained by the assumption that the DipA channels did not close completely when they were occupied by the different compounds or that only a fraction of the DipA channels closed completely. As previously described (Andersen *et al.* 2003), equation 3.3 allowed a much better fit, which took this problem into account,

$$\frac{G_{max} - G_{(c)}}{G_{max}} = \left(1 - \frac{G_{\infty}}{G_{max}}\right) \cdot \frac{K \cdot c}{K \cdot c + 1} \qquad \text{(Eq 3.3)}$$

with G_{∞} as the conductance at very high substrate concentration, i.e. the fraction that did not respond to the dicarboxylate compounds.

3.4. Results

3.4.1. Purification and identification of a new pore-forming protein in the outer membrane of *B. burgdorferi* Δ*p66*

The outer membrane fraction (OMF) of *B. burgdorferi* B31 Δp66 contains a variety of proteins as shown by SDS-PAGE (Fig. 3.1, left panel). Previous black lipid bilayer experiments with OMFs of *B. burgdorferi* Δ*p66* and *B. burgdorferi* Δ*p13*/Δ*p66* (Pinne *et al.* 2007) indicated that the preparations contained high channel-forming activities in the conductance range between 10 and 100 pS which are not related to P13, Oms28, P66 and BesC. Also the recent identification of an 80 pS-porin in closely related relapsing fever spirochetes suggested the possible presence of a similar pore-forming protein in the *B. burgdorferi* OMF (Thein *et al.* 2008b). To identify the corresponding protein component, approximately 100 ng of the OMF of *B. burgdorferi* Δp66 (Pinne *et al.* 2007), a knock-out mutant of the 11 nS pore P66, was subjected to hydroxyapatite chromatography. The fraction eluted at an ionic strength of 250 mM KCl showed high channel-forming activity of 50 pS in 1 M KCl which differed clearly from the pore-forming activities of P13, Oms28, P66 and BesC. To check the purity of the protein fraction exhibiting the channel formation, 100 μl of the corresponding fraction were precipitated and subjected to a 12% SDS-PAGE. Pore formation was found exclusively in fractions containing a band that corresponded to a molecular mass of 36 kDa (Fig. 3.1, right panel).
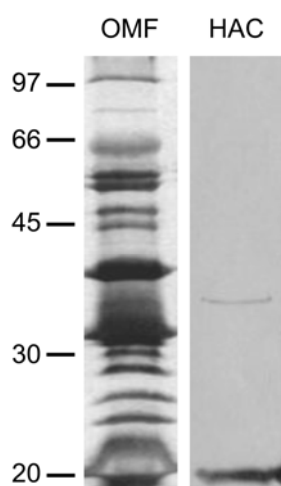
Figure 3.1. Analysis of purified DipA. Approximately 1-10 ng of outer membrane fraction (OMF) of *B. burgdorferi* B31 Δp66 or hydroxyapatite chromatography-purified (HAC) DipA was separated by 12% SDS-PAGE and silver-stained. The positions of molecular mass standards in kDa are shown at the left panel.

To identify the gene coding for this 36 kDa protein, silver-stained protein bands of the SDS-PAGE gel were tryptically digested, analyzed by mass spectrometry and identified by peptide mass fingerprinting. The fraction eluted from the hydroxyapatite column at an ionic strength of

250 mM KCl contained besides the 36 kDa protein a second band visible through all fractions, which corresponded to a molecular mass of about 20 kDa. Mass spectrometry identified this band as OspA and OspB precursors, well-studied cell surface proteins, which are present in very high copy numbers in the OMF of *B. burgdorferi*. Detailed molecular and structural analyses of OspA and OspB (Bergström *et al.* 1989; Caporale *et al.* 1994; Ding *et al.* 2000) and the fact that fractions next to one with pore-forming activity contained exclusively the OspA/OspB band and did not exhibit pore-forming activity suggested that these proteins are not pore-forming components. Thus, the 36 kDa protein was clearly defined as pore-forming component in the hydroxyapatite fraction and being responsible for the formation of the 50 pS pores. The gene of the protein band with the apparent molecular mass of 36 kDa was identified as "hypothetical protein *bb0418*" (GenBank accession number NP_212552) of *B. burgdorferi* B31, now designated as *dipA*, for dicarboxylate-specific porin A. The partial peptides which were found by mass spectrometry and were used for the identification of DipA are marked in figure 3.2. Searches within the published genomes of *B. garinii* PBi and *B. afzelii* PKo revealed homologous genes of *dipA* in these closely related Lyme disease agents.

3.4.2. Analysis of the DipA amino acid sequences of *B. burgdorferi*, *B. garinii* and *B. afzelii* DipA

The DipA sequences of *B. burgdorferi*, *B. garinii* and *B. afzelii* are shown in figure 3.2. The three species' DipA share an amino acid sequence identity of 88% demonstrating that the proteins are highly conserved while most of their sequence heterogeneity is found in N-terminal regions. Strikingly, *B. burgdorferi* DipA is 57% identical with the porin Oms38 of the relapsing fever species *B. duttonii* (Thein *et al.* 2008b), which even showed akin biophysical properties (see below). As known from other spirochetal outer membrane proteins and porins N-terminal amino acids serve as signal peptide and are cleaved under *in vivo* conditions (Cullen *et al.* 2004). Predicted N-terminal cleavage sites (Bendtsen *et al.* 2004) of *B. burgdorferi*, *B. garinii* and *B. afzelii* DipA are marked by an arrowhead in figure 3.2. Further computational analysis (Bagos *et al.* 2004; Gromiha *et al.* 2004) predicted putative ß-strands (red boxes in Fig. 3.2), that suggested that the secondary structure of DipA may contain 14 ß-sheets similar as is known for the ß-barrels of well-studied bacterial porins (Schirmer 1998; Charbit 2003).
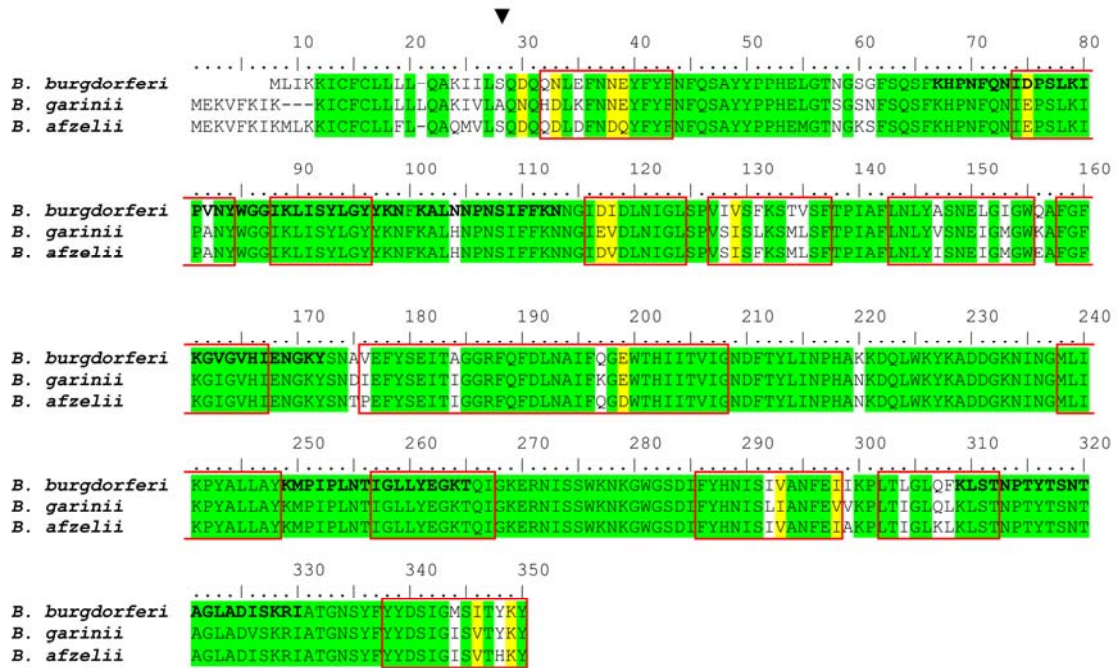
Figure 3.2. DipA amino acid sequences of *B. burgdorferi* B31, *B. garinii* PBi and *B. afzelii* PKo. Conserved amino acids in three species are highlighted in green, similar in yellow. The predicted cleavage site of the N-terminal signal peptide of DipA of *B. burgdorferi* B31 is marked by an arrowhead (Bendtsen *et al.* 2004). Partial peptide sequences obtained by mass spectrometry are in bold. Predicted ß-sheet transmembrane domains in the three proteins are framed in red (Bagos *et al.* 2004; Gromiha *et al.* 2004).

3.4.3. Immunoblot analysis of outer membranes and purified *B. burgdorferi* DipA

For immunoblot analysis antiserum was raised against a recombinant polypeptide representing the 90 C-terminal amino acids of *B. burgdorferi* DipA. Using this antiserum immunoblots of different Lyme disease and relapsing fever *Borrelia* OMFs and a fraction containing purified *B. burgdorferi* DipA were performed (Fig. 3.3). The results demonstrate that anti-DipA polyserum detected clearly DipA in the OMFs of the Lyme disease species *B. burgdorferi*, *B. afzelii* and *B. garinii*. Furthermore, the immunoblot showed also strong signals within the OMFs of the relapsing fever species *B. crocidurae*, *B. duttonii*, *B. hermsii*, *B. hispanica* and *B. recurrentis*, which indicated cross-reactivity of the anti-DipA polyserum with the DipA homologue Oms38 (Thein *et al.* 2008b). In addition, there was also a signal visible within the hydroxyapatite chromatography fraction that showed pore-forming activity (Fig. 3.3, HAC).
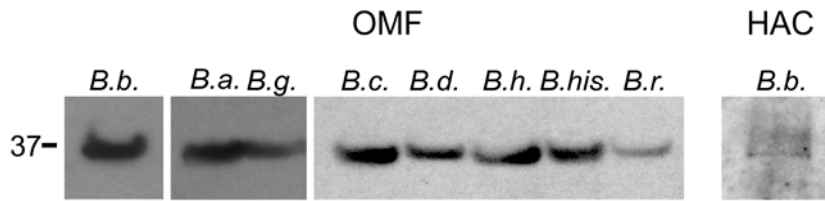
Figure 3.3. Detection of DipA in Lyme disease and relapsing fever spirochetes. Immunoblot analysis with antiserum against *B. burgdorferi* DipA resulted in clear signals of DipA and its homologues in the outer membrane fractions (OMF) of the Lyme disease agents *B. burgdorferi* (*B. b.*), *B. afzelii* (*B. a.*), *B. garinii* (*B. g.*) and the relapsing fever agents *B. crocidurae* (*B. c.*), *B. duttonii* (*B. d.*), *B. hermsii* (*B. h.*), *B. hispanica* (*B. his*) and *B. recurrentis* (*B. r.*). The immunoblot signal of the hydroxyapatite chromatography (HAC) purified *B. burgdorferi* (*B. b.*) DipA is on the right. The position of molecular mass standard in kDa is shown at the left.

3.4.4. Single-channel experiments

DipA-mediated channel formation was studied in detail. The addition of small amounts of DipA to a black lipid bilayer membrane caused a substantial conductance increase due to the formation of small ion-permeable channels similar to pore-forming events caused by other bacterial porins (Benz 1994b). Under conditions of appropriate amplification and low protein concentration, the recording of single insertional events into the membrane could be resolved as conductance steps with an average single-channel conductance of 50 pS in 1 M KCl (Fig. 3.4.A). Fig. 3.4.B shows a histogram of the current fluctuations observed with DipA in 1 M KCl. The data suggested that the current fluctuations are rather homogeneous. Interestingly, the 50 pS channel-forming activity of DipA could be abolished after preincubation with DipA-specific polyclonal antiserum, which also demonstrated antibody binding to DipA (data not shown).
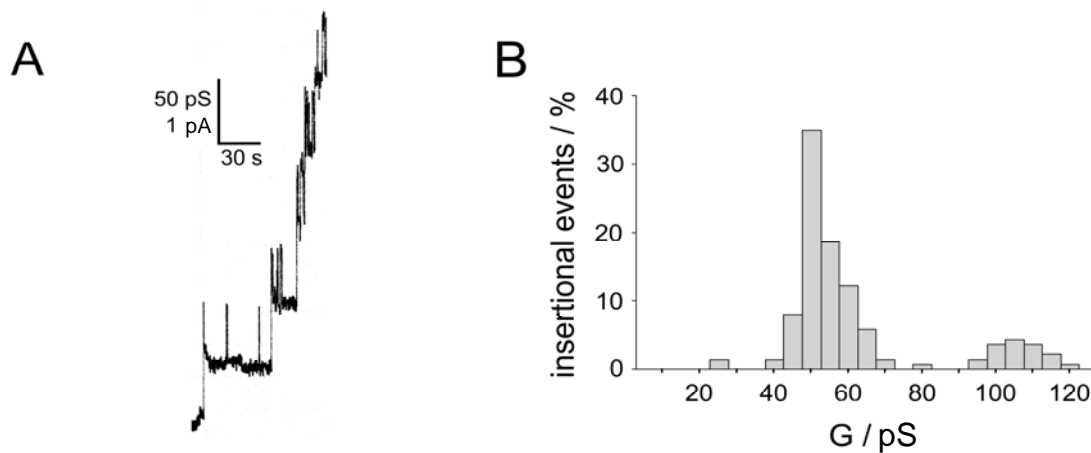
Figure 3.4. Pore-forming activity of DipA. (A) Single-channel conductance observed for DipA in a diphytanoyl phosphatidylcholine/*n*-decane (PC) membrane. About 10 ng ml^{-1} of purified DipA was added to a PC lipid bilayer bathed in 1 M KCl. (B) Histogram of individual single-channel events observed for purified DipA. The average single-channel conductance was 50 pS for a total number of 140 insertional events; temperature = 20°C; voltage = 20 mV.

Single-channel experiments were also performed with other electrolytes as LiCl and KCH₃COO to obtain more information on the properties of the channels formed by DipA. By statistical analysis of at least 100 conductance steps, the single-channel conductance of DipA was evaluated as a function of different electrolytes and different concentrations. The results are summarized in Table 3.1 and suggested anion selectivity of the channel. There was some influence of the mobility of anions on conductance (45 pS in 1 M KCH₃COO, pH 7), whereas change of the cation did not influence conductance (50 pS in 1 M LiCl). Table 3.1 shows also the average single-channel conductance of DipA, G, as a function of the KCl concentration in the aqueous phase. The single channel conductance in different KCl concentrations was a linear function of the electrolyte concentration.

Table 3.1. Average single-channel conductance (G) of DipA in different electrolyte solutions.

Electrolyte	Concentration	G
	(M)	(pS)
KCl	0.1	8
	0.3	20
	1	50
	3	140
LiCl	1	50
KCH₃COO (pH 7)	1	45

The membranes were formed from diphytanoyl phosphatidylcholine dissolved in *n*-decane. The aqueous electrolyte solutions were unbuffered and had a pH of ~6 unless otherwise indicated; temperature = 20°C; voltage = 20 mV. The average single-channel conductance, G, was calculated from at least 30 single insertional events of DipA.

3.4.5. Voltage dependence

Some Gram-negative bacterial porins show voltage-dependent closure despite the fact that no voltage dependent closure was observed so far in *in vivo* experiments (Sen *et al.* 1988; Lakey *et al.* 1989; Benz 1994b). A multi-channel experiment with at least 100 reconstituted DipA channels was performed to check the protein for a possible voltage-dependence. The application of membrane potentials ranging from -120 V to +120 V did not show any influence on the conductance demonstrating that DipA did not show voltage-dependent closure.

3.4.6. Selectivity measurements

Selectivity measurements were performed to quantify the permeability of the DipA channel for anions relative to cations. The selectivity was checked by multi-channel experiments under zero-current conditions. Membranes were formed in 100 mM electrolyte solution and purified DipA was added to the aqueous phase when the membranes were in the black state. After incorporation of at least 100 channels into the membrane, five-fold salt gradients were established by addition of small amounts of 3 M salt solution to one side of the membrane. The permeability ratios of cations over anions through DipA could be calculated using the Goldman-Hodgkin-Katz equation (Benz *et al.* 1979). They revealed together with the zero-current membrane potential that DipA is anion selective (Table 3.2). The potential on the more diluted side of the membrane was negative for KCl (-10.1 mV) and LiCl (-11.9 mV), suggesting preferential movement of anions through the DipA channel for these salts (Table 3.2). In contrast, the zero-current membrane potential was positive (7.5 mV) using KCH_3COO as electrolyte, suggesting preferential movement of potassium over acetate ions. This means that also cations could have a certain permeability through DipA because the ratios of the permeability coefficients P_{cation}/P_{anion} were 0.57 (in KCl), 0.47 (in LiCl) and 1.65 (in KCH_3COO). Furthermore the selectivity of the channel for anions in KCH_3COO could be influenced (P_{cation}/P_{anion} = 0.79) by adding 1 mM oxaloacetate (in 10 mM Tris-HCl pH 7.5) to the KCl solution, indicating that this substrate has a certain binding affinity to DipA (see below).

Table 3.2. Zero-current membrane potentials (V_m) of diphytanoyl phosphatidylcholine/*n*-decane membranes in the presence of DipA measured for a five-fold concentration gradient of different electrolytes.

Electrolyte	V_m	P_c/P_a
	(mV)	
KCl	-10.1	0.57
LiCl	-11.9	0.47
KCH_3COO (pH 7)	7.5	1.65
KCl + 1 mM Oxaloacetate	-7.6	0.79

V_m is defined as the difference between the potential at the dilute side (100 mM) and the potential at the concentrated side (500 mM). The aqueous electrolyte solutions were buffered with 10 mM Tris-HCl (pH 7.5); temperature = 20°C; The permeability ratio P_c/P_a was calculated using the Goldman-Hodgin-Katz equation (Benz *et al.*, 1979) from at least three individual experiments.

3.4.7. Inhibition of ion permeation through DipA by addition of dicarboxylates

Single-channel measurements demonstrated that DipA formed very small pores with a conductance much smaller than that of typical general diffusion pores (Benz 2001). The small single-channel conductance and the fact that growth of *Borrelia* is highly dependent on the uptake of nutrients (Barbour 1984; Fraser *et al.* 1997) suggested that DipA could be a channel specific for essential substances and contained a binding site for those chemicals in a similar way as the carbohydrate-specific *E. coli* channel LamB (Ferenci *et al.* 1980; Benz *et al.* 1986).

To test this hypothesis, titration experiments using different classes of substrates were performed as described previously for titration of LamB with carbohydrates (Benz *et al.* 1986; Benz *et al.* 1987). Interestingly, most classes of substrates including carbohydrates, such as glucose, fructose, sucrose, maltose and lactose, nucleosides, such as adenosine, and other anionic molecules, such as acetate, carbonate, phosphate and adenosine triphosphate, did not show any interaction with DipA. However, partial channel block was observed for dicarboxylates, which was studied in detail. For these experiments an electrolyte was chosen containing 0.1 M KCl, 1 mM Tris-HCl, pH 7.5, close to the chloride concentration in the blood of mammals to work under conditions close to the physiological ones. This means that the experiments were performed at a pH at least 1 unit above the pK_s of the carboxylic groups in the aqueous phase to guarantee dissociation of all carboxylic groups of the dicarboxylates by at least 90%. DipA was reconstituted into lipid bilayer membranes. After the reconstitution of channels had slowed down considerably and the membrane conductance was approximately stationary, concentrated solutions of different dicarboxylates were added to the aqueous phase at both sides of the membrane while stirring to allow equilibration. To exclude conductance decrease caused by pH and dilution effects during the addition of certain solutes, all tested substrates were dissolved in 0.1 M KCl, 1 mM Tris-HCl, pH 7.5 and the conductivity of the bathing solution was checked before and after each titration experiment.

Fig. 3.5 shows experiments using malate (Fig. 3.5.A), 2-oxoglutarate (Fig. 3.5.B) and phthalate (Fig. 3.5.C) as potential substrates of DipA. The addition of these dicarboxylates led to a dose-dependent block of DipA-mediated membrane conductance, which decreased by 23% in the case of malate, 29% in the case of 2-oxoglutarate and 25% in the case of phthalate at substrate concentrations of 27 mM, 9 mM and 4 mM, respectively. To study the complete binding potential of DipA for the substrates, titration experiments were performed with a variety of dicarboxylates and other related anions with high biological relevance (Table 3.3). All anions

listed in this Table blocked the ion current through DipA with a maximum block of channel conductance ranging from 20% for pyruvate to 31% for oxaloacetate
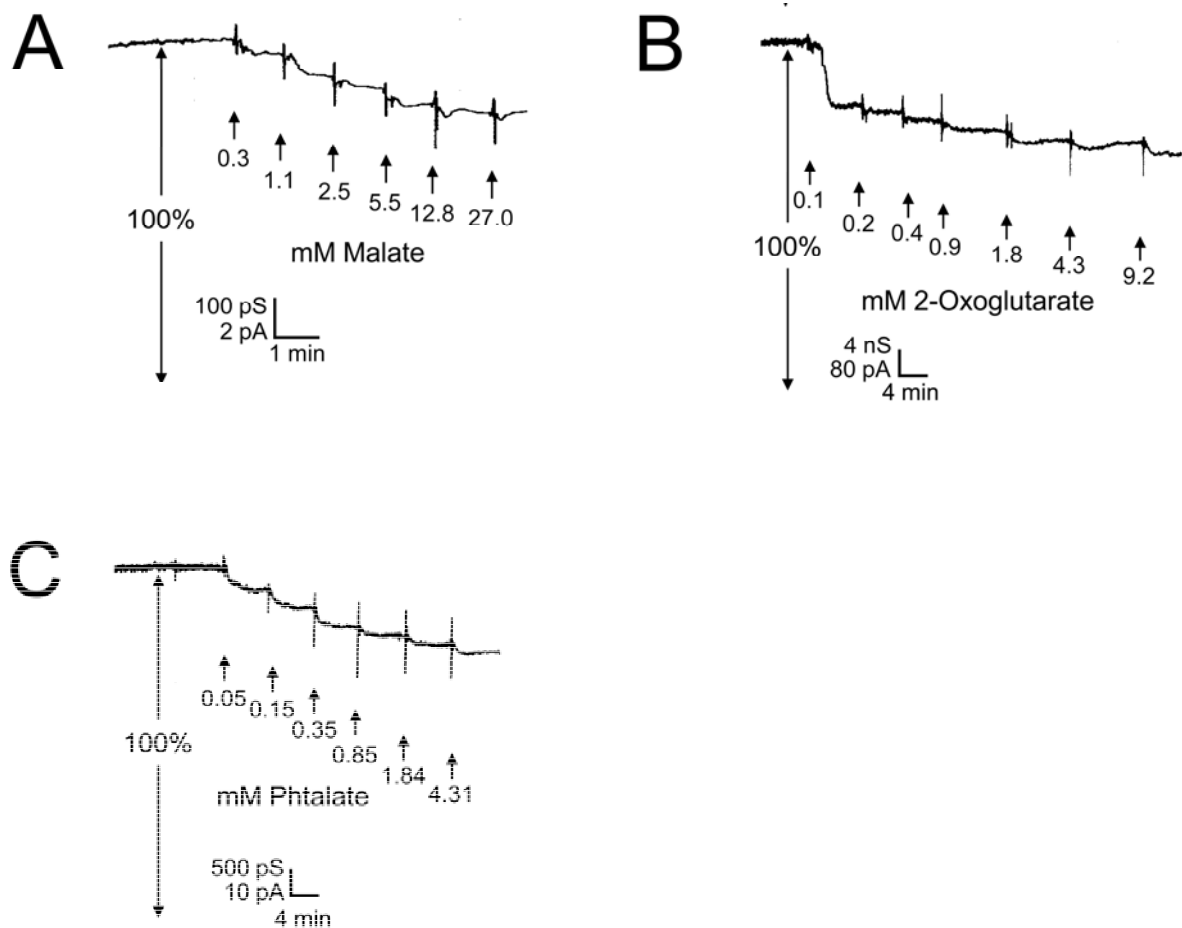
Figure 3.5. Titration of membrane conductance induced by DipA with malate (A), 2-oxoglutarate (B) and phthalate (C). The membrane was formed from diphytanoyl phosphatidylcholine/*n*-decane. The aqueous phase contained ~100 ng ml^{-1} DipA protein, 0.1 M KCl, 10 mM Tris-Cl, pH 7.5 and dicarboxylates at concentrations as indicated; temperature = 20°C; voltage = 20 mV.

3.4.8. Study of the binding affinity of different dicarboxylates to DipA

The titration experiments with DipA were analyzed in a similar way as used for the characterization of carbohydrate-binding channels of Gram-negative bacteria (Benz *et al.* 1986; Benz *et al.* 1987). The data of figure 3.5 and of similar experiments were analyzed using equation 3, which means that Lineweaver-Burk plots were performed as shown in figure 3.6. The straight lines in figure 3.6 correspond to stability constants, *K*, for malate 926 l/mol (K_s = 1.08 mM) (Fig. 3.6.A), for 2-oxoglutarate 20,298 l/mol (K_s = 0.05 mM) (Fig. 3.6.B) and for phthalate 5, 152 l/mol (K_s = 0.19 mM) (Fig. 3.6.C).
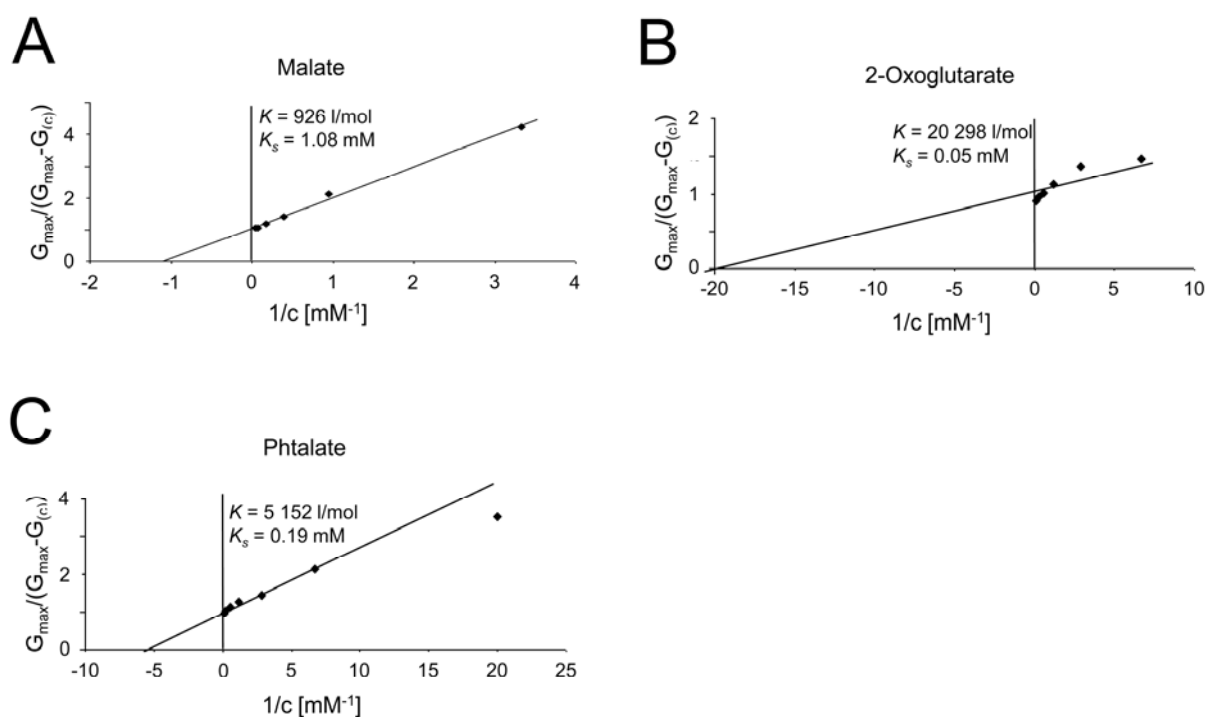
Figure 3.6. Lineweaver-Burk plots of the inhibition of membrane conductance by malate (A), 2-oxoglutarate (B) and phthalate (C). The data were taken from figure 3.5 and analyzed using equation 3.3. The straight lines correspond to stability constants *K*, for malate binding of 926 l/mol (K_s = 1.08 mM), for 2-oxoglutarate 20 298 l/mol (K_s = 0.05 mM) and for phthalate 5 152 l/mol (K_s = 0.19 mM).

Table 3.3 summarizes the results of all titration experiments. Binding of dicarboxylic anions yielded high stability constants for oxaloacetate (*K* = 19,881 ± 5,064 l/mol), succinate (*K* = 6,072 ± 2,205 l/mol), malate (*K* = 1,291 ± 516 l/mol) and 2-oxoglutarate (*K* = 3,517 ± 138 l/mol). This means that binding of the tested compounds to the DipA channel showed a significant

specificity. C_4-dicarboxylates with terminal groups next to one of the carboxylic groups showed considerable differences in their stability constants. The binding constant was maximal for oxaloacetate ($K = 19,881 \pm 5,064$ l/mol) which contains a polar oxo group next to one of the carboxylic groups. Succinate, a dicarboxylate without any side groups, showed a significantly lower binding affinity ($K = 6,072 \pm 2,205$ l/mol). For malate and aspartate, which contain a hydroxyl group and a positively charged amino group, respectively, next to one of the carboxyl acid groups, the stability constants were even smaller ($K = 1,291 \pm 516$ l/mol and $1,332 \pm 452$ l/mol, respectively).

The use of the unsaturated C_4-dicarboxylic anions fumarate and maleate yielded a stability constant for fumarate ($K = 416 \pm 38$ l/mol) that was remarkably low. The *trans* position of the carboxylic groups seemed to reduce significantly the affinity to the binding site of DipA. In contrast, the stability constant of maleate with a *cis* position of the carboxylic groups allowed maximal binding interaction resulting in a drastic increase of the stability constant ($K = 28,320 \pm 948$ l/mol). Experiments with 2-oxoglutarate demonstrated that an increase of the carbon chain length of the C_4 oxaloacetate to a C_5-dicarboxylic anion affected the binding affinity drastically and resulted in a decrease of the stability constant from $19,881 \pm 5,064$ l/mol (oxaloacetate) to $3,517 \pm 138$ l/mol (2-oxoglutarate). Phthalate, an aromatic C_8-dicarboxylic anion, exhibited a stability constant of $5,653 \pm 709$ l/mol indicating that binding of bigger compounds is still possible. Interestingly, the use of bigger dicarboxylates did not result in a higher maximum inhibition of channel conductance, which was also 25% for phthalate and in the same range of block than for the other dicarboxylates tested here.

Titration experiments with citrate revealed a high stability constant ($K = 13,044 \pm 2,661$ l/mol), pointing out that a third carboxylic group in the organic anions leads to further increase of the binding affinity compared to 2-oxoglutarate that lacks the third acid group and has a polar oxo group instead. For aspartate and glutamate, containing positively charged amino groups next to one of the carboxylic groups, the stability constants were relatively low ($1,332 \pm 452$ l/mol and $1,247 \pm 593$ l/mol, respectively), indicating a certain influence of the positively charged amino group on the binding affinity. For the monocarboxylic C_3-anion pyruvate the observed binding affinity was very low ($K = 473 \pm 34$ l/mol) and comparable to the value of fumarate ($K = 416 \pm 38$ l/mol).

Taking all results of the binding affinities together, the DipA channel showed rather high stability constants in the range from 416 l/mol to 28,320 l/mol for a wide spectrum of organic anions containing one, two or three carboxylic acid groups. The highest stability constants were measured for C_4-dicarboxylic anions such as maleate and oxaloacetate. Furthermore, these results

revealed distinctive binding specificities of DipA to certain substrates depending on the number of carboxylic acid groups and on side groups of the anions like oxo, hydroxyl or amino groups.

Table 3.3. Stability constants, *K*, for the binding of different organic anions to the DipA channel.

Organic anion	K	K_s	maximum inhibition of channel conductance	n
	(l/mol)	*(mM)*	*(%)*	
Dicarboxylic anions (C4)				
Oxaloacetate	19,881 ± 5,064	0.05 ± 0.01	31	5
Succinate	6,072 ± 2,205	0.18 ± 0.06	24	2
Malate	1,291 ± 516	0.87 ± 0.33	23	2
Stereospecific				
Fumarate	416 ± 38	2.42 ± 0.22	28	2
Maleate	28,320 ± 948	0.04 ± 0.00	23	2
Dicarboxylic anion (C5)				
2-Oxoglutarate	3,517 ± 138	0.35 ± 0.16	29	3
Aromatic dicarboxylic anion (C8)				
Phthalate	5,653 ± 709	0.18 ± 0.02	25	2
Tricarboxylic anion (C6)				
Citrate	13,044 ± 2,661	0.08 ± 0.02	24	2
Other substrates				
Aspartate	1,332 ± 452	0.82 ± 0.33	27	3
Glutamate	1,247 ± 593	0.90 ± 0.43	22	2
Pyruvate	473 ± 34	2.12 ± 0.15	20	2

The organic anions are important key metabolites of *Borrelia* species. The membranes were formed from diphytanoyl phosphatidylcholine dissolved in *n*-decane. The buffered aqueous phase (1 mM Tris-HCl pH 7.5) contained purified DipA in the nanogramm range and 0.1 M KCl; temperature = 20°C; voltage = 20 mV. The stability constants were derived from titration experiments similar to those shown in Fig. 3.3. The stability constant, *K*, is given as the mean of *n* experiments ± SD. K_s is the half-saturation constant.

3.5. Discussion

3.5.1. A comparison with relapsing fever *Borrelia* suggested the presence of an additional pore-forming component in the outer membrane of *B. burgdorferi*

A few outer membrane-spanning proteins of *B. burgdorferi* have been characterized so far, four have pore-forming activity and are therefore considered to be porins: These are P13, Oms28, whose possible function as a porin has recently been questioned (Mulay *et al.* 2007) and P66 (Skare *et al.* 1996; Skare *et al.* 1997; Nilsson *et al.* 2002; Östberg *et al.* 2002). In addition, BesC, a channel-tunnel part of efflux systems, has been identified (Bunikis *et al.* 2008). All these proteins form pores with a conductance in 1 M KCl that is larger than that observed for the pore-forming activity in this study. In recent studies, porin Oms38 with an obvious single-channel conductance in the pS-range was identified in relapsing fever *Borrelia* (Thein *et al.* 2008b). Searches within the genome of *B. burgdorferi* revealed a gene homologous to *oms38* called "hypothetical protein *bb0418*" with unknown function. These findings indicated that the OMF of *B. burgdorferi* could possibly contain further pore-forming components beside the described ones which have similar properties as Oms38 of relapsing fever *Borrelia*. In fact we identified in this study a pore-forming protein with a molecular mass of about 36 kDa in the outer membrane of *B. burgdorferi*. The porin was purified and termed DipA, for dicarboxylate-specific porin A, considering its possible function as a specific porin for carboxylates.

3.5.2. Identification of *B. burgdorferi* DipA

Using hydroxyapatite chromatography, DipA could be purified from the OMF of *B. burgdorferi* in the same way as the purification of the DipA homologue Oms38 of relapsing fever *Borrelia* (Thein *et al.* 2008b). SDS-PAGE analysis revealed a high degree of purity of DipA after protein precipitation and silver-staining of the gel. In addition to the identification using mass spectrometry, immunoblot analysis clearly confirmed that the 36 kDa band in the outer membrane of *B. burgdorferi* is the DipA protein responsible for the pore formation. This could further be demonstrated by block of its pore-forming ability by preincubation with antiserum against DipA. Presumably, the specific antiserum bound to DipA and blocked its reconstitution and thus its pore-forming capacity.

The 20 kDa protein band additionally visible on SDS-PAGE after purification across the hydroxyapatite column is definitely not responsible for pore-formation because fractions next to

that with pore-forming activity contained exclusively this 20 kDa band and did not exhibit any pore-forming activity. This band could clearly be identified by mass spectrometry as OspA and OspC precursors, well-studied outer surface proteins of *B. burgdorferi* (Bergström *et al.* 1989; Caporale *et al.* 1994; Ding *et al.* 2000). Thus, detailed molecular and structural analyses of these proteins supported the view that they are lipoproteins without any channel-forming ability.

3.5.3. Amino acid sequences of *B. burgdorferi*, *B. garinii* and *B. afzelii* DipA

Tryptic digestion followed by sequencing of purified DipA peptides allowed the identification of the corresponding gene within the genome of *B. burgdorferi*. Further searches revealed the genes of DipA homologues present in the related LD species *B. garinii* and *B. afzelii*. The deduced amino acid sequences of the three LD species' DipA share an identity of 88%, which means that the identities between the DipA homologues are very high, comparable with the high homology of other porins in these species (Bunikis *et al.* 1995; Noppa *et al.* 2001). From this point of view we assumed that structure and function of the DipA homologues are identical under *in vivo* conditions. Strikingly, *B. burgdorferi* DipA is also 57% identical with the porin Oms38 of the relapsing fever (RF) agent *B. duttonii* (Thein *et al.* 2008b). This high amino acid identity is in agreement with immunoblot results, which showed that DipA-specific antiserum reacted with analogous protein domains of DipA and Oms38 in OMFs of both LD and RF *Borrelia*. And in addition, similar biophysical characteristics (see below) of DipA and Oms38 underlined this finding on the amino acid level and suggested that these proteins are homologous.

DipA is located in the outer membrane meaning that this protein needs to contain an N-terminal signal peptide with a putative recognition sequence for the leader peptidase similar to those of other spirochetal outer membrane proteins (Cullen *et al.* 2004). The predicted signal peptide for *B. burgdorferi* DipA is 20 amino acids long and contains positive charges at the N-terminus, properties which are typical for borrelian signal peptides (Cullen *et al.* 2004). Further predictions indicated that the deduced sequences of *B. garinii* and *B. afzelii* DipA contain similar N-terminal extensions that are responsible for their transport into the periplasm as is known for other spirochetal porins (Cullen *et al.* 2004).

Computational analyses predicted putative β-sheet regions in the primary sequences of *B. burgdorferi*, *B. garinii* and *B. afzelii* DipA. The secondary structure predictions supported the idea that the proteins may form a β-barrel cylinder consisting of about 14 β-sheets similar as is known for most Gram-negative bacterial porins (Benz 1994b; Saier 2000; Delcour 2002; Charbit 2003).

3.5.4. Biophysical properties of DipA

The single-channel conductance of 50 pS differs clearly from the comparatively huge single-channel conductances of 600 pS (Skare *et al.* 1996), 3.5 nS (Östberg *et al.* 2002) and 9.6 nS (Skare *et al.* 1997) of the other *B. burgdorferi* porins and from the BesC channel tunnel (300 pS) (Bunikis *et al.* 2008). Anyway, the DipA pore showed a small single-channel conductance comparable to the ones of the substrate-specific *E. coli* channels Tsx (10 pS) (Maier *et al.* 1988) and LamB (160 pS) (Benz *et al.* 1986). The reconstitution and biophysical properties of DipA were similar to the ones observed for the homologue Oms38 (Thein *et al.* 2008b). Congruently with Oms38, during some single-channel measurements initial sharp peaks and superpositions of the stable 50 pS state of the pore (see Fig. 3.4) have been observed, which could be interpreted as additional transient states of the DipA channels. An anion selectivity of the DipA channels was indicated by single-channel measurements in LiCl and KCH_3COO and could be confirmed by zero-current potential measurements. Interestingly, the selectivity for anions could be reduced by the addition of 1 mM oxaloacetate to the KCl solution, which presumably bound to the channel and resulted in a partial shielding of exposed charges. This result suggested the possibility that DipA could contain a binding site for dicarboxylates.

3.5.5. Specificity of DipA for dicarboxylates

The growth of *Borrelia* depends strictly on nutrients provided by their hosts as demonstrated by the fastidious growth requirements of serum-supplemented mammalian tissue-culture medium for *in vitro* cultivation (Barbour 1984). In addition, it is known that *B. burgdorferi* lacks genes encoding proteins of the tricarboxylic acid cycle or oxidative phosphorylation and for *de novo* synthesis of amino acids and nucleotides (Fraser *et al.* 1997). This implicates that essential compounds or precursor of these compounds have to be imported into the cell.

Dicarboxylates, such as malate, succinate, oxaloacetate and 2-oxoglutarate, are major intermediates of the tricarboxylic acid cycle and mainly used for synthesis of amino acids. For example, oxaloacetate and 2-oxoglutarate are important substrates for the biosynthesis of asparagine, aspartic acid and glutamic acid, respectively, which are essential proteinogenic amino acids. In addition, C_4-dicarboxylates other than succinate can be metabolized due to the lack of a functional tricarboxylic acid cycle in anaerobic energy metabolism of most bacteria (Janausch *et al.* 2002). Taking these points into consideration, a potential dependence of the growth of *Borrelia* on this group of chemicals is likely. Consequently DipA plays an important role in the uptake of

dicarboxylates across the outer membrane. It is noteworthy that DipA is not the first identified membrane channel that is specific for dicarboxylates. Previous studies revealed that the channel of spinach leaf peroxisomes is specific for this group of chemicals (Reumann *et al.* 1998). Interestingly, in bacteria, the PorB porin of *Chlamydia trachomatis* is the first identified pore-forming outer membrane protein being specific for dicarboxylates. It plays a crucial role in feeding the chlamydial tricarboxylic acid cycle and providing carbon and energy production intermediates (Kubo *et al.* 2001).

Porins with a similar small single-channel conductance as DipA often contain specific substrate-binding sites (Ferenci *et al.* 1980; Benz *et al.* 1986; Hancock *et al.* 1986; Benz *et al.* 1988b), which suggested that DipA could possibly be a substrate-specific porin of *B. burgdorferi*. This assumption was tested and the substrate-specificity could be demonstrated by multi-channel experiments which revealed that DipA has a high affinity for dicarboxylates. Despite the observed high affinity for these organic acids, it was not possible to measure the permeability of DipA for these metabolites. Anyway, in analogy to other bacterial specific porins, it is likely that the DipA binding site with its high affinity for dicarboxylic anions increases the permeability of the channel for these metabolites as has been demonstrated previously: the presence of a binding site leads to an accelerated transport of carbohydrate through LamB and of phosphate transport through OprP, especially at very low substrate concentrations (Benz *et al.* 1987; Benz 1994b). Thus, the permeability of a substrate-specific porin can surpass that of a general diffusion pore by orders of magnitude in spite of its smaller cross-section (Benz *et al.* 1987).

The detailed study of the DipA specificity revealed that the stability constant depends strongly on the specific structure of the organic anion showing a maximum for C_4-dicarboxylates. Even if the observed stability constants are low compared to those of other substrate-specific bacterial porins such as LamB or Tsx of *E. coli* (Benz *et al.* 1987; Benz *et al.* 1988b) they are in the same range as values observed for the binding of dicarboxylates to the channel of spinach leaf peroxisomes (Reumann *et al.* 1998) and higher than stability constants of specific porins for nicotinamide adenosine dinucleotides (Andersen *et al.* 2003). Even under saturated substrate concentrations the channel conductance of DipA could be maximally blocked by 30%, which means that there are still ions able to pass the pore as known from other porins (Andersen *et al.* 2003). Even phthalate, which is much bigger than the other tested chemicals, could not lead to an enhanced block of the channel conductance. This could indicate that the binding site is possibly not fully located in the interior of the channel but at the entrance or at a surface-exposed loop. The binding site could lead to increased concentrations of dicarboxylates in the close proximity of the pore and therefore to an accelerated uptake. Anyway, our data suggested together with the

observed anion selectivity that the DipA binding site consists of positively charged groups, which could be located even in a binding pocket of the channel.

Taking these findings together, a porin could be identified in the outer membrane of *B. burgdorferi*, designated as DipA. DipA does not form general diffusion pores, but a small channel whose permeability properties are determined by charge effect at a permeability filter. Thus, DipA is the first identified *Borrelia* porin exhibiting a substrate specificity and therefore has presumably a well-defined function. Furthermore, this study supplements the knowledge of the outer membrane protein composition of LD species. This could lead to a basis for a successful drug design, more information concerning the physiology of the spirochetes and discover a surface-exposed protein that could function as a potential vaccine candidate.

Chapter 4

THE P66 PORIN IS PRESENT IN BOTH
LYME DISEASE AND RELAPSING FEVER SPIROCHETES:
A COMPARISON OF THE BIOPHYSICAL PROPERTIES
OF SIX P66 SPECIES

4.1. Summary

The genus *Borrelia* is the cause of the two human diseases Lyme disease (LD) and relapsing fever (RF). Both LD and RF *Borrelia* species are obligate parasites and dependent on nutrients provided by their hosts. The first step of nutrient availability is accomplished by water-filled channels, so called-porins, across the outer membrane of these bacteria. So far, the knowledge of the porin composition in the outer membrane is divergent comparing the agents of the two borrelian-caused diseases. Only one porin is described in relapsing fever species to date, whereas four porins are known to be present in Lyme disease agents. Thereof, the *Borrelia burgdorferi* outer membrane protein P66 is a well investigated outer membrane channel with the additional function as an adhesin. After reconstitution in artificial membranes it is able to form pores with an extremely high single channel conductance of 9.6 nS in 1 M KCl. The aim of this study was to explore whether the P66 porin is expressed and similarly capable of pore formation in both Lyme disease and relapsing fever *Borrelia*. Therefore, the Lyme disease species *B. burgdorferi*, *B. afzelii*, *B. garinii* and the relapsing fever species *B. duttonii*, *B. recurrentis* and *B. hermsii* were investigated for the presence of a P66 homologue. A search in current published relapsing fever genomes, comprising the ones of *B. duttonii*, *B. recurrentis* and *B. hermsii*, indicated that they all contained P66 homologues. The deduced P66 amino acid sequences of the Lyme disease and relapsing fever agents were compared and revealed an inter-species amino acid identity of 41%. The P66 homologues of the six species were purified to homogeneity by anion exchange chromatography and their pore-forming capabilities and biophysical properties were compared by using the black lipid bilayer assay. Except of the P66 homologue of *B. hermsii* all purified proteins were highly active in artificial membranes and formed pores with a very high single-channel conductance between 9 and 11 nS in 1 M KCl. The homologous proteins did not show any selectivity between cations and anions and exhibited some voltage-dependent closure.

4.2. Introduction

The outer membrane of Gram-negative bacteria plays an important role in the physiology of these organisms. All nutrients or antibiotics either hydrophilic or hydrophobic have to cross this permeability barrier. Only hydrophilic solutes smaller than the exclusion limit specific for a given Gram-negative bacteria can pass the outer membrane. This means that this barrier has special sieving properties. Bacteria with limited biosynthetic capacity, such as *Borrelia* species are dependent on the uptake of even more nutrients across their cell envelope (Fraser *et al.* 1997). Uptake of nutrients across the outer membranes of Gram-negative bacteria occurs by few membrane-spanning, pore-forming proteins, so-called porins. Most porins form wide water-filled channels in the outer membrane which sort solutes of different structures mostly according to their molecular weights. Other porins are solute specific and contain binding sites for classes of solutes (Benz *et al.* 1988a; Benz 1994b; Nikaido 2003; Benz *et al.* 2004). Within the *Borrelia* genus, the knowledge of the porin composition is divergent comparing the agents of the two borrelian-caused diseases, Lyme disease (LD) species and relapsing fever (RF) species. In terms of porins, the LD species *Borrelia burgdorferi* is well-studied, while the porin content of RF agents is only poorly understood.

To date, four porins are primarily identified in *B. burgdorferi*: (1) P13 (Nilsson *et al.* 2002; Östberg *et al.* 2002), which is not well understood in structure and function, (2) Oms28 (Skare *et al.* 1996), which was recently questioned to have porin-like properties (Mulay *et al.* 2007), (3) DipA, which is specific for dicarboxylates (Thein *et al.* 2008c) and (4) P66, which is the object of this study. P66 is a well-studied pore-forming outer membrane protein present in Lyme disease *Borrelia* (Bunikis *et al.* 1995; Skare *et al.* 1997; Coburn *et al.* 1999; Defoe *et al.* 2001; Coburn *et al.* 2003; Pinne *et al.* 2007). *B. burgdorferi* P66 was shown to form pores in artificial membranes with an unusual extremely high single channel conductance of 9.6 nS in 1 M KCl (Skare *et al.* 1997). Furthermore, P66 acts as an adhesin which can bind to β3-integrin (Coburn *et al.* 1999; Defoe *et al.* 2001; Coburn *et al.* 2003). In addition, the study of P66 is also of special interest because of the presence of surface-exposed domains (Bunikis *et al.* 1995; Bunikis *et al.* 1996) exhibiting a certain immunogenic potential (Barbour *et al.* 2008), a property which could be of interest in the search of vaccination candidates against European LD *Borrelia*.

In contrast to LD species, the porin knowledge in terms of relapsing fever *Borrelia* is rather limited. There are indications of several pore-forming activities in outer membrane preparations of RF spirochetes (Shang *et al.* 1998; Thein *et al.* 2008b) and genes with a high homology to *B. burgdorferi p13*, *oms28* and *p66* can be found in the published genomes of the RF

agents *B. duttonii*, *B. recurrentis* and *B. hermsii*. Nevertheless, only one porin is described in RF species in detail. Oms38 forms channels in artificial lipid bilayers with a small single channel conductance of 80 pS in 1 M KCl (Thein *et al.* 2008b).

The aim of this work was to show whether bifunctional P66 porins are present in both LD and RF species *Borrelia* and to study if these porins were similarly capable of pore formation in model lipid membranes. Therefore, P66 homologues of six different species were analyzed. The three LD species *B. burgdorferi*, *B. garinii* and *B. afzelii*, chosen to be included in this work, are the primary agents of the disease in Europe (Wilske 2003). Three RF species were also selected for this study and represent the worldwide distribution of the agents of this disease: *B. duttonii* and *B. hermsii* are mainly responsible for the tick-borne RF in sub-Saharan Africa and North America, respectively, (Goubau 1984; Dworkin *et al.* 2002; Schwan *et al.* 2007) and *B. recurrentis* is the main agent of the louse-borne RF (Bryceson *et al.* 1970). P66 homologues of these species were purified by anion exchange chromatography to homogeneity and their pore-forming capabilities and properties were compared and investigated in detail by using the black lipid bilayer assay.

4.3. Material and Methods

4.3.1. Bacterial strains and growth conditions

The strains used in this study were *B. burgdorferi* B31, *B. afzelii* pKo, *B. garinii* PBi, *B. duttonii* 1120K3, *B. recurrentis* A1 and *B. hermsii* HS1. Bacteria were grown in Barbour-Stoenner-Kelly-II (BSKII) medium (Barbour 1984) supplemented with 10% rabbit serum and 1.4% gelatine at 37°C until cell density reached approximately 10^7-10^8 cells ml^{-1} followed by harvesting of the bacteria by centrifugation.

4.3.2. Isolation of outer membrane proteins and purification of the P66 homologues

Outer membrane fractions (OMFs) of the mentioned *Borrelia* strains were prepared as described elsewhere (Magnarelli *et al.* 1989). To purify native P66, the OMFs were solubilized in 2% (v/v) lauryl dimethyl amine oxide (LDAO; Sigma) and purified by fast performance liquid chromatography (FPLC) on a MonoQ column (GE Healthcare). The column was washed with 15 ml of 0.4% (v/v) LDAO buffered in 10 mM Tris HCl, pH 8.0. Proteins bound to the column were eluted using the above mentioned washing buffer supplemented with a 0 – 1 M linear NaCl gradient. Pure P66 was eluted from the column at a NaCl concentration of about 190 mM.

4.3.3. SDS-PAGE and Immunoblotting

Sodium dodecyl sulfate-polyacrylamide gel electrophoresis (SDS-PAGE) was performed according to the Laemmli gel system (Laemmli 1970). 100 μl of FPLC fractions were precipitated by the protocol of Wessel and Flügge (Wessel *et al.* 1984). Proteins were separated by 12% SDS-PAGE under denatured conditions (boiled for 10 min in 4x SDS sample buffer before loading the gel) by using a Bio-Rad electrophoresis system. The gels were silver-stained (Blum *et al.* 1987). For immunoblots, a tank blot system (Amersham Biosciences) was used as previously described (Towbin *et al.* 1979). Bound antibodies were detected using peroxidase-conjugated anti-rabbit antibodies (DAKO A/S) and enhanced chemiluminescence reagents according to the manufacturer's instructions (Amersham Biosciences). The production and use of polyclonal rabbit serum against *B. burgdorferi* P66 has been described previously (Sadziene *et al.* 1992; Bunikis *et al.* 1995).

4.3.4. Planar lipid bilayer assays

The methods used for black lipid bilayer experiments have been described previously (Benz *et al.* 1978). The instrumentation consisted of a Teflon chamber with two compartments separated by a thin wall and connected by a small circular hole with an area of 0.4 mm^2. The membranes were formed from a 1% (w/v) solution of diphytanoyl phosphatidylcholine (PC) (Avanti Polar Lipids, Alabaster, AL) in *n*-decane. The porin-containing protein fractions were 1:1 diluted in 1% Genapol (Roth) and added to the aqueous phase after the membrane had turned black. The membrane current was measured with a pair of Ag/AgCl electrodes with salt bridges switched in series with a voltage source and a highly sensitive current amplifier (Keithley 427). The temperature was kept at 20°C throughout.

Zero-current membrane potential measurements were performed by establishing a salt gradient across membranes containing approximately 100 pore-forming proteins as it has been described earlier (Benz *et al.* 1979; Ludwig *et al.* 1986). The zero-current membrane potentials were measured with a high impedance electrometer (Keithley 617). Voltage-dependence of the porin channels was checked following the method described elsewhere (Mirzabekov *et al.* 1996), using membrane potentials as high as -100 to +100 mV.

4.4. Results

4.4.1. *In silico* comparison of LD and RF P66

Searches in published genomes of LD and RF *Borrelia* revealed the presence of P66 homologues in all species. To obtain more information about the homology of P66 sequences of different species, P66 sequences of six selected LD and RF *Borrelia* were compared. The deduced amino acid sequences from P66 of the Lyme disease species *B. burgdorferi* B31, *B. afzelii* pKo, *B. garinii* PBi and the relapsing fever species *B. duttonii* Ly, *B. recurrentis* A1 and *B. hermsii* HS1 are presented in figure 4.1 (GenBank accession numbers NP_212737, YP_710051, YP_073044, NC_011229, NC_011244 and AAC38306, respectively). The six sequences are rather consistent in their amino acid number ranging between 598 (*B. h.*) and 621 (*B. g.*) and show partially highly conserved domains. Comparison of the amino acid sequences of P66 from the different LD and RF *Borrelia* revealed 41% inter-species identity. While the three LD species' P66 share a sequence identity of 90%, a fact that was already shown by Bunikis *et al.* (Bunikis *et al.* 1995), P66 of the three relapsing fever strains are identical by 67% of their amino acid sequence. Strikingly, the P66 sequence identity of *B. duttonii* and *B. recurrentis* is outstanding high, reaching an identity score of 98%.

Computational analysis (Bendtsen *et al.* 2004) predicted a potential leader peptidase I cleavage site between amino acid residues at position 21 and 22 of the full length sequence (marked by an arrowhead in figure 4.1). This prediction is congruent with previous indications of the cleavage site for *B. burgdorferi*, *B. afzelii* and *B. garinii* P66 (Bunikis *et al.* 1995) and studies about the N-terminal signal peptide of *B. burgdorferi* porins (Cullen *et al.* 2004). Thus, the first 21 amino acids of all analyzed species' P66 seem to serve as signal peptides and are responsible for the transport across the cytoplasmic membrane.

To get an idea of a possible secondary and tertiary structure of P66, further computational predictions (Gromiha *et al.* 2004) were used and congruent secondary structure predictions in the P66 sequences of all six species were compared. The predictions suggested putative β-sheet regions (red framed in figure 4.1) within all six species' P66 sequences and allowed the concept of β –barrel proteins with 20 to 22 transmembrane β-sheets which could form a β-barrel cylinder as it is known from other well-studied porins (Saier 2000; Delcour 2002; Charbit 2003).
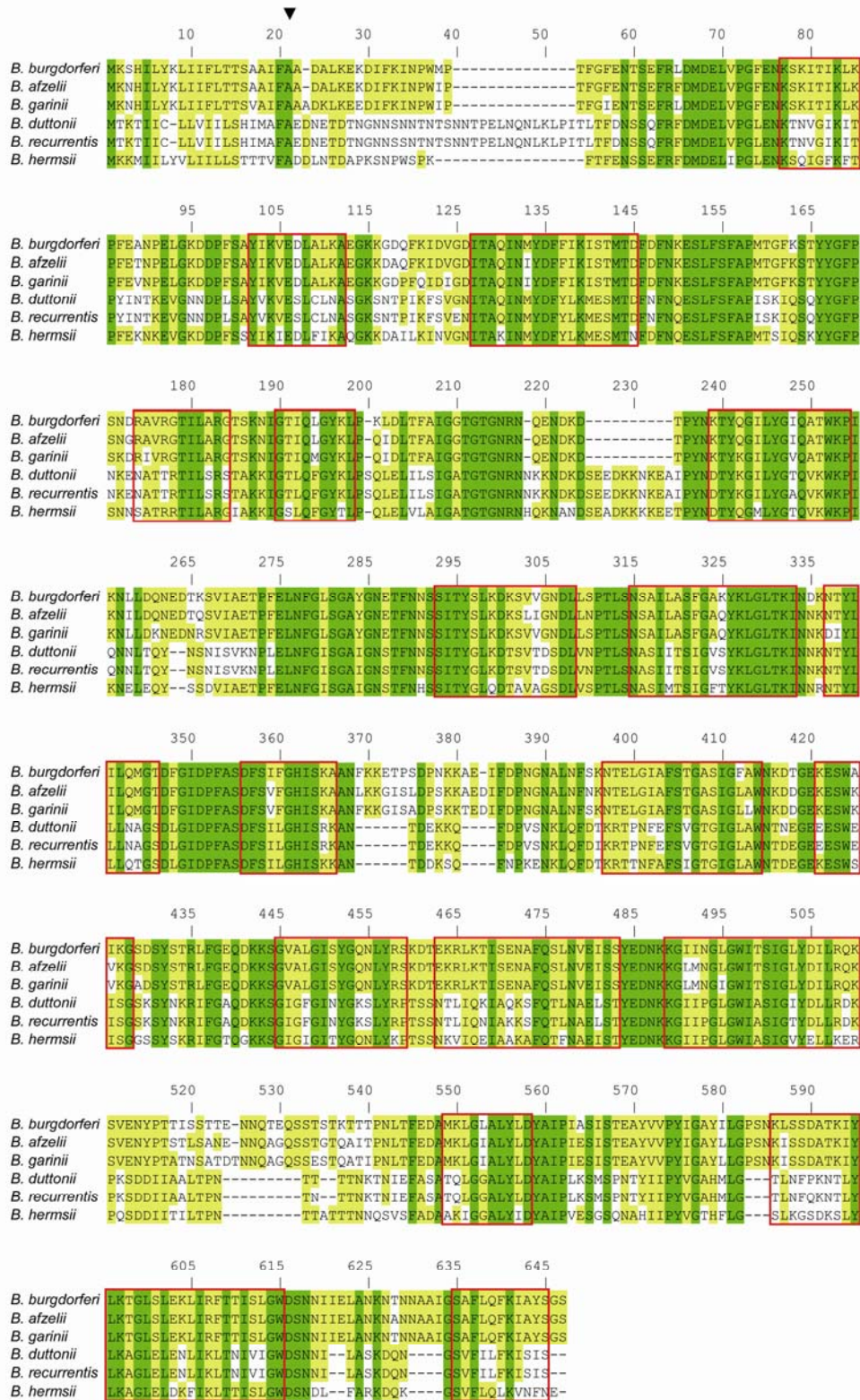
Figure 4.1. Amino acid sequences of P66 from Lyme disease agents (*B. burgdorferi, B. afzelii, B. garinii*) and relapsing fever agents (*B. duttonii, B. recurrentis, B. hermsii*). Amino acids identical in all six strains are shaded in green, identical amino acids in at least three species are highlighted in yellow. The sequences of all six species' P66 share an identity of 41%. P66 of the LD species are identical in 90% and the amino acid sequences of the RF species are 67% identical. The putative N-terminal cleavage site of all six species' P66 is marked by an arrowhead (Bendtsen *et al.* 2004). Predicted β-sheet transmembrane regions (Gromiha *et al.* 2004) congruent in all six species are framed in red and allow the conception of β-barrel protein consisting of 20-22 β-sheets.

4.4.2. Purification and identification of the P66 homologues in LD and RF species

For the purification of P66 homologues of the different LD and RF species approximately 100 ng of the corresponding outer membrane fraction (OMF) were dissolved in 1 ml 2% LDAO and applied to an anion exchange chromatography as it has been successfully performed previously for the purification of *B. burgdorferi* P66 (Skare *et al.* 1997; Pinne *et al.* 2007). At a concentration of around 190 mM NaCl in the buffer, pure P66 was eluted from the column. This purification protocol was also used to purify P66 homologues from OMFs of the LD species *B. burgdorferi*, *B. afzelii*, *B. garinii* and the RF species *B. duttonii*, *B. recurrentis* and *B. hermsii*. Thereafter, the presence of putative P66 homologues was checked by 12% SDS-PAGE. The gels clearly demonstrated that the proteins eluted from the column were purified to homogeneity and exhibited a molecular mass of 66 kDa for all LD and RF strains (Fig. 4.2).
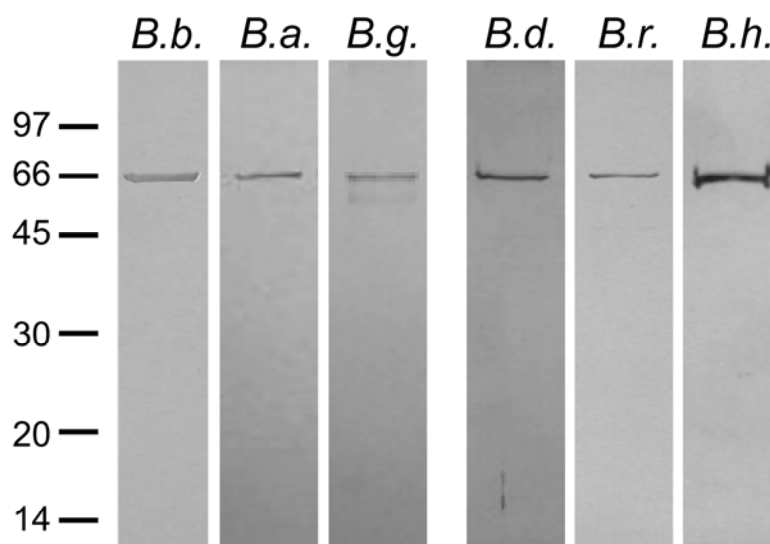
Figure 4.2. SDS-PAGE analysis of purified P66 of *B. burgdorferi* (*B. b.*), *B. afzelii* (*B. a.*), *B. garinii* (*B. g.*), *B. duttonii* (*B. d.*), *B. recurrentis* (*B. r.*) and *B. hermsii* (*B. h.*). 100 μl anion exchange chromatography-fractions containing the purified P66 homologues were separated by 12% SDS-PAGE and silver-stained. The positions of molecular mass standards in kDa are shown at the left.

Western blots with polyserum against *B. burgdorferi* P66 suggested clearly that the fractions that were eluted at an ionic strength of 190 mM NaCl from the column contained proteins homologous to P66 (Fig. 4.3). This means that the 66 kDa proteins derived from *B. burgdorferi*, *B. afzelii*, *B. garinii* and the RF species *B. hermsii* were homologues of P66. Interestingly, the polyserum did not cross-react with the 66 kDa proteins purified from the outer membranes of the RF species *B. duttonii* and *B. recurrentis*, even when the Western blots were performed with high concentrations of OMFs to exclude a protein concentration-dependent loss of the detection

signal by purification (data not shown). This means presumably that the P66 proteins of these two species did not contain epitopes which are sufficient homologous to *B. burgdorferi* P66 to enable a binding of the *B. burgdorferi*-derived polyserum. However, following reconstitution of the purified proteins in artificial membranes and studying their pore-forming activity confirmed the assumption that the purified proteins of these two RF species are P66 homologues because it was similar to that described previously for *B. burgdorferi* P66 (Skare *et al.* 1997) (see below).
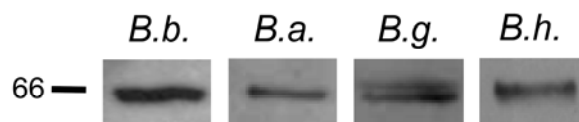
Figure 4.3. Detection of P66 in Lyme disease and relapsing fever spirochetes. Immunoblot analysis with polyserum against *B. burgdorferi* P66 resulted in clear signals of P66 and its homologues in the outer membrane fractions of the Lyme disease agents *B. burgdorferi* (*B. b.*), *B. afzelii* (*B. a.*), *B. garinii* (*B. g.*) and the relapsing fever agent *B. hermsii* (*B. h.*). Immunoblots with OMFs of *B. duttonii* and *B. recurrentis* did not exhibit any signal corresponding to putative P66 homologues (data not shown). The position of molecular mass standard in kDa is shown at the left.

4.4.3. Single-channel analyses of P66 homologues

Previous studies demonstrated that *B. burgdorferi* P66 forms pores with an atypical extremely high single-channel conductance of 9.6 nS in 1 M KCl (Skare *et al.* 1997). To compare biophysical properties of P66 from LD and RF *Borrelia* we performed a detailed characterization of the P66 homologues in black lipid bilayer membranes. After the membranes were in the black state, P66 was added in low concentration (approx. 1 ng/ml) to one or both sides of the membranes. Subsequently, the membrane current increased in a step-like manner caused by reconstitution of single P66 molecules. Figure 4.4 shows a typical single-channel recording in the presence of one LD (*B. burgdorferi*) and one RF (*B. duttonii*) P66, respectively. P66 from *B. burgdorferi*, *B. afzelii*, *B. garinii*, *B. duttonii* and *B. recurrentis* were similarly highly active in the lipid bilayer assay and well defined conductance steps could also be resolved in these cases after reconstitution of P66 proteins in black lipid bilayers (data not shown). Interestingly, the P66 homologue purified from *B. hermsii* OMF did not show any pore-forming activity in the black lipid bilayer assay. Three different samples isolated independently from different OMFs of *B. hermsii* were used to purify the P66 homologue, but none of the obtained fractions of pure protein showed pore-forming activity. Similarly, no pore-forming activity was observed when OMF from *B. hermsii* treated with detergents was directly added to the aqueous phase bathing black lipid bilayers.
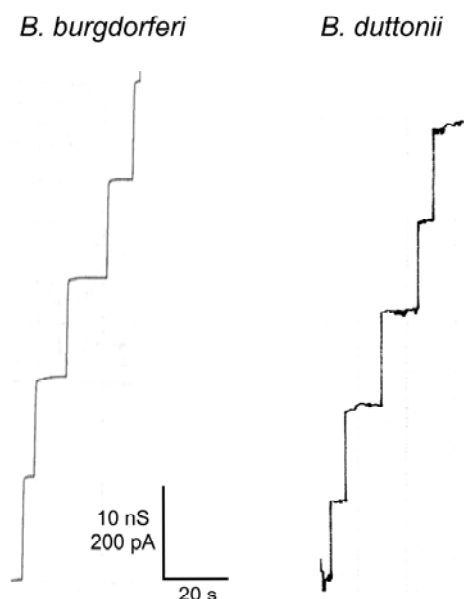
Figure 4.4. Pore-forming activity associated with purified P66 from one LD agent, *B. burgdorferi*, and one RF agent, *B. duttonii*, representatively. Single-channel conductance steps in a diphytanoyl phosphatidylcholine/*n*-decane membrane illustrated representatively for P66 of one LD species, *B. burgdorferi*, and one RF species, *B. duttonii*. Highly diluted, purified P66 at a concentration of about 10 ng ml^{-1} was added to the membrane bathed in 1 M KCl. The applied voltage was 20 mV and the temperature was 20°C throughout. Similar well-defined conductance steps were observed during the reconstitution of P66 from *B. afzelii*, *B. garinii* and *B. recurrentis* in black lipid bilayer membranes.

The single-channel conductance of the P66 homologues with pore-forming capability was studied as a function of different KCl concentrations and different electrolytes. Statistical evaluations of at least 100 reconstituted channels per measurement were used to calculate the average single-channel conductance. The histograms of the current fluctuations of the experiments in 1 M KCl are given in figure 4.5. Similarly, the results of all single-channel measurements are summarized in table 4.1. The single channel data clearly demonstrate that the single-channel conductances for P66 of LD and RF *Borrelia* in 1 M KCl were in the range between 9 and 11 nS. Further measurements in different KCl concentrations from 0.1 to 3 M revealed that the single channel conductance was approximately a linear function of the electrolyte concentration (Table 4.1). This indicates that the different P66 channels did not contain a binding site for ions.
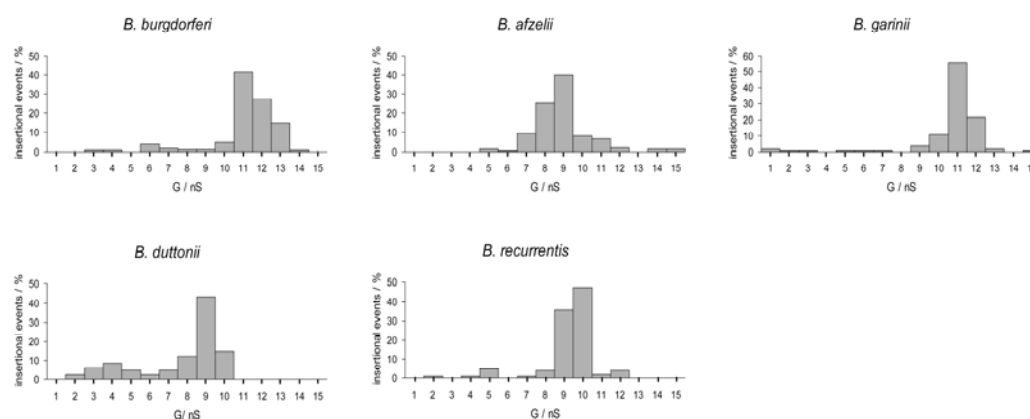
Figure 4.5. Histograms of individual single-channel events observed for purified P66 of the LD species *B. burgdorferi*, *B. afzelii*, *B. garinii* and the RF species *B. duttonii* and *B. recurrentis*. For each histogram a total number of at least 100 insertional events of the respective P66 homologues into a diphytanoyl phosphatidylcholine/*n*-decane membrane were evaluated. The average single-channel conductances (*G*) were of values in the range between 9 and 11 nS. The aqueous phase contained 1 M KCl; the applied voltage was 20 mV and the temperature was 20°C throughout.

Additional information about the ion selectivity of the pores was obtained from single-channel experiments with salts containing ions other than K^+ and Cl^- such as LiCl and KCH_3COO. The results are summarized in table 4.1 and suggest that cations and anions from different salts influenced the single-channel conductance indicating that the P66 channels are wide and water-filled without any obvious preference for one sort of ions, which means that all P66 homologues are more or less non-selective. Similar results were obtained for all P66 homologues studied here. The data showed that cations and anions had a certain permeability through the P66 channels that followed approximately their mobility sequence in the aqueous phase.

Table 4.1. Average single-channel conductances of P66 of *B. burgdorferi* (*B. b.*), *B. afzelii* (*B. a.*), *B. garinii* (*B. g.*), *B. duttonii* (*B.d.*) and *B. recurrentis* (*B. r.*) in different electrolyte solutions. *B. hermsii* (*B. h.*) P66 did not exhibit any pore-forming activity in black lipid bilayers.

		B. b.	*B. a.*	*B. g.*	*B. d.*	*B. r.*	*B. h.*
Electrolyte	Concentration (*M*)			*G* (*nS*)			
KCl	0.1	1.3	1.3	1.5	0.8	1.25	*n.a.*
	0.3	3.5	3.5	3.5	2.25	2.75	*n.a.*
	1	11.0	9.0	11.0	9.0	9.5	*n.a.*
	3	30	33	35	20	25	*n.a.*
LiCl	1	7.3	7.0	8.0	5.0	6.0	*n.a.*
KCH_3COO (pH 7)	1	6.7	6.5	6.5	4.0	5.0	*n.a.*

The membranes were formed from diphytanoyl phosphatidylcholine dissolved in *n*-decane. The single-channel conductance was measured in unbuffered electrolyte solutions (approx. pH 6) unless otherwise indicated at 20 mV applied voltage and 20°C. The average single-channel conductance, *G*, was calculated from at least 100 single events of the respective P66. *n.a.* means not active in the black lipid bilayer.

4.4.4. Selectivity measurements

Zero-current membrane potential measurements were performed to quantify the selectivity of the P66 in KCl, LiCl and KCH_3COO. After reconstitution of 100 to 1,000 channels into PC membranes, the initial salt concentration of 100 mM was raised fivefold on one side of the membrane, and the zero-current potential was measured 5 minutes after the increase in salt gradient across the membrane. For KCl and LiCl, the more diluted side of the membrane

(100 mM) always became negative, whereas slightly positive membrane potentials were observed for KCH_3COO (data not shown). Analysis of the membrane potential using the Goldman-Hodgin-Katz equation (Benz *et al.* 1979) confirmed the assumption that the P66 channels are permeable for both anions and cations, because the calculated values of the permeability ratio of cations over anions (P_c/P_a) in KCl were in the range between 0.8 and 1.0. The P_c/P_a ratios (mean of three individual measurements) of all P66 homologues are summarized in table 4.2. The results of measurements in LiCl and KCH_3COO confirmed that the selectivity of P66 channels was dependent on the mobility of the ions in the aqueous phase. Thus, replacement of K^+ by the less mobile Li^+ resulted in P_c/P_a values in the range between 0.5 and 0.8, while the replacement of Cl^- by the less mobile CH_3COO^- resulted in P_c/P_a values in the range between 1.1 and 1.5 (Table 4.2). The selectivity was highly consistent for all P66 homologues measured in this study. It furthermore resembled previous results obtained from *B. burgdorferi* P66, which also suggested that this channel was also non-selective for ions used here and in the previous study (Skare *et al.* 1997).

Table 4.2. Permeability ratios P_c/P_a of diphytanoyl phosphatidylcholine/*n*-decane membranes in the presence of respective P66 homologues measured for a five-fold concentration gradient of different electrolytes.

	B. b.	*B. a.*	*B. g.*	*B. d.*	*B. r.*
Electrolyte	Permeability ratios P_c/P_a				
KCl	0.8	1.0	0.8	0.9	0.9
LiCl	0.5	0.7	0.5	0.6	0.8
KCH_3COO (pH 7)	1.5	1.2	1.4	1.1	1.2

The permeability ratios P_c/P_a were calculated using the Goldman-Hodgin-Katz equation (Benz *et al.* 1979) from at least three individual experiments. Therefore, the difference between the potential at the diluted side (100 mM) and the potential at the concentrated side (500 mM) was defined. The aqueous electrolyte solutions were unbuffered (approx. pH 6) unless otherwise indicated. The temperature was 20°C throughout.

4.4.5. Voltage-dependence

Previous studies demonstrated a certain voltage-dependence for *B. burgdorferi* P66 (Skare *et al.* 1997). To investigate if the P66 homologues of all LD and RF *Borrelia* species used in this study exhibited also voltage-dependent closure, appropriate multi-channel experiments were performed. Protein was added to both sides of the membrane and after incorporation of at least

100 pores into the membrane, different potentials were applied to the membrane, beginning with +20 mV followed by -20 mV. The experiments were performed with potentials ranging from -100 to +100 mV. For both positive and negative potentials applied to the membrane the current decreased in an exponential manner. The results indicated a fairly symmetric response of the P66 homologues to the applied voltages. The experiments were analyzed in the following way. The membrane conductance (G) as a function of voltage, V_m, was measured as soon as the closing of channels reached an equilibrium, i.e. after the exponential decay of the membrane current following the voltage step V_m. G was divided by the initial value of the conductance G_0 (which was approximately a linear function of the voltage) obtained immediately after the turning-on of the voltage.
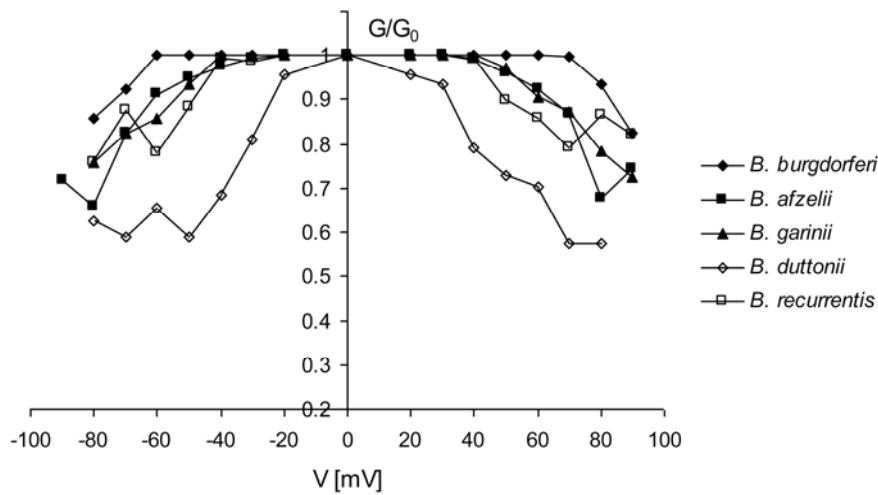
Figure 4.6. Voltage dependence of P66 homologues of different LD and RF species. The ratio of the conductance, G, at an applied voltage, V, divided by the initial value of the conductance G_0, immediately after the turning-on of the voltage. Highly diluted, purified P66 at a concentration of about 10 ng ml^{-1} was added to diphytanoyl phosphatidylcholine/n-decane membranes and after reconstitution of approximately 100 pores the different potentials were applied. The measurements were highly reproducible and the values in the diagram represent the mean of three measurements per species. The aqueous phase contained 1 M KCl; the temperature was 20°C throughout.

The data of P66 homologues of all investigated *Borrelia* species are illustrated in figure 4.6 and corresponded to a symmetric voltage-dependence of the channels (mean of three measurements per species). The measurements were highly reproducible and demonstrated that all tested P66 proteins showed significant conductance decreases beginning at a certain applied voltage. Interestingly, the current-voltage relationships showed some species-specific differences. For P66 of *B. afzelii*, *B. garinii* and *B. recurrentis*, the voltage-dependent closure started at potentials as high as +/- 40 mV and the conductance decreased by approximately 30% at applied potentials of +/- 80 mV and higher. *B. burgdorferi* P66 started to show voltage-dependent closure at potentials as

high as + 70 and -60 mV reaching a maximal conductance decrease by approximately 20%. This means that we observed some differences to the published data of Skare et al. (Skare *et al.* 1997), which revealed a voltage-dependence beginning at +/- 40 mV with a maximum decrease in conductance by about 90%. In comparison to the other P66 species, the conductance decrease of the *B. duttonii* P66 homologue was initiated at potentials as low as +/- 20 mV with a maximum conductance decrease by approximately 40%. Thus, these data revealed that P66 of the different species all showed similar voltage-dependent behaviour with slight species-specific differences in the potential for the start of conductance decrease.

4.5. Discussion

4.5.1. The high interspecies homology of P66 indicated similar functionality in LD and RF *Borrelia* species

Previous studies on the function of *B. burgdorferi* P66 indicated that the protein acted as both adhesin and pore-forming protein in the outer membrane (Skare *et al.* 1997; Coburn *et al.* 1999; Coburn *et al.* 2003; Pinne *et al.* 2007). This bifunctionality of P66 suggests a certain importance and relevance of this protein in function and assembly of the *B. burgdorferi* outer membrane. The aim of this work was to investigate the expression and pore-forming functionality of P66 homologues in other *Borrelia* species than *B. burgdorferi*. Previous studies demonstrated the presence and high homology (approx. 90% identity in the amino acid sequence) of P66 in the closely related LD species *B. afzelii* and *B. garinii* (Bunikis et al. 1995). To analyze if P66 homologues were also present in the RF *Borrelia*, we performed a search in all relapsing fever *Borrelia* genomes known to date. These comprise the main African RF pathogen *B. duttonii*, the pathogen of louse-borne RF, *B. recurrentis*, and the main American RF pathogen *B. hermsii*. The results confirmed the presence of P66 homologues in all species, which showed a rather high interspecies amino acid identity (41%). Interestingly, the length of 21 amino acids of the predicted N-terminal signal peptide is identical for all five P66 species. This means that the mature proteins start consistently after alanine at amino acid position 21 of the sequences. This is in agreement with the previous analysis of the N-terminal cleavage site of *B. burgdorferi* P66 (Cullen *et al.* 2004). The many identical domains of the homologous P66 proteins (shaded in green in Fig. 4.1) indicated a conserved structure and function within all species included in this study.

The highly conserved domains of P66 could possibly play key roles in the formation of the channel structure and may be responsible for the formation of up to 20 to 22 β-sheets as the consensus of predicted transmembrane domains in all P66 homologues suggested. Thus, a putative β-barrel structure of P66 is strongly indicated as it is known from Gram-negative porins (Benz 1994b; Saier 2000; Delcour 2002; Charbit 2003). Indeed, a previous topology model of P66 based on proteinase K cleavage, antibody reactivity of surface-exposed P66 regions and computational analyses predicted only two transmembrane domains. One exhibited α-helical content which is in strong contrast to the β-barrel concept of P66 suggested here (Bunikis *et al.* 1995). However, as these points have been used as basis for the previously published topology model, proteinase K cleavage and antibody reactivity of extracellular domains does not exclude

the hypothesis of a β-barrel cylinder formed by P66. Enzymes and antibodies could also have an access to one of the putative surface-exposed loops of P66. The α-helical topology model, which contains only two transmembrane domains, is probably not sufficient to account for the undoubtedly pore-forming character of P66. However, detailed investigations of the P66 structure by X-ray analyses of crystals remain to be done to show if the protein structure was mainly based on α-helices as a previous publication indicated (Bunikis *et al.* 1995) or if β-sheets formed the backbone of this pore-forming protein.

4.5.2. Purification and identification of the P66 homologues

The P66 homologues analyzed in this study could be purified to homogeneity using anion exchange chromatography across a Mono-Q column as it has been previously shown for the purification of *B. burgdorferi* P66 (Skare *et al.* 1997; Pinne *et al.* 2007). All the P66 homologues showed similar binding properties to the column material, which is not a surprise considering the high conservation of their amino acid sequences. SDS-PAGE revealed a very high degree of purity of the proteins, even under the very sensitive conditions of silver-staining of protein bands (Fig. 4.2).

Identification of the 66 kDa protein bands as P66 homologues was achieved by performing Western blots of the purified fractions using anti-P66 polyserum (raised against a partial sequence of *B. burgdorferi* P66). The blots showed clear signals in the corresponding fractions of *B. burgdorferi*, *B. afzelii* and *B. garinii* and *B. hermsii*, clearly indicating that the fractions contained homologues of P66. In contrast to this, there was no signal detectable in the fractions derived from the *B. duttonii* and *B. recurrentis* OMFs. Probably, the polyserum did not cross-react with the putative P66 homologues within these fractions. Reasons for that fact could be based on variations in the amino acid sequences of *B. burgdorferi* P66 and the homologues from these two relapsing fever species. As shown in figure 4.1 there are several identical amino acid residues present in the sequences of *B. duttonii* and *B. recurrentis* which differ from those of the other *Borrelia* species' P66 sequences and could possibly be responsible for the loss of Western blot detection of these proteins. Anyway, biophysical properties of the *B. duttonii* and *B. recurrentis* fractions containing the 66 kDa proteins identified them undoubtedly as P66 homologues (see below).

4.5.3. The P66 proteins of the studied species exhibit similar biophysical properties in artificial membranes

The pure P66 homologues were obtained by anion-exchange chromatography. Although electrophysiological properties of *B. burgdorferi* P66 were described elsewhere in detail (Skare *et al.* 1997), measurements were also performed with this protein in order to compare the biophysical properties of all P66 homologues under identical conditions. We measured a single-channel conductance of *B. burgdorferi P66* in 1M KCl of 11.0 nS. This value differed only slightly from the previously published values of 9.6 nS and 12.6 nS that were related to *B. burgdorferi* P66 in previous publications (Skare *et al.* 1995; Skare *et al.* 1997). One possible explanation of the observed differences in the large channel conductance could be due to the application of different detergents during the isolation and purification procedures that could result in minor conformational changes thereby causing small single-channel conductance differences. Additional measurements demonstrated clearly that P66 from *B. afzelii*, *B. garinii*, *B. duttonii* and *B. recurrentis* formed consistently well-defined channels with single-channel conductances in 1 M KCl that were in the range of 9 to 11 nS similar to the pores formed by *B. burgdorferi* P66. The small variations in single-channel conductance are probably due to minor species-specific differences of intrinsic pores properties which could be based on amino acid exchanges in the sequences as it is shown in figure 4.1.

The P66 homologue of *B. hermsii* was clearly identified by SDS-PAGE and Western blot (see figure 4.2 and 4.3). But unlike the high pore-forming activity of the P66 homologues of all other tested species, *B. hermsii* P66 did not exhibit any activity in the black lipid bilayer. This finding is in agreement with single-channel experiments using whole *B. hermsii* OMF. There was no indication in these experiments that channels could be formed with a single-channel conductance in the range of 9-11 nS that would be similar to the conductance of the other P66 species (Shang *et al.* 1998; Thein *et al.* 2008a). It is possible that *B. hermsii* P66 is affected by the procedure of outer membrane isolation and purification as it was used in this study. Additional analyses using milder isolation conditions have to be done to explain the P66 functionality in *B. hermsii*.

The results of the selectivity measurements of the membrane active P66 homologues were consistent with one another and revealed that the channels do not preferentially filter one type of ions. All P66 channels used in this study were permeable for both cations and anions at approximately the same rate. This was clearly demonstrated by the permeability ratios of cations over anions in KCl close to unity as calculated from the very low zero-current membrane

potentials. Further electrophysiological data revealed that also the voltage-dependent closing of all pore-forming P66 homologues was similar indicating a certain dependence of the applied voltage on the single-channel conductance. In comparison to previous studies that showed a high degree of closure (about 80% decrease in conductance at applied voltages of +/-100 mV) (Skare *et al.* 1997), the *B. burgdorferi* P66 conductance could be decreased by about 20% at comparable applied voltages. This disagreement could be due to the same reasons which are responsible for the observed variances in single-channel conductances (see above).

The high similarity of the observed electrophysiological properties of the different P66 homologues including single-channel measurements, selectivity measurements and voltage-dependence is not surprising, considering the high amino acid identity of the P66 sequences. Anyway, the data obtained in this study revealed clearly that the important, bifunctional protein P66 is expressed in both Lyme disease and relapsing fever *Borrelia* species. Furthermore, our results could elucidate that the P66 homologues of *B. burgdorferi*, *B. afzelii*, *B. garinii*, *B. duttonii* and *B. recurrentis* are capable of formation of pores with high single-channel conductances in the range of 9 to 11 nS with similar biophysical properties. It remains unclear, if this high, electrophysiologically determined, single-channel conductance is due to likewise enormous diameter of the P66 pore as suggested previously (Skare *et al.* 1997). Additional experiments have to be done to specify the two putative functions of P66 *in vivo* and to clarify the relation to its poorly understood structure.

THE USE OF NONELECTROLYTES AS MOLECULAR TOOLS REVEALS THE CHANNEL SIZE AND THE OLIGOMERIC CONSTITUTION OF THE *BORRELIA BURGDORFERI* PORIN P66

5.1. Summary

The outer membrane protein P66 of the Lyme disease spirochete *Borrelia burgdorferi* exhibits dual functions. It acts as adhesin that can bind to β-integrin and is capable of pore formation with the atypical extremely high single-channel conductance of 11 nS in 1 M KCl. This study focused on the questions what is the apparent channel diameter and what is the constitution of a protein with such an outstanding high single-channel conductance. To answer these questions, a channel sizing was performed. Therefore, the P66 single-channel conductance was analyzed in black lipid bilayers in the presence of different nonelectrolytes with known hydrodynamic radii. The filling of the channel with these nonelectrolytes was calculated and revealed that nonelectrolytes with hydrodynamic radii smaller than 0.94 nm enter the pore, whereas neutral molecules with greater radii did either block the channel or were not able to enter the channel. Thus, the effective diameter of the P66 channel lumen was determined to be about 1.9 nm. Furthermore, the P66-induced membrane conductance could be blocked by 80-90% after addition of the nonelectrolytes PEG 400, PEG 600 and maltohexaose in the low millimolar range. The nonelectrolyte-induced block of the channel could also be used for the study of current noise through the P66 channel. The analysis of the power density spectra of P66 after blockage with nonelectrolytes revealed $1/f$-noise indicating that there was no chemical reaction responsible for channel block. The blockage of one P66 single-channel conductance unit of 11 nS occurred by seven subconducting states, thus indicating a heptameric organization of the P66 oligomer. This organization of P66 as a heptamer could be confirmed by Blue native PAGE and immunoblot analysis, which demonstrated that P66 forms a complex with a mass of approximately 440 kDa.

5.2. Introduction

The P66 protein is present in the outer membranes of Lyme disease and relapsing fever spirochetes (Thein *et al.* 2008a). P66 of the Lyme disease species *Borrelia burgdorferi* is well described and exhibits dual functions. (1) It was shown to act as an adhesin which can bind to β3-integrin (Coburn *et al.* 1999; Defoe *et al.* 2001; Coburn *et al.* 2003). (2) And strikingly, it acts as a porin in the outer membrane because its capability of pore-formation could clearly be demonstrated by studies in planar lipid membranes (Skare *et al.* 1997; Pinne *et al.* 2007; Thein *et al.* 2008a). In addition, P66 contains surface-exposed domains (Bunikis *et al.* 1995; Bunikis *et al.* 1996) and exhibits a certain immunogenic potential (Barbour *et al.* 2008). Considering these properties, P66 seems to be an outer membrane protein with a promising potential in terms of a vaccine candidate against Lyme disease.

The electrophysiological properties of the *B. burgdorferi* P66 channel have been studied previously in detail. P66 is able to form pores in planar lipid bilayers with the enormously high single-channel conductance of 11 nS in 1 M KCl (Thein *et al.* 2008a). The channels are nonselective for small anions and cations and exhibit voltage-dependent closure (Skare *et al.* 1997; Thein *et al.* 2008a). The extremely high single-channel conductance is atypical and rare for Gram-negative bacterial porins. However, certain spirochetal porins exhibit also an extremely high single-channel conductance, such as the one of the major outer membrane proteins of *Spirochaeta aurantia*, which forms pores with a conductance of 7.7 nS in 1 M KCl (Kropinski *et al.* 1987) and the one of the major surface protein of *Treponema denticola*, Msp, a 53-kDa species (forming 1.8 nS pores in 0.1 M KCl) (Egli *et al.* 1993). So far, beside selectivity and estimated pore diameters, very little is understood about the apparent pore size and the structure of these outer membrane channels. In terms of P66, the channel diameter was calculated to be about 2.6 nm estimated from the observed single-channel conductance (Skare *et al.* 1997), which would be a rather large diameter compared to other pore-forming outer membrane proteins (Benz 1985).

The calculation of the P66 channel diameter was based on the assumption that the conductance of the channel is equal to the conductivity of a simple cylinder of aqueous salt solution. The length of the cylinder was taken to be equal to the thickness of the membrane. This method has to be considered as zero-order approximation, because it does not take into account such important parameters as the form of the channel and repulsion of the ions from the hydrophobic zone of the lipid membrane. Thus, the calculated value of the P66 diameter appears to be rather preliminary and the apparent size and the structure of channels with such high single-channel conductances as P66 remained only poorly understood so far. Hence, the question

arose what is the apparent channel diameter of P66 and its molecular organization in the outer membrane of *Borrelia* species. To answer this question, the conductance of the P66 channel reconstituted in planar lipid membranes in the presence of noncharged molecules, so-called nonelectrolytes (NEs), was studied as a function of the size of the spherical NEs. When the NEs can enter the P66 channel they will reduce its conductance as has been shown previously (Krasilnikov 2002). This means that the molecular mass cut-off for NEs and their hydrodynamic radii could provide a measure of the pore diameter. However, he partitioning of NEs into channels is not accounted accurately by any theory, nevertheless these polymers were used successfully to determine the effective diameters of a number of polyene- and protein-induced channels (Holz *et al.* 1970; Krasilnikov *et al.* 1992; Vodyanoy *et al.* 1992; Sabirov *et al.* 1993; McKim *et al.* 1994; Kaulin *et al.* 1998; Krasilnikov *et al.* 1998; Berestovsky *et al.* 2001; Krasilnikov 2002; Rostovtseva *et al.* 2002; Ternovsky *et al.* 2004). Besides, this method avoids the potentially strong coulombic interactions that occur between ionic probes and ion channels containing fixed charges.

Some NEs were able to block the P66 channel and allowed therefore a detailed analysis of the P66 properties in multi- and single-channel measurements by titration of the P66-induced conductance. The results suggested that P66 forms a high molecular mass oligomer with many single conductive units. This finding was confirmed by Blue Native PAGE and Western blotting analysis.

5.3. Materials and Methods

5.3.1. Isolation and purification of P66 protein

Pure P66 was obtained by anion exchange chromatography of outer membrane fractions of *B. burgdorferi* B31 (Magnarelli *et al.* 1989) as it has been described previously (Pinne *et al.* 2007; Thein *et al.* 2008a).

5.3.2. Planar lipid bilayer assays

The methods used for black lipid bilayer experiments have been described previously (Benz *et al.* 1978). The instrumentation consisted of a Teflon chamber with two compartments separated by a thin wall and connected by a small circular hole with an area of 0.4 mm^2. The membranes were formed from a 1% (w/v) solution of diphytanoyl phosphatidylcholine (PC) (Avanti Polar Lipids, Alabaster, AL) in *n*-decane. The porin-containing protein fractions were 1:1 or 1:100 diluted in 1% Genapol (Roth) and added to the aqueous phase after the membrane had turned black. The membrane current was measured with a pair of Ag/AgCl electrodes with salt bridges switched in series with a voltage source and a highly sensitive current amplifier (Keithley 427). The temperature was kept at 20°C throughout.

In the experiments carried out to determine the channel diameter the electrolyte solution also contained 20% (w/v) of an appropriate NE as described previously (Krasilnikov *et al.* 1992; Sabirov *et al.* 1993; Krasilnikov *et al.* 1998). The following NEs were used: ethylene glycol (Sigma), glycerol (Sigma), arabinose (Sigma), sorbitol (Sigma), maltose (Sigma), polyethylene glycol (PEG) 300, PEG 400 (Fluka), PEG 600 (Fluka), PEG 900 (Fluka), PEG 1000 (Fluka), PEG 2000 (Fluka), PEG 3000 (Fluka) and PEG 6000 (Fluka). Polyethylene glycols were the molecules of choice in our studies because in aqueous solutions they have a spherical shape (Rempp 1957; Mark 1965).

The conductivity of each buffer was measured with a multi-range conductivity meter (Knick laboratory conductivity meter 702) using a 4-electrode sensor (Knick ZU 6985 conductivity sensor).

Blocking of P66 conductance by NEs was investigated in the same way as the binding of maltooligosaccharides to carbohydrate-specific porins (Benz *et al.* 1986; Benz *et al.* 1987). Blockage of the channel conductance by NEs could be detected by a reduced ion flux through the channel. The measurements were performed with single- or multi-channel experiments under

stationary conditions. The highly diluted protein was added to black diphytanoyl phosphatidylcholine/*n*-decane membranes. After the stable reconstitution of one P66 single-channel conductance unit of 11 nS, titrations on the single-channel level were started. For multi-channel experiments the membrane conductance increased upon reconstitution of numerous channels. After about 90 minutes the conductance was stationary. At that point of time NEs were added in defined concentrations to both sides of the membrane while stirring constantly to allow equilibration. If the compounds blocked the P66 channel, the membrane conductance decreased in a dose-dependent manner as result of the restricted ion flux.

The noise analysis was performed as has been described previously (Andersen *et al.* 1995; Jordy *et al.* 1996; Wohnsland *et al.* 1997; Denker *et al.* 2005). In brief, the membrane current was measured with a pair of silver/silver chloride electrodes switched in series with a battery-operated voltage source and a current amplifier (Keithley 427 with a four pole filter). Feedback resistors of the current amplifier were between 0.01 and 10 GΩ. The amplified signal was monitored with a strip chart recorder (Rikadenki) and fed simultaneously through a low-pass filter (4 Pole Butterworth Low-pass Filter) into an AD-converting card of an IBM-compatible PC. The digitalized data were analyzed with a home-made fast Fourier-transformation program. The spectra were composed of 400 points and they were averaged 128 or 256 times. The obtained power density spectra were further analyzed using commercial graphics programs.

5.3.3. Evaluation of the channel filling with nonelectrolytes

The conception to determine the pore size of P66 by the use of NEs is based on previously published considerations (Krasilnikov *et al.* 1992; Sabirov *et al.* 1993; Krasilnikov *et al.* 1995; Krasilnikov *et al.* 1998). This type of evaluation can be used to determine the apparent size of the channel constriction by analyzing the relationship between the single channel conductance in the presence of NEs and the NEs' hydrodynamic radii. For a more precise measurement of the channel radius the channel filling (*F*) was used in this study in a similar manner as published elsewhere (Krasilnikov *et al.* 1998). Therefore, it is assumed that an ion channel can be treated as an equivalent ohmic resistor with resistance (*R*). This assumption can be extended to all channels with a linear current-voltage relationship. This condition is fulfilled for P66 as the current-voltage relationship of the channel was linear as described in previous studies (Thein *et al.* 2008a).

R can be seen as composed of one part corresponding to the portion of the channel length filled with the NE (F) and another part corresponding to the portion without NE (1-F). Thus, R can be written as:

$$R = [F/(A\mathrm{X}_i) + (1\text{-}F)/(A\mathrm{X}_o)] \qquad \text{(Eq. 5.1)}$$

with $A = \pi r^2/l$, l is the channel length and r its radius, and X_o and X_i are the conductivities of the solution without and with NE, respectively. In assumption that $A\mathrm{X}_o$ is equal to the ion channel conductance in a solution without NE (G_o), it can be shown that the filling (F) is given by:

$$F = [(G_o\text{-}G_i)/\ G_i]/[(\mathrm{X}_o\ \text{-}\mathrm{X}_i)/\ \mathrm{X}_i] \qquad \text{(Eq. 5.2)}$$

where G_o is the single-channel conductance in a solution without NE (1 M KCl), G_i is the single-channel conductance in the presence of a solution containing 20% (w/v) of an NE with access to the channel interior, X_0 is the conductivity of the solution without NE (1 M KCl), and X_i is the conductivity of the solution containing 20% (w/v) of a given NE.

Assuming that the filling of the channel by two of the smallest NE, in our study ethylene glycol and glycerol, is close to the maximum possible level, the filling can be calculated in terms of percentage ($F\%$):

$$F\% = 2F_i/(F_1+F_2)*100\% \qquad \text{(Eq. 5.3)}$$

where F_i is the filling in the presence of a given NE and F_1 and F_2 represent filling in the presence of ethylene glycol and glycerol in the bathing solution, respectively.

5.3.4. Blue Native PAGE and Western blotting analyses

Blue native polyacrylamide gel electrophoresis (Blue native PAGE) was performed according to previously published protocols (Wittig *et al.* 2006). 50 μl (approximately 50 ng) of purified P66 was separated in a 4-13% Blue native PAGE. The NativeMark Unstained (Invitrogen) and the HMW Native Marker (Amersham Biosciences) were used as molecular mass standards. For visualization of the proteins, the Blue native gels were silver stained according to a previously published protocol (Schägger 2006).

For Western blotting, a tank blot system (Amersham Biosciences) was used as described elsewhere (Towbin *et al.* 1979). Bound antibodies were detected using peroxidase-conjugated anti-rabbit antibodies (DAKO A/S) and enhanced chemiluminescence reagents according to the

manufacturer's instructions (Amersham Biosciences). The production and use of polyclonal rabbit serum against *B. burgdorferi* P66 has been described in previous studies (Sadziene *et al.* 1992; Bunikis *et al.* 1995).

5.4. Results

5.4.1. Effects of nonelectrolytes on P66 single-channel conductance

B. burgdorferi P66 forms pores with a mean single-channel conductance of 11 nS in 1 M KCl according to previous studies (Thein *et al.* 2008a). The single-channel conductance of *B. burgdorferi* P66 was measured in 1 M KCl solutions containing in addition 20% (w/v) of appropriate NE molecules with defined hydrodynamic radii ranging from 0.26 nm (for the highly permeant ethylene glycol) up to 2.50 nm (for the nonpermeant PEG 6000). NEs with a hydrodynamic radius smaller than the pore radius should enter the channel and reduce the channel conductance as described in Material and Methods, whereas larger NEs that cannot enter the channel should have little or no effect on the ionic current (Sabirov *et al.* 1991; Krasilnikov 2002). By statistical analysis of at least 100 reconstituted P66 channels into diphytanoyl phosphatidylcholine membranes the mean single-channel conductance in the presence of the different NEs was evaluated. Histograms of four representative measurements together with the recordings of single-channel traces are illustrated in figure 5.1.
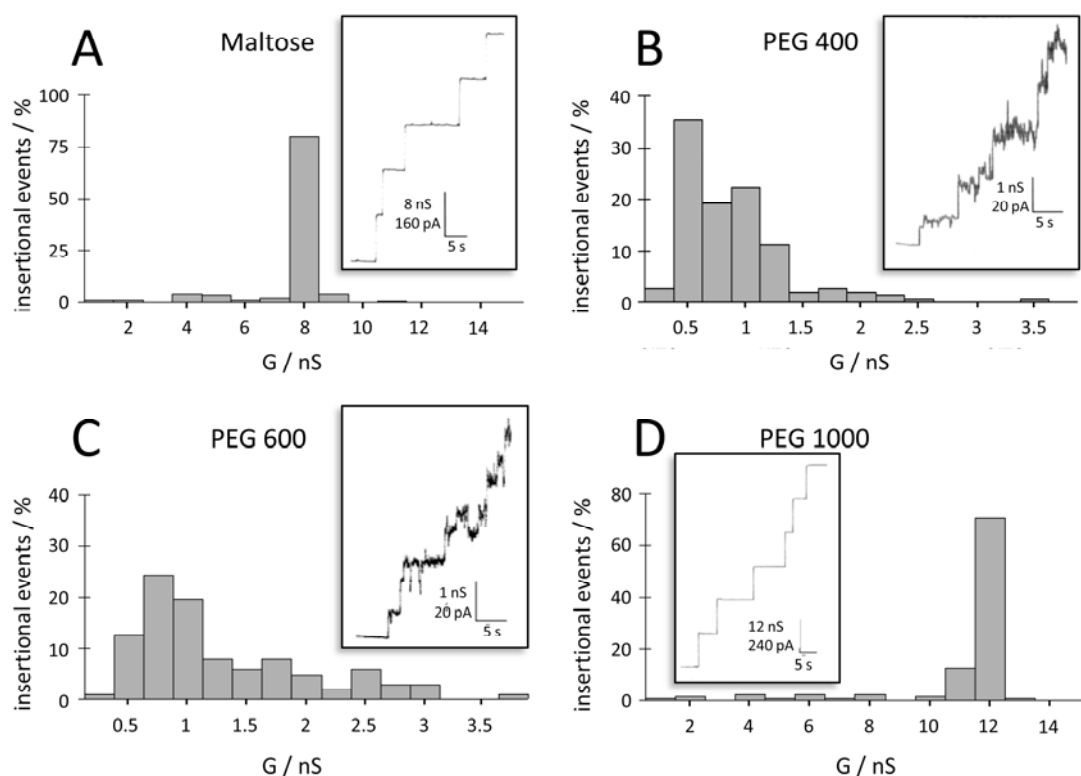
Figure 5.1. Distribution of the single-channel conductances of P66 in the presence of nonelectrolytes. Histograms were constructed from the evaluation of at least 100 insertional events into a diphytanoyl phosphatidylcholine membrane in the presence of 20% (w/v) maltose (A), PEG 400 (B), PEG 600 (C) and PEG 1000 (D) in the bathing solution 1 M KCl. The insets show original recordings of the single-channel current vs. time. The base lines of these recordings represent the zero current level.

In the presence of small well permeant NEs with hydrodynamic radii up to 0.60 nm, such as ethylene glycol, glycerol, arabinose, sorbitol, maltose and PEG 300, the single-channel conductance decreased proportional to that of the bulk solution conductivity (Table 5.1). On the other hand, large nonpermeant NEs with hydrodynamic radii between 0.94 and 2.50 nm, such as PEG 1000, PEG 3000 and PEG 6000, did not show any effect on the single channel conductance. Surprisingly, the addition of PEG 400 and PEG 600 (hydrodynamic radii of 0.70 and 0.80 nm, respectively) to the bathing solution resulted in an exceptional low single-channel conductance of 0.9 nS that was not proportional to the bulk aqueous conductivity. This effect seemed to be due to a highly specific interaction between the polymer and the channel interior resulting in a blockage of the conductance and was further investigated in a separate set of experiments (see below).

Table 5.1. Average single-channel conductances of P66 in the presence of nonelectrolytes in the bathing solution.

Nonelectrolyte	Mr (g/mol)	r (nm)	G (nS)	X ($mS\ cm^{-1}$)
None	-	-	11.0	110.3
Ethylene glycol	62	0.26	6.5	57.2
Glycerol	92	0.31	5.5	49.1
Arabinose	150	0.34	7.0	63.7
Sorbitol	182	0.39	7.5	57.8
Maltose	360	0.50	8.0	73.8
PEG 300	300	0.60	7.5	45.5
PEG 400	400	0.70	0.9	46.4
PEG 600	600	0.80	0.9	54.1
PEG 1000	1000	0.94	12.0	49.5
PEG 3000	3000	1.44	10.5	48.9
PEG 6000	6000	2.50	10.5	50.5

Average single-channel conductances G are expressed as mean of at least 100 insertional steps into a diphytanoyl phosphatidylcholine membrane in the presence of the respective nonelectrolyte at a concentration of 20% (w/v) in the bathing solution 1 M KCl. Mr = molecular mass; r = hydrodynamic radius; Mr and r of the nonelectrolytes were taken from previous publications (Krasilnikov *et al.* 1992; Sabirov *et al.* 1993; Krasilnikov *et al.* 1998); X = conductivity of the solutions, T = 24.5°C for measurements of X.

5.4.2. P66 pore size estimation

In order to characterize the pore size, the conductance decrease as a function of the molecular mass and the hydrodynamic radii of the uncharged polymers was evaluated (Table 5.1). The ratios of the single-channel conductance in the presence of NEs to that in the absence of NEs are shown in figure 5.2. The obtained results suggested that NEs with a mean molecular mass (Mr) of ≤ 600 g/mol and a hydrodynamic radius (r) ≤ 0.8 nm enter the pore whereas NEs with a $Mr \geq 1000$ g/mol and $r \geq 0.94$ nm are not permeable and cannot enter the P66 channel. The effective radius of a water-filled channel is obviously equal to the minimal size of a not permeable NE, i.e. a polymer that does not decrease G.
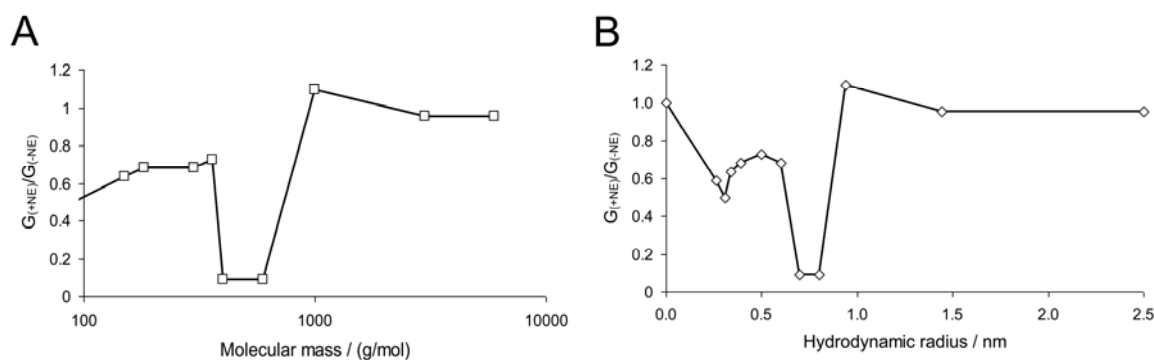

Figure 5.2. Dependence of the single-channel conductance of P66 on the molecular mass (A) and the hydrodynamic radius (B) of the nonelectrolytes. $G_{(+NE)}/G_{(-NE)}$ is the ratio of the mean single-channel channel conductance in the presence of NEs (taken from table 1) to that in the absence of NEs (11 nS (Thein *et al.* 2008a)). Molecular masses and hydrodynamic radii of the nonelectrolytes were taken from table 1.

It is convenient to introduce the channel filling in order to correctly determine the size of the P66 channel (Krasilnikov *et al.* 1998). The channel filling F and the channel filling in terms of percentage $F\%$ were calculated according to equations 5.2 and 5.3 and are listed in table 5.2. The results of the dependence of $F\%$ on the hydrodynamic radii of the NEs are shown in figure 5.3. If the radius of the NEs did not exceed 0.34 nm, $F\%$ was always close to 100%, as it was the case for ethylene glycol ($r = 0.26$ nm), glycerol ($r = 0.31$ nm) and arabinose ($r = 0.34$ nm). Further increase of r caused a decrease in the filling parameter. In this way sorbitol ($r = 0.39$ nm) is able to fill the channel by only 65.8% and PEG 300 ($r = 0.60$ nm) by 42.6%. Channel filling by PEG 400 and PEG 600 was not included in this diagram because $F\%$ of these NEs exceeded 100% by several orders of magnitude indicating a special interaction between channel interior and NE that was not reported to date in similar studies. This interaction presumably reflects particular effects of these NEs on the channel conductance different to those of the other small used NEs and are

probably caused by specific interactions between PEG 400 and PEG 600 and the channel interior. Maltose with a larger radius than sorbitol and PEG 300 ($r = 0.50$ nm) filled approximately 100% of the channel, probably due to slightly specific interactions with the channel interior similar to those of PEG 400 and PEG 600. For a better understanding of the interactions of PEG 400 and PEG 600 with the P66 channel we deviced a separate set of experiments (see below). Beside these deviations, PEGs with $r \geq 0.94$ did not enter the channel at all and caused a decrease of the channel filling close to zero as in the case for PEG 1000, PEG 3000 and PEG 6000.

Table 5.2. Filling of the P66 channel with nonelectrolytes.

Nonelectrolyte	r (*nm*)	F	$F\%$
Ethylene glycol	0.26	0.75	96.8
Glycerol	0.31	0.80	106.7
Arabinose	0.34	0.78	100.6
Sorbitol	0.39	0.51	65.8
Maltose	0.50	0.76	98.1
PEG 300	0.60	0.33	42.6
PEG 400	0.70	*nl.*	*nl.*
PEG 600	0.80	*nl.*	*nl.*
PEG 1000	0.94	-0.07	9.0
PEG 3000	1.44	0.04	5.2
PEG 6000	2.50	0.04	5.2

F and *F%* are the ion channel filling and the ion channel filling in terms of percentage, respectively, in the presence of 20% (w/v) nonelectrolytes in the bathing solution 1 M KCl. *F* and *F%* were calculated according to Eq. 5.2 and Eq. 5.3, respectively. *nl.* means neglected: the channel filling of PEG 400 and PEG 600 was neglected and not included in this table, because the calculated values of *F* and *F%* were pointless high due to possible interactions of these compounds with the channel interior (for details see text). *r* = hydrodynamic radius of the nonelectrolyte taken from previous publications (Krasilnikov *et al.* 1992; Sabirov *et al.* 1993; Krasilnikov *et al.* 1998).

As proposed from the plot in figure 5.3, the effective radius of the P66 channel can be estimated from the abscissa of the intersection point of the linear part of the dependence of *F%* on the hydrodynamic radii of the NEs with the lower plateau. The error of the pore radius estimation

may be derived from the standard deviation of NEs radii, usually around 0.1 - 0.2 nm (Krasilnikov *et al.* 1992). Thus, evaluation of the obtained data with this method indicated that the precise value of the effective P66 radius is about 0.94 ± 0.1 nm.
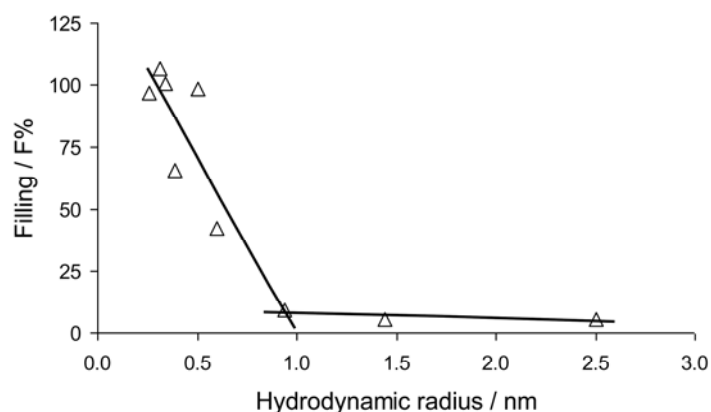

Figure 5.3. Dependence of the channel filling *F%* on the hydrodynamic radii of nonelectrolytes. *F%* for each nonelectrolyte was calculated according to Eq. 5.3. Lines are best fits to the experimental points. The channel filling of PEG 400 and PEG 600 was not included in this diagram, because the calculated values of *F* and *F%* were pointless high and not utilizable due to possible interactions of these compounds with the channel interior (for details see text). The horizontal lines connect the points derived from measurements in the presence of PEG 1000, PEG 3000 and PEG 6000. The other line regression was used to describe the points for the nonelectrolytes with radii ranging from 0.26 nm to 0.6 nm. Hydrodynamic radii of the nonelectrolytes were taken from table 5.2.

5.4.3. Interactions of nonelectrolytes with the P66 channel

The results of P66 single-channel measurements demonstrated that the addition of PEG 400 and PEG 600 caused a decrease of the channel conductance to a higher extent (i.e., ~92% for both PEGs) than they decreased the bulk conductivity (i.e., by 58% and 51%, respectively). To investigate if this finding was caused by a specific interaction of the PEGs with the P66 channels, we performed multi-channel titration experiments as described previously (Benz *et al.* 1986; Benz *et al.* 1987) using different NEs, such as fructose, glucose, maltose, sucrose, PEG 400, PEG 600, maltohexaose and related carbohydrates. P66 was reconstituted into lipid bilayer membranes. After the saturation of channel reconstitution concentrated solutions of different NEs were added to the aqueous phase at both sides of the membrane while stirring to allow equilibration. The addition of small amounts of NEs to the bathing solution caused a substantial, dose-dependent blockage of the conductance. Figure 5.4 shows representative experiments with PEG 600 (Fig. 5.4.A) and maltohexaose (Fig. 5.4.B). The P66-induced conductance could be

blocked by 80% after addition of 4.5 mM PEG 400 or PEG 600 and by approx. 90% after the addition of 45 mM maltohexaose. The kinetics of the decrease of P66-mediated conductance after addition of PEG 400 or PEG 600 was remarkably slow, lasting about 10-30 min, compared to the effect after addition of maltohexaose, which was somewhat faster (see Figure 5.4). Titrations with smaller NE molecules such as the monosaccharides fructose and glucose or the disaccharides maltose and sucrose did not lead to any blockage of the P66-induced conductance (data not shown).
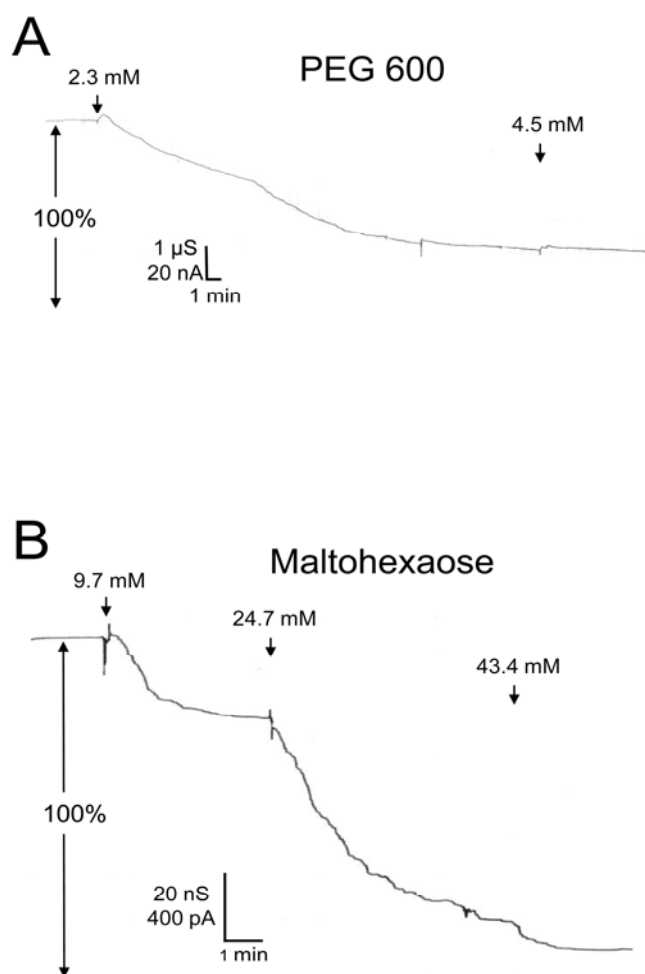
Figure 5.4. Titration of the P66-induced membrane conductance with PEG 600 (A) and maltohexaose (B).

The membrane was formed with diphytanoyl phosphatidylcholine/n-decane. The aqueous phase contained ~100 ng ml^{-1} P66, 1 M KCl and respective nonelectrolytes in the concentration as indicated; temperature = 20°C;
applied voltage = 20 mV.

5.4.4. Effect of nonelectrolytes on the P66-induced membrane conductance at single-channel level

Additional measurements were performed to study PEG 400-induced block of the P66 channel on the single-channel level. P66 was added in very small concentration to both sides of a black

PC membrane. After reconstitution of one single 11 nS unit, the defined single-channel conductance of P66 (Thein *et al.* 2008a), in the membrane, 90 mM PEG 400 was added at both sides of the membrane. The addition of PEG 400 resulted in a substantial blockage of the ionic current through the channel. The recording of such a measurement is shown in figure 5.5 and revealed a PEG-induced, stepwise closing of P66 in seven substates. The conductance of all substates was fairly homogenous and was on average about 1.5 nS. Only sporadic fluctuations of the substates were observed indicating that they were not irreversibly closed. However, they opened with the same conductance of 1.5 nS in 1 M KCl.
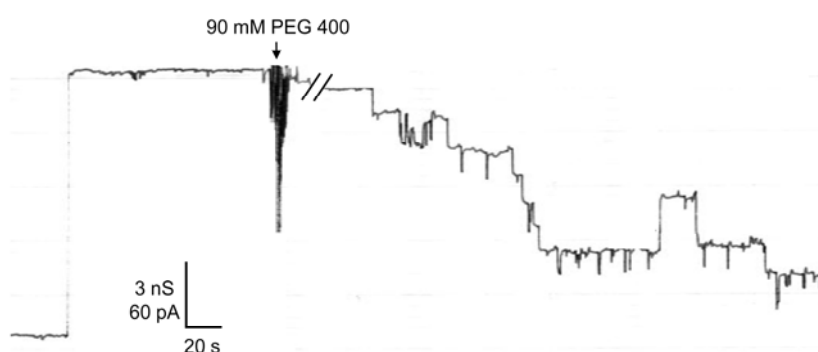
Figure 5.5. PEG 400-induced blockage of P66 on the single-channel level. Small amounts of highly diluted P66 (1:1000 in 1% Genapol) was added to both sides of a diphytanoyl phosphatidylcholine membrane. After reconstitution of one single 11 nS P66 unit, 90 mM PEG 400 was added to both sides of the membrane. The P66 conductance was blocked stepwise exhibiting subconducting steps of approximately 1.5 nS; temperature = 20°C; applied voltage = 20 mV.

5.4.5. Measurements of the current noise through the open and the nonelectrolyte-induced closed state of the P66 channel

The data of Fig. 5.4 indicated that the decrease in conductance after addition of PEG 600 is remarkably slow and lasting 10-30 min, although continuous stirring should result in much faster equilibration of the aqueous phase. To gather some information on the blocking process and its binding kinetics, we studied the current noise of the blocked P66 channels. Parallel to the titration measurements, the frequency-dependence of the spectral density of the current noise was analysed using fast Fourier transformation. Fig. 5.6 illustrates an example of a measurement with PEG 600. Before addition of NEs, a reference spectrum was taken to obtain the current noise of the open P66 channel, which exhibited $1/f$-noise in the frequency range between 10 Hz and 100 Hz (Fig. 5.6, trace 1). The increase of the spectral density at frequencies above about 300 Hz was caused by intrinsic noise of the preamplifier that produces a frequency-dependent

current noise through the membrane capacity C_m. The reference spectrum was subtracted from each spectrum taken after the successive addition of NEs in increasing concentrations. Figure 5.6, trace 2 shows a spectrum taken after addition of PEG 600 (9.6 mM; the reference spectrum of trace 1 was subtracted). The current noise spectrum of P66 after addition of PEG 600 could be fited to a $1/f$-function and is shifted to higher spectral density as compared to the reference spectrum (see Fig. 5.6, trace 2). In further measurements, the concentration of PEG 600 was increased in defined steps. At other concentrations of PEG 600 (18.7 mM and 30.0 mM) the power density spectrum corresponded to that of traces 3 and 4, respectively, in figure 5.6, which also could be fited to a $1/f$-function. This type of noise is expected for diffusion processes through open channels (Wohnsland *et al.* 1997; Bezrukov *et al.* 2000). The spectral density of current noise through P66 channels could also be fitted to $1/f$ functions after addition of PEG 400 and maltohexaose (data not shown).
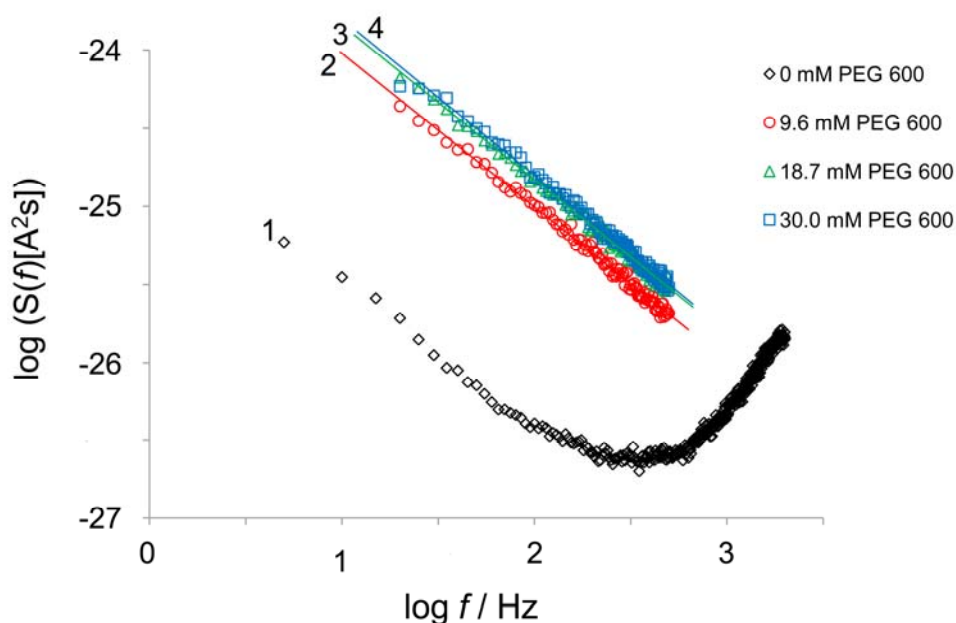
Figure 5.6. Power density spectrum of PEG 600-induced current noise of 61 P66 channels. Trace 1 shows the control, the aqueous phase contained 1 M KCl. For traces 2, 3 and 4 the aqueous phase contained 9.6 mM, 18.7 mM and 30.0 mM PEG 600, respectively, and the power density spectrum of trace 1 was subtracted from each of those traces. PEG 400- and maltohexaose-induced current noises resulted in similar power density spectra (data not shown).

5.4.6. Blue native PAGE analysis of the P66 constitution

The blockage of the P66 conductance on the single-channel level suggested the presence of conductive substates within the P66 channel. This could be caused for example by assuming that

the P66 channel represents an oligomer formed by different P66 monomers. Normal SDS-PAGE did not indicate the formation of P66 oligomers. To check for such a possibility, approximately 50 ng of pure P66 were analyzed in a 4-13% Blue native PAGE and silver stained. For a precise determination of the molecular mass two separate molecular mass standards were used (see Material and Methods). The obtained results clearly demonstrated that pure native P66 is forming a complex that corresponds to a molecular mass of approximately 440 kDa (Figure 5.7, left panel). To verify the presence of P66 within this high molecular mass protein band, an immunoblot of the Blue native PAGE was performed using polyserum against *B. burgdorferi* P66 in a similar manner as it has been used in previous studies (Sadziene *et al.* 1992; Bunikis *et al.* 1995). The strong positive immunoblot signal confirmed the presence of P66 within this high molecular mass protein complex (Figure 5.7, right panel).
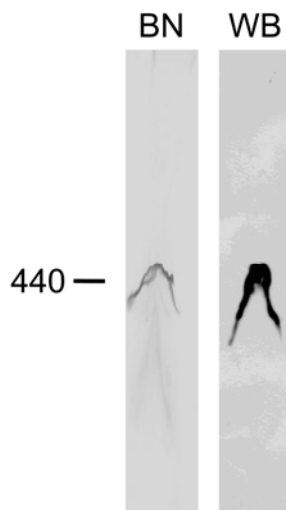
**Figure 5.7. Blue native (BN) PAGE and Western blotting (WB) analysis of the purified P66 complex.** Approximately 50 ng of purified P66 was applied on a 4-13% Blue native PAGE and silver stained (BN, left panel). Western blotting of this BN-PAGE using polyserum against *B. burgdorferi* P66 resulted in a clear signal (WB, right panel). The position of molecular mass standard in kDa is shown at the left.

5.5. Discussion

5.5.1. The effective pore diameter of P66 is smaller than predicted

Estimations based on the previously reported single-channel conductance of 9.6 nS predicted that the P66 channel should have a diameter of 2.6 nm (Skare *et al.* 1997). This large diameter is comparable to similarly large diameters estimated for other spirochetal porins such as that of the major outer membrane protein of *Spirochaeta aurantia* (Kropinski *et al.* 1987) and that of the major surface protein of *Treponema denticola*, Msp, a 53-kDa species (Egli *et al.* 1993), which have estimated diameters of 2.3 and 3.4 nm, respectively. However, the estimation of the pore diameter as has previously been used for the calculation for that of P66 and the other spirochetal porins represents only a rough estimate (Skare *et al.* 1997). This is caused by an oversimplification of the theoretical approach assuming that the cylindrical channels have approximately the same length as the membrane thickness and that the channel interiors have the same conductance as the bulk aqueous conductivity. This rough estimate does not take into account several effects that may influence ion conductance through a channel such as the action of image force, a more hydrophobic interior or that channel friction hinders ion movement (Markin *et al.* 1974; Sizonenko 1995). Thus, to get an idea of the effective pore diameter of a channel with such an extremely high single-channel conductance as P66, pore sizing by use of NEs seemed to be a suitable method as has been demonstrated previously (Krasilnikov 2002).

The estimation of the P66 pore size based on our single-channel measurements with different NEs indicated an effective pore diameter of less than 1.9 nm. This value is significantly smaller than the prediction of 2.6 nm (Skare *et al.* 1997). Reasons for this difference could be due to specific properties of the channel interior. Although the estimation of the pore diameter by the use of NEs could be more precise, it still encounters some difficulties and assumptions, which may interfere with the correct evaluation of the diameter. One could be the smearing of the molecular mass of the PEGs over a considerable range, which could influence the channel filling and thus the estimated radius. However, this effect is accounted and may influence only the standard deviation of the estimated radius. In addition, it is not clear if the PEG 400 and PEG 600 molecules used in this study retain their spherical structure inside the P66 channel. The consistency of the pore sizing with NEs and the comparison with results of electron microscopical investigation of ion channel structures suggests that this point does not represent a major problem (Krasilnikov *et al.* 1992). The pore diameter of less than 1.9 nm is in the range of the size of several other Gram-negative bacterial porins and other membrane channels, that were

characterized by the use of NEs, such as *Bacillus anthracis* $(PA_{63})_7$ ($d \approx 2$ nm) (Nablo *et al.* 2008), *Staphylococcus aureus* α-toxin ($d \approx 1.35$ nm) (Krasilnikov *et al.* 1992) and the colicin Ia ion channel ($d \approx 1$ nm) (Krasilnikov *et al.* 1998). These three channels exhibit single-channel conductances of ~180 pS in 1 M KCl (Orlik *et al.* 2005), 775 pS in 1 M KCl (Menestrina *et al.* 2003) and ~90 pS in 1.77 M KCl (Krasilnikov *et al.* 1998), respectively. P66 has an apparent channel diameter close to the one of *Bacillus anthracis* $(PA_{63})_7$, but its single-channel conductance is about 60-fold higher than the $(PA_{63})_7$ one. This high discrepancy cannot only be explained by special effects of the channel lumen and the molecular organization of the P66 complex as discussed below in more detail.

5.5.2. The effects of PEG 400 and PEG 600 on the P66 single-channel conductance are caused by a special interaction with the channel interior

Membrane experiments in the presence of 20% PEG 400 or PEG 600 resulted in drastically reduced single-channel conductance. The decrease of ion flux through the channel was significantly greater than the measured decrease of the bulk conductivity after addition of NEs and was also observed during multi-channel measurements, which revealed that the P66 conductance could be blocked by 80-90% after the addition of PEG 400, PEG 600 and maltohexaose. Interestingly, the kinetics of conductance decrease after addition of these compounds was very slow, an observation that differs from substrate-binding porins (Andersen *et al.* 1998; Orlik *et al.* 2002; Denker *et al.* 2005). This finding enforced the assumption that specific interactions of PEG 400, PEG 600 and maltohexaose with the channel interior result in the block of the ion flux through the pore. Measurements of the current noise through open and NE-induced closed states of P66 channels should reveal the possible binding kinetics of this interaction during the blocking effect. Current noise measurements and the analyses of the resulting power density spectra obtained by Fourier-transformation allow to study the binding kinetics of substrate-specific porins (Andersen *et al.* 1995; Jordy *et al.* 1996; Andersen *et al.* 1998; Orlik *et al.* 2002). In these cases the noise is of Lorentzian type. Analysis of this Lorentzian type of noise yields the rate constants and thus a determination of the binding kinetics. In contrast, open channel noise of general diffusion porins and porins with a binding site for a specific substrate is a $1/f$-noise (Wohnsland *et al.* 1997; Bezrukov *et al.* 2000; Denker *et al.* 2005).

Open P66 channels exhibited $1/f$-noise before addition of NEs, similar as the noise of other open porin channels (Wohnsland *et al.* 1997). But in contrast to well-studied substrate-specific porins, P66 channels exhibited also $1/f$-noise after blockage of the P66-induced conductance by

addition of NEs. 1/*f*-noise is known to describe diffusion processes through open bacterial channels (Wohnsland *et al.* 1997; Bezrukov *et al.* 2000), meaning that there was no chemical reaction, e.g. substrate binding, detectable during the interaction of NEs with the P66 channel. This phenomenon is exceptional for substrate-specific porins and detailed kinetics during the blockage of the P66-induced conductance remain unclear.

Anyway, these studies were focusing more on the blocking effect of P66-induced membrane conductance than on the determination of permeation kinetics and the possible spectrum of the P66 substrate-specificity. Thus, further investigations have to be done to understand the binding and permeation kinetics of NEs in more detail. In particular, the interacting domains of both the NEs and the P66 lumen are not known and can only be derived definitely from deeper structural insights such as X-ray analyses of P66 crystals.

5.5.3. The discrepancy between single-channel conductance and effective diameter suggested that the channel-forming domain of P66 is composed of several subunits

Several experimental observations suggest that the P66 channel is not formed by a P66 monomer alone. First of all, the size of the channel as derived from measurement with NEs does not agree with its extremely high single-channel conductance of about 11 nS in 1 M KCl (Thein *et al.* 2008a). Furthermore, the stepwise block of the P66 channel with certain NEs occurred in substates with a conductance of about 1.5 nS in 1 M KCl. All these results suggested that the P66 channel may be formed by a bundle of pores. To support this view, purified P66 was investigated by Blue native PAGE, a method that allows the determination of native protein masses and oligomeric states of protein complexes (Wittig *et al.* 2006).

In Blue native PAGE a 440 kDa protein band was observed. This high molecular mass agreed with the data discussed above. P66 could indeed form a hexamer or a heptamer in its membrane-active configuration because seven 66 kDa monomers could form an oligomer with a calculated molecular mass of approximately 460 kDa. Furthermore, the six or seven substates with a conductance of about 1.5 nS could match the 11 nS conductance of the oligomer. Taken together the results presented here suggested that the individual P66 molecules are forming a high molecular mass protein complex: The individual channels in the oligomer act like molecular sieves with a molecular mass cut-off of approximately 600 g/mol and an exclusion size of approximately 1.9 nm.

CONCLUSIONS

6.1. Conclusions of this thesis

This thesis provides insight into the composition and also the constitution and functionality of porins from both relapsing fever and Lyme disease spirochetes. The identification and detailed biochemical and biophysical characterizations of *Borrelia* porins within this thesis represent an important step forward in understanding the outer membrane pathways for nutrient uptake of these strictly host-dependent, pathogenic spirochetes. Anyway, further studies, including genetic manipulations, growth experiments and X-ray analyses of protein crystals, remain to be done to understand the structure of *Borrelia* porins in more detail. As this thesis contributed strongly to the understanding of the nutrient uptake of *Borrelia* species by porins, it provides a new viewpoint of porins of Lyme disease and relapsing fever species.

For Lyme disease species four putative porins are described to date, namely P13, Oms28, DipA and P66 (Skare *et al.* 1996; Skare *et al.* 1997; Östberg *et al.* 2002; Thein *et al.* 2008c). Subsequently, the question arises what are the particular tasks of all those proteins. In particular, P13 was shown to form pores in artificial lipid membranes, but its small size of 13 kDa and its N- and C-terminal processing (Noppa *et al.* 2001; Nilsson *et al.* 2002) leave many questions unanswered, i.e. what is the structure and the functionality of this protein and is it really able to function as a porin *in vivo*. Similarly, controversal studies are known for Oms28. It was shown to exhibit pore-forming capability (Skare *et al.* 1996), but hitherto, it was also questioned to have porin-like properties (Mulay *et al.* 2007). So, it remains still unclear, what is the actual role of Oms28 in the *Borrelia* outer membrane. In contrast to those two proteins, the newly identified DipA seems to function like a typical porin as it is known from other porins of Gram-negative bacteria (Benz 2001). According to unequivocal predictions, its β-barrel structure follows the ones of well-studied porins. In addition, a certain function could be attributed to DipA as it was shown to be a porin specific for the permeation of dicarboxylates (Thein *et al.* 2008c). This is the first concrete function related to any *Borrelia* porin. Finally, P66 is a protein with an unusual exteremely high single-channel conductance (Skare *et al.* 1997; Thein *et al.* 2008a). As revealed in this thesis, the pore-formation seems to be due to an atypical constitution of this protein

compared to other Gram-negative porins, such as OmpF from *Escherichia coli* (Lou *et al.* 1996; Benz 2001). Taking all the obtained findings of Lyme *Borrelia* porins together, these species are undoubtedly dependent on the constitution and functionality of porins in their outer membranes. Anyway, structure and constitution of those pore-forming proteins seem to partly differ from those of other Gram-negative bacteria as findings of previous studies and this thesis indicated. This is not a surprise, looking at the peculiar biology of spirochetes and their outstanding position in the taxonomy of Gram-negative bacteria.

Moreover, this thesis provides the first time insight into the porin content of relapsing fever spirochetes. As a result, two porins are now described for representatives of these species, namely Oms38 and P66 (Thein *et al.* 2008a; Thein *et al.* 2008b). According to findings within this thesis, both proteins seem to function in a similar manner as their homologues in Lyme disease species. The first, Oms38, is highly homologous to the Lyme disease porin DipA and exhibited similar biophysical properties (Thein *et al.* 2008b). Nevertheless, further studies remain to be done to demonstrate if Oms38 is also specific for the permeation of dicarboxylates as it was shown for DipA. The related properties of Lyme disease and relapsing fever P66 proteins suggested strongly that the proteins act similarly in the agents of both diseases. Beside the identification and characterization of Oms38 and P66, there are additional indications for porins within relapsing fever species. For instance, searches in current published genomes of relapsing fever species revealed the presence of a gene homologous to the *p13* one of Lyme disease species, indicating that homologues of this putative Lyme disease porin are also present in relapsing fever agents. Anyway, further studies have do be done to elucidate the complete porin content of relapsing fever species.

6.2. Outlook

One major gap in the *Borrelia* porin knowledge is the lack of definite structural insights. Structural investigations of *Borrelia* porins are mainly based on computational predictions and often very imprecise, as in the case of P13, or even contradictory, as in the case of Oms28 and P66. To elucidate the apparent structures of *Borrelia* porins, X-ray analyses of protein crystals have to be done. This would also be very helpful to understand the structure-related functionality of those proteins in detail.

Besides, future studies should also focus on the production of recombinant *Borrelia* porins. Investigations of recombinant proteins and mutated forms of those would allow a closer understanding of the particular protein domains, e.g. identify substrate-binding sites of the

channels. Furthermore, immunological investigations using native and recombinant *Borrelia* porins could enable the identification of surface-exposed protein domains of Lyme disease and relapsing fever species. A profound knowledge of surface-exposed proteins, such as porins, is one precondition for the production of a successful vaccine and the drug design against the two borrelian-born diseases.

APPENDIX

7.1. References

Achouak, W., Heulin, T. and Pages, J. M. (2001). "Multiple facets of bacterial porins." <u>FEMS Microbiol Lett</u> **199**(1): 1-7.

Alberti, S., Marques, G., Hernandez-Alles, S., Rubires, X., Tomas, J. M., Vivanco, F. and Benedi, V. J. (1996). "Interaction between complement subcomponent C1q and the *Klebsiella pneumoniae* porin OmpK36." <u>Infect Immun</u> **64**(11): 4719-4725.

Andersen, C., Cseh, R., Schulein, K. and Benz, R. (1998). "Study of sugar binding to the sucrose-specific ScrY channel of enteric bacteria using current noise analysis." <u>J Membr Biol</u> **164**(3): 263-274.

Andersen, C., Jordy, M. and Benz, R. (1995). "Evaluation of the rate constants of sugar transport through maltoporin (LamB) of *Escherichia coli* from the sugar-induced current noise." <u>J Gen Physiol</u> **105**(3): 385-401.

Andersen, C., Maier, E., Kemmer, G., Blass, J., Hilpert, A. K., Benz, R. and Reidl, J. (2003). "Porin OmpP2 of *Haemophilus influenzae* shows specificity for nicotinamide-derived nucleotide substrates." <u>J Biol Chem</u> **278**(27): 24269-24276.

Aron, L., Alekshun, M., Perlee, L., Schwartz, I., Godfrey, H. P. and Cabello, F. C. (1994). "Cloning and DNA sequence analysis of bmpC, a gene encoding a potential membrane lipoprotein of *Borrelia burgdorferi*." <u>FEMS Microbiol Lett</u> **123**(1-2): 75-82.

Bagos, P. G., Liakopoulos, T. D., Spyropoulos, I. C. and Hamodrakas, S. J. (2004). "A Hidden Markov Model method, capable of predicting and discriminating beta-barrel outer membrane proteins." <u>BMC Bioinformatics</u> **5**: 29.

Baranton, G., Marti Ras, N. and Postic, D. (1998). "*Borrelia burgdorferi*, taxonomy, pathogenicity and spread." <u>Ann Med Interne (Paris)</u> **149**(7): 455-458.

Baranton, G., Postic, D., Saint Girons, I., Boerlin, P., Piffaretti, J. C., Assous, M. and Grimont, P. A. (1992). "Delineation of *Borrelia burgdorferi* sensu stricto, *Borrelia garinii* sp. nov., and group VS461 associated with Lyme borreliosis." <u>Int J Syst Bacteriol</u> **42**(3): 378-383.

Barbour, A. G. (1984). "Isolation and cultivation of Lyme disease spirochetes." <u>Yale J Biol Med</u> **57**(4): 521-525.

Barbour, A. G. (1990). "Antigenic variation of a relapsing fever *Borrelia* species." <u>Annu Rev Microbiol</u> **44**: 155-171.

Barbour, A. G. (1993). "Linear DNA of *Borrelia* species and antigenic variation." Trends Microbiol **1**(6): 236-239.

Barbour, A. G. (2002). Antigenic variation of relapsing fever *Borrelia* and other pathogenic bacteria. Mobile DNA II. Washington, D.C., American Society for Microbiology**:** 972-994.

Barbour, A. G., Carter, C. J. and Sohaskey, C. D. (2000). "Surface protein variation by expression site switching in the relapsing fever agent *Borrelia hermsii*." Infect Immun **68**(12): 7114-7121.

Barbour, A. G., Dai, Q., Restrepo, B. I., Stoenner, H. G. and Frank, S. A. (2006). "Pathogen escape from host immunity by a genome program for antigenic variation." Proc Natl Acad Sci U S A **103**(48): 18290-18295.

Barbour, A. G. and Hayes, S. F. (1986). "Biology of *Borrelia* species." Microbiol Rev **50**(4): 381-400.

Barbour, A. G., Jasinskas, A., Kayala, M. A., Davies, D. H., Steere, A. C., Baldi, P. and Felgner, P. L. (2008). "A genome-wide proteome array reveals a limited set of immunogens in natural infections of humans and white-footed mice with *Borrelia burgdorferi*." Infect Immun.

Belisle, J. T., Brandt, M. E., Radolf, J. D. and Norgard, M. V. (1994). "Fatty acids of *Treponema pallidum* and *Borrelia burgdorferi* lipoproteins." J Bacteriol **176**(8): 2151-2157.

Benach, J. L., Bosler, E. M., Hanrahan, J. P., Coleman, J. L., Habicht, G. S., Bast, T. F., Cameron, D. J., Ziegler, J. L., Barbour, A. G., Burgdorfer, W., Edelman, R. and Kaslow, R. A. (1983). "Spirochetes isolated from the blood of two patients with Lyme disease." N Engl J Med **308**(13): 740-742.

Bendtsen, J. D., Nielsen, H., von Heijne, G. and Brunak, S. (2004). "Improved prediction of signal peptides: SignalP 3.0." J Mol Biol **340**(4): 783-795.

Benz, R. (1985). "Porin from bacterial and mitochondrial outer membranes." CRC Crit Rev Biochem **19**(2): 145-190.

Benz, R. (1994a). "Permeation of hydrophilic solutes through mitochondrial outer membranes: review on mitochondrial porins." Biochim Biophys Acta **1197**(2): 167-196.

Benz, R. (1994b). Solute uptake through bacterial outer membranes. Bacterial Cell Wall. G. J. M. Hackenbek R. Amsterdam, Elsevier Science B. V.**:** 397-423.

Benz, R. (2001). Porins - structure and function. Microbial Transport Systems. G. Winkelmann. Weinheim/Germany, WILEY-VCH Verlag GmbH**:** 227-246.

Benz, R. (2004). Structure and function of mitochondrial (eukaryotic) porins. Structure and Function of Prokaryotic and Eukaryotic Porins. R. Benz. Weinheim/Germany WILEY-VCH Verlag GmbH**:** 259-284.

Benz, R. and Bauer, K. (1988a). "Permeation of hydrophilic molecules through the outer membrane of gram-negative bacteria. Review on bacterial porins." Eur J Biochem **176**(1): 1-19.

Benz, R., Janko, K., Boos, W. and Läuger, P. (1978). "Formation of large, ion-permeable membrane channels by the matrix protein (porin) of *Escherichia coli*." <u>Biochim Biophys Acta</u> **511**(3): 305-319.

Benz, R., Janko, K. and Läuger, P. (1979). "Ionic selectivity of pores formed by the matrix protein (porin) of *Escherichia coli*." <u>Biochim Biophys Acta</u> **551**(2): 238-247.

Benz, R. and Orlik, F. (2004). Functional reconstitution and properties of specific porins. <u>Structure and function of prokaryotic and eukaryotic porins</u>. R. Benz. Weinheim/Germany, WILEY-VCH Verlag GmbH**:** 183-212.

Benz, R., Schmid, A., Maier, C. and Bremer, E. (1988b). "Characterization of the nucleoside-binding site inside the Tsx channel of *Escherichia coli* outer membrane. Reconstitution experiments with lipid bilayer membranes." <u>Eur J Biochem</u> **176**(3): 699-705.

Benz, R., Schmid, A., Nakae, T. and Vos-Scheperkeuter, G. H. (1986). "Pore formation by LamB of *Escherichia coli* in lipid bilayer membranes." <u>J Bacteriol</u> **165**(3): 978-986.

Benz, R., Schmid, A. and Vos-Scheperkeuter, G. H. (1987). "Mechanism of sugar transport through the sugar-specific LamB channel of *Escherichia coli* outer membrane." <u>J Membr Biol</u> **100**(1): 21-29.

Berestovsky, G. N., Ternovsky, V. I. and Kataev, A. A. (2001). "Through pore diameter in the cell wall of *Chara corallina*." <u>J Exp Bot</u> **52**(359): 1173-1177.

Bergström, S., Bundoc, V. G. and Barbour, A. G. (1989). "Molecular analysis of linear plasmid-encoded major surface proteins, OspA and OspB, of the Lyme disease spirochaete *Borrelia burgdorferi*." <u>Mol Microbiol</u> **3**(4): 479-486.

Bernardini, M. L., Sanna, M. G., Fontaine, A. and Sansonetti, P. J. (1993). "OmpC is involved in invasion of epithelial cells by *Shigella flexneri*." <u>Infect Immun</u> **61**(9): 3625-3635.

Beveridge, T. J. (1981). "Ultrastructure, chemistry, and function of the bacterial wall." <u>Int Rev Cytol</u> **72**: 229-317.

Bezrukov, S. M. and Winterhalter, M. (2000). "Examining noise sources at the single-molecule level: 1/f noise of an open maltoporin channel." <u>Phys Rev Lett</u> **85**(1): 202-205.

Blum, H., Beier, H. and Gross, H. J. (1987). "Improved silver staining of plant proteins, RNA and DNA in polyacrylamide gels." <u>Electrophoresis</u> **8**: 93-99.

Bos, M. P., Robert, V. and Tommassen, J. (2007). "Biogenesis of the gram-negative bacterial outer membrane." <u>Annu Rev Microbiol</u> **61**: 191-214.

Brandt, M. E., Riley, B. S., Radolf, J. D. and Norgard, M. V. (1990). "Immunogenic integral membrane proteins of *Borrelia burgdorferi* are lipoproteins." <u>Infect Immun</u> **58**(4): 983-991.

Brasseur, D. (1985). "Tick-borne relapsing fever in a premature infant." <u>Ann Trop Paediatr</u> **5**(3): 161-162.

Bryceson, A. D., Parry, E. H., Perine, P. L., Warrell, D. A., Vukotich, D. and Leithead, C. S. (1970). "Louse-borne relapsing fever." <u>Q J Med</u> **39**(153): 129-170.

Bunikis, I., Denker, K., Östberg, Y., Andersen, C., Benz, R. and Bergström, S. (2008). "An RND-type efflux system in *Borrelia burgdorferi* is involved in virulence and resistance to antimicrobial compounds." <u>PLoS Pathog</u> **4**(2): e1000009.

Bunikis, J., Noppa, L. and Bergström, S. (1995). "Molecular analysis of a 66-kDa protein associated with the outer membrane of Lyme disease *Borrelia*." <u>FEMS Microbiol Lett</u> **131**(2): 139-145.

Bunikis, J., Noppa, L., Ostberg, Y., Barbour, A. G. and Bergström, S. (1996). "Surface exposure and species specificity of an immunoreactive domain of a 66-kilodalton outer membrane protein (P66) of the *Borrelia* spp. that cause Lyme disease." <u>Infect Immun</u> **64**(12): 5111-5116.

Burgdorfer, W. (1984). "Discovery of the Lyme disease spirochete and its relation to tick vectors." <u>Yale J Biol Med</u> **57**(4): 515-520.

Burgdorfer, W. (1991). "Lyme borreliosis: ten years after discovery of the etiologic agent, *Borrelia burgdorferi*." <u>Infection</u> **19**(4): 257-262.

Burgdorfer, W., Barbour, A. G., Hayes, S. F., Benach, J. L., Grunwaldt, E. and Davis, J. P. (1982). "Lyme disease-a tick-borne spirochetosis?" <u>Science</u> **216**(4552): 1317-1319.

Butler, T., Hazen, P., Wallace, C. K., Awoke, S. and Habte-Michael, A. (1979). "Infection with *Borrelia recurrentis*: pathogenesis of fever and petechiae." <u>J Infect Dis</u> **140**(5): 665-675.

Cadavid, D. and Barbour, A. G. (1998). "Neuroborreliosis during relapsing fever: review of the clinical manifestations, pathology, and treatment of infections in humans and experimental animals." <u>Clin Infect Dis</u> **26**(1): 151-164.

Cadavid, D., Pennington, P. M., Kerentseva, T. A., Bergström, S. and Barbour, A. G. (1997). "Immunologic and genetic analyses of VmpA of a neurotropic strain of *Borrelia turicatae*." <u>Infect Immun</u> **65**(8): 3352-3360.

Caimano, M. J., Yang, X., Popova, T. G., Clawson, M. L., Akins, D. R., Norgard, M. V. and Radolf, J. D. (2000). "Molecular and evolutionary characterization of the cp32/18 family of supercoiled plasmids in *Borrelia burgdorferi* 297." <u>Infect Immun</u> **68**(3): 1574-1586.

Canica, M. M., Nato, F., du Merle, L., Mazie, J. C., Baranton, G. and Postic, D. (1993). "Monoclonal antibodies for identification of *Borrelia afzelii* sp. nov. associated with late cutaneous manifestations of Lyme borreliosis." <u>Scand J Infect Dis</u> **25**(4): 441-448.

Caporale, D. A. and Kocher, T. D. (1994). "Sequence variation in the outer-surface-protein genes of *Borrelia burgdorferi*." <u>Mol Biol Evol</u> **11**(1): 51-64.

Carter, C. J., Bergström, S., Norris, S. J. and Barbour, A. G. (1994). "A family of surface-exposed proteins of 20 kilodaltons in the genus *Borrelia*." <u>Infect Immun</u> **62**(7): 2792-2799.

Casjens, S., Palmer, N., van Vugt, R., Huang, W. M., Stevenson, B., Rosa, P., Lathigra, R., Sutton, G., Peterson, J., Dodson, R. J., Haft, D., Hickey, E., Gwinn, M., White, O. and Fraser, C. M. (2000). "A bacterial genome in flux: the twelve linear and nine circular extrachromosomal DNAs in an infectious isolate of the Lyme disease spirochete *Borrelia burgdorferi*." <u>Mol Microbiol</u> **35**(3): 490-516.

Charbit, A. (2003). "Maltodextrin transport through lamb." <u>Front Biosci</u> **8**: s265-274.

Chenna, R., Sugawara, H., Koike, T., Lopez, R., Gibson, T. J., Higgins, D. G. and Thompson, J. D. (2003). "Multiple sequence alignment with the Clustal series of programs." <u>Nucleic Acids Res</u> **31**(13): 3497-3500.

Coburn, J., Chege, W., Magoun, L., Bodary, S. C. and Leong, J. M. (1999). "Characterization of a candidate *Borrelia burgdorferi* beta3-chain integrin ligand identified using a phage display library." <u>Mol Microbiol</u> **34**(5): 926-940.

Coburn, J. and Cugini, C. (2003). "Targeted mutation of the outer membrane protein P66 disrupts attachment of the Lyme disease agent, *Borrelia burgdorferi*, to integrin alphavbeta3." <u>Proc Natl Acad Sci U S A</u> **100**(12): 7301-7306.

Coburn, J., Fischer, J. R. and Leong, J. M. (2005). "Solving a sticky problem: new genetic approaches to host cell adhesion by the Lyme disease spirochete." <u>Mol Microbiol</u> **57**(5): 1182-1195.

Cook, G. C. (2003). <u>Manson's tropical diseases</u>, Saunders London.

Cox, D. L., Akins, D. R., Bourell, K. W., Lahdenne, P., Norgard, M. V. and Radolf, J. D. (1996). "Limited surface exposure of *Borrelia burgdorferi* outer surface lipoproteins." <u>Proc Natl Acad Sci U S A</u> **93**(15): 7973-7978.

Cox, D. L. and Radolf, J. D. (2001). "Insertion of fluorescent fatty acid probes into the outer membranes of the pathogenic spirochaetes *Treponema pallidum* and *Borrelia burgdorferi*." <u>Microbiology</u> **147**(Pt 5): 1161-1169.

Cullen, P. A., Haake, D. A. and Adler, B. (2004). "Outer membrane proteins of pathogenic spirochetes." <u>FEMS Microbiol Rev</u> **28**(3): 291-318.

de Silva, A. M. and Fikrig, E. (1997). "Arthropod- and host-specific gene expression by *Borrelia burgdorferi*." <u>J Clin Invest</u> **99**(3): 377-379.

Delcour, A. H. (2002). "Structure and function of pore-forming beta-barrels from bacteria." <u>J Mol Microbiol Biotechnol</u> **4**(1): 1-10.

Denker, K., Orlik, F., Schiffler, B. and Benz, R. (2005). "Site-directed mutagenesis of the greasy slide aromatic residues within the LamB (maltoporin) channel of *Escherichia coli*: effect on ion and maltopentaose transport." <u>J Mol Biol</u> **352**(3): 534-550.

Ding, W., Huang, X., Yang, X., Dunn, J. J., Luft, B. J., Koide, S. and Lawson, C. L. (2000). "Structural identification of a key protective B-cell epitope in Lyme disease antigen OspA." <u>J Mol Biol</u> **302**(5): 1153-1164.

Dworkin, M. S., Schwan, T. G. and Anderson, D. E., Jr. (2002). "Tick-borne relapsing fever in North America." <u>Med Clin North Am</u> **86**(2): 417-433, viii-ix.

Eckerskorn, C. and Lottspeich, F. (1993). "Structural characterization of blotting membranes and the influence of membrane parameters for electroblotting and subsequent amino acid sequence analysis of proteins." <u>Electrophoresis</u> **14**(9): 831-838.

Egli, C., Leung, W. K., Muller, K. H., Hancock, R. E. and McBride, B. C. (1993). "Pore-forming properties of the major 53-kilodalton surface antigen from the outer sheath of *Treponema denticola*." Infect Immun **61**(5): 1694-1699.

Eicken, C., Sharma, V., Klabunde, T., Lawrenz, M. B., Hardham, J. M., Norris, S. J. and Sacchettini, J. C. (2002). "Crystal structure of Lyme disease variable surface antigen VlsE of *Borrelia burgdorferi*." J Biol Chem **277**(24): 21691-21696.

Eicken, C., Sharma, V., Klabunde, T., Owens, R. T., Pikas, D. S., Hook, M. and Sacchettini, J. C. (2001). "Crystal structure of Lyme disease antigen outer surface protein C from *Borrelia burgdorferi*." J Biol Chem **276**(13): 10010-10015.

Eiffert, H., Lotter, H., Jarecki-Khan, K. and Thomssen, R. (1991). "Identification of an immunoreactive non-proteinaleous component in *Borrelia burgdorferi*." Med Microbiol Immunol **180**(5): 229-237.

Felsenfeld, O. (1965). "Borreliae, Human Relapsing Fever, and Parasite-Vector-Host Relationships." Bacteriol Rev **29**: 46-74.

Felsenfeld, O. (1971). "*Borrelia*: Strains, vectors, human and animal Borreliosis." Green, St. Louis, MO.

Ferenci, T., Schwentorat, M., Ullrich, S. and Vilmart, J. (1980). "Lambda receptor in the outer membrane of *Escherichia coli* as a binding protein for maltodextrins and starch polysaccharides." J Bacteriol **142**(2): 521-526.

Fraser, C. M., Casjens, S., Huang, W. M., Sutton, G. G., Clayton, R., Lathigra, R., White, O., Ketchum, K. A., Dodson, R., Hickey, E. K., Gwinn, M., Dougherty, B., Tomb, J. F., Fleischmann, R. D., Richardson, D., Peterson, J., Kerlavage, A. R., Quackenbush, J., Salzberg, S., Hanson, M., van Vugt, R., Palmer, N., Adams, M. D., Gocayne, J., Weidman, J., Utterback, T., Watthey, L., McDonald, L., Artiach, P., Bowman, C., Garland, S., Fuji, C., Cotton, M. D., Horst, K., Roberts, K., Hatch, B., Smith, H. O. and Venter, J. C. (1997). "Genomic sequence of a Lyme disease spirochaete, *Borrelia burgdorferi*." Nature **390**(6660): 580-586.

Freitag, H., Genchi, G., Benz, R., Palmieri, F. and Neupert, W. (1982). "Isolation of mitochondrial porin from *Neurospora crassa*." FEBS Lett **145**(1): 72-76.

Fuchs, P. C. and Oyama, A. A. (1969). "Neonatal relapsing fever due to transplacental transmission of *Borrelia*." JAMA **208**(4): 690-692.

Goldstein, S. F., Buttle, K. F. and Charon, N. W. (1996). "Structural analysis of the *Leptospiraceae* and *Borrelia burgdorferi* by high-voltage electron microscopy." J Bacteriol **178**(22): 6539-6545.

Goubau, P. F. (1984). "Relapsing fevers. A review." Ann Soc Belg Med Trop **64**(4): 335-364.

Gromiha, M. M., Ahmad, S. and Suwa, M. (2004). "Neural network-based prediction of transmembrane beta-strand segments in outer membrane proteins." J Comput Chem **25**(5): 762-767.

Guggenheim, J. N. and Haverkamp, A. D. (2005). "Tick-borne relapsing fever during pregnancy: a case report." J Reprod Med **50**(9): 727-729.

Guo, B. P., Norris, S. J., Rosenberg, L. C. and Hook, M. (1995). "Adherence of *Borrelia burgdorferi* to the proteoglycan decorin." Infect Immun **63**(9): 3467-3472.

Haake, D. A. (2000). "Spirochaetal lipoproteins and pathogenesis." Microbiology **146 (Pt 7)**: 1491-1504.

Hancock, R. E. and Benz, R. (1986). "Demonstration and chemical modification of a specific phosphate binding site in the phosphate-starvation-inducible outer membrane porin protein P of *Pseudomonas aeruginosa*." Biochim Biophys Acta **860**(3): 699-707.

Hefty, P. S., Jolliff, S. E., Caimano, M. J., Wikel, S. K. and Akins, D. R. (2002). "Changes in temporal and spatial patterns of outer surface lipoprotein expression generate population heterogeneity and antigenic diversity in the Lyme disease spirochete, *Borrelia burgdorferi*." Infect Immun **70**(7): 3468-3478.

Hinnebusch, B. J., Barbour, A. G., Restrepo, B. I. and Schwan, T. G. (1998). "Population structure of the relapsing fever spirochete *Borrelia hermsii* as indicated by polymorphism of two multigene families that encode immunogenic outer surface lipoproteins." Infect Immun **66**(2): 432-440.

Holz, R. and Finkelstein, A. (1970). "The water and nonelectrolyte permeability induced in thin lipid membranes by the polyene antibiotics nystatin and amphotericin B." J Gen Physiol **56**(1): 125-145.

Ichihara, S., Hussain, M. and Mizushima, S. (1981). "Characterization of new membrane lipoproteins and their precursors of *Escherichia coli*." J Biol Chem **256**(6): 3125-3129.

Janausch, I. G., Zientz, E., Tran, Q. H., Kroger, A. and Unden, G. (2002). "C4-dicarboxylate carriers and sensors in bacteria." Biochim Biophys Acta **1553**(1-2): 39-56.

Johnson, R. C. (1977). "The spirochetes." Annu Rev Microbiol **31**: 89-106.

Jordy, M., Andersen, C., Schulein, K., Ferenci, T. and Benz, R. (1996). "Rate constants of sugar transport through two LamB mutants of *Escherichia coli*: comparison with wild-type maltoporin and LamB of *Salmonella typhimurium*." J Mol Biol **259**(4): 666-678.

Kaulin, Y. A., Schagina, L. V., Bezrukov, S. M., Malev, V. V., Feigin, A. M., Takemoto, J. Y., Teeter, J. H. and Brand, J. G. (1998). "Cluster organization of ion channels formed by the antibiotic syringomycin E in bilayer lipid membranes." Biophys J **74**(6): 2918-2925.

Kehl, K. S., Farmer, S. G., Komorowski, R. A. and Knox, K. K. (1986). "Antigenic variation among *Borrelia* spp. in relapsing fever." Infect Immun **54**(3): 899-902.

Kraiczy, P., Skerka, C., Kirschfink, M., Zipfel, P. F. and Brade, V. (2001). "Mechanism of complement resistance of pathogenic *Borrelia burgdorferi* isolates." Int Immunopharmacol **1**(3): 393-401.

Krasilnikov, O. V. (2002). Sizing channels with neutral polymers. Structure and Dynamics of Confined Polymers. K. Press. Dordrecht, Netherlands, Kasianowicz, J. J., Kellermayer M. S. Z., Deamer, D. W.**:** 97-115.

Krasilnikov, O. V., Da Cruz, J. B., Yuldasheva, L. N., Varanda, W. A. and Nogueira, R. A. (1998). "A novel approach to study the geometry of the water lumen of ion channels: colicin Ia channels in planar lipid bilayers." J Membr Biol **161**(1): 83-92.

Krasilnikov, O. V., Sabirov, R. Z., Ternovsky, V. I., Merzliak, P. G. and Muratkhodjaev, J. N. (1992). "A simple method for the determination of the pore radius of ion channels in planar lipid bilayer membranes." FEMS Microbiol Immunol **5**(1-3): 93-100.

Krasilnikov, O. V., Yuldasheva, L. N., Nogueira, R. A. and Rodrigues, C. G. (1995). "The diameter of water pores formed by colicin Ia in planar lipid bilayers." Braz J Med Biol Res **28**(6): 693-698.

Kropinski, A. M., Parr, T. R., Jr., Angus, B. L., Hancock, R. E., Ghiorse, W. C. and Greenberg, E. P. (1987). "Isolation of the outer membrane and characterization of the major outer membrane protein from *Spirochaeta aurantia*." J Bacteriol **169**(1): 172-179.

Kubo, A. and Stephens, R. S. (2001). "Substrate-specific diffusion of select dicarboxylates through *Chlamydia trachomatis* PorB." Microbiology **147**(Pt 11): 3135-3140.

Kumaran, D., Eswaramoorthy, S., Luft, B. J., Koide, S., Dunn, J. J., Lawson, C. L. and Swaminathan, S. (2001). "Crystal structure of outer surface protein C (OspC) from the Lyme disease spirochete, *Borrelia burgdorferi*." EMBO J **20**(5): 971-978.

Laemmli, U. K. (1970). "Cleavage of structural proteins during the assembly of the head of bacteriophage T4." Nature **227**(5259): 680-685.

Lakey, J. H. and Pattus, F. (1989). "The voltage-dependent activity of *Escherichia coli* porins in different planar bilayer reconstitutions." Eur J Biochem **186**(1-2): 303-308.

Lam, T. T., Nguyen, T. P., Fikrig, E. and Flavell, R. A. (1994). "A chromosomal *Borrelia burgdorferi* gene encodes a 22-kilodalton lipoprotein, P22, that is serologically recognized in Lyme disease." J Clin Microbiol **32**(4): 876-883.

Larsson, C., Andersson, M., Pelkonen, J., Guo, B. P., Nordstrand, A. and Bergström, S. (2006). "Persistent brain infection and disease reactivation in relapsing fever borreliosis." Microbes Infect **8**(8): 2213-2219.

Lathrop, S. L., Ball, R., Haber, P., Mootrey, G. T., Braun, M. M., Shadomy, S. V., Ellenberg, S. S., Chen, R. T. and Hayes, E. B. (2002). "Adverse event reports following vaccination for Lyme disease: December 1998-July 2000." Vaccine **20**(11-12): 1603-1608.

Lou, K. L., Saint, N., Prilipov, A., Rummel, G., Benson, S. A., Rosenbusch, J. P. and Schirmer, T. (1996). "Structural and functional characterization of OmpF porin mutants selected for larger pore size. I. Crystallographic analysis." J Biol Chem **271**(34): 20669-20675.

Ludwig, O., De Pinto, V., Palmieri, F. and Benz, R. (1986). "Pore formation by the mitochondrial porin of rat brain in lipid bilayer membranes." Biochim Biophys Acta **860**(2): 268-276.

Madigan, M. T., Martinko, J. M. and Parker, J. (2000). "Brock biology of microorganisms."

Magnarelli, L. A., Anderson, J. F. and Barbour, A. G. (1989). "Enzyme-linked immunosorbent assays for Lyme disease: reactivity of subunits of *Borrelia burgdorferi*." J Infect Dis **159**(1): 43-49.

Maier, C., Bremer, E., Schmid, A. and Benz, R. (1988). "Pore-forming activity of the Tsx protein from the outer membrane of *Escherichia coli*. Demonstration of a nucleoside-specific binding site." J Biol Chem **263**(5): 2493-2499.

Makabe, K., Tereshko, V., Gawlak, G., Yan, S. and Koide, S. (2006). "Atomic-resolution crystal structure of *Borrelia burgdorferi* outer surface protein A via surface engineering." Protein Sci **15**(8): 1907-1914.

Marconi, R. T. and Garon, C. F. (1992). "Identification of a third genomic group of *Borrelia burgdorferi* through signature nucleotide analysis and 16S rRNA sequence determination." J Gen Microbiol **138**(3): 533-536.

Mark, J. E., Flory, P.J. (1965). "The configuration of the polyoxyethylene chain." J. Am. Chem. Soc. **87**: 1415-1422.

Markin, V. S. and Chizmadzhev, Y. A. (1974). Induced Ion Transport, Nauka, Moscow.

McKim, S. and Hinton, J. F. (1994). "Evidence of xenon transport through the gramicidin channel: a 129Xe-NMR study." Biochim Biophys Acta **1193**(1): 186-198.

Menestrina, G., Dalla Serra, M., Comai, M., Coraiola, M., Viero, G., Werner, S., Colin, D. A., Monteil, H. and Prevost, G. (2003). "Ion channels and bacterial infection: the case of beta-barrel pore-forming protein toxins of *Staphylococcus aureus*." FEBS Lett **552**(1): 54-60.

Merino, S., Nogueras, M. M., Aguilar, A., Rubires, X., Alberti, S., Benedi, V. J. and Tomas, J. M. (1998). "Activation of the complement classical pathway (C1q binding) by mesophilic *Aeromonas hydrophila* outer membrane protein." Infect Immun **66**(8): 3825-3831.

Mirzabekov, T. A., Skare, J. T., Shang, E. S., Blanco, D. R., Miller, J. N., Lovett, M. A. and Kagan, B. L. (1996). "Electrical properties of porins from *Borrelia burgdorferi*." Biophys. J. **70**(2): A205.

Moser, I., Schroeder, W. and Salnikow, J. (1997). "*Campylobacter jejuni* major outer membrane protein and a 59-kDa protein are involved in binding to fibronectin and INT 407 cell membranes." FEMS Microbiol Lett **157**(2): 233-238.

Mulay, V., Caimano, M. J., Liveris, D., Desrosiers, D. C., Radolf, J. D. and Schwartz, I. (2007). "*Borrelia burgdorferi* BBA74, a periplasmic protein associated with the outer membrane, lacks porin-like properties." J Bacteriol **189**(5): 2063-2068.

Nablo, B. J., Halverson, K. M., Robertson, J. W. F., Nguyen, T. L., Panchal, R. G., Gussio, R., Bavari, S., Krasilnikov, O. V. and Kasianowicz, J. J. (2008). "Sizing the *Bacillus anthracis* PA63 Channel with Nonelectrolyte Poly (Ethylene Glycols)." Biophysical Journal **95**(3): 1157.

Nadelman, R. B. and Wormser, G. P. (1998). "Lyme borreliosis." Lancet **352**(9127): 557-565.

Nikaido, H. (2003). "Molecular basis of bacterial outer membrane permeability revisited." Microbiol Mol Biol Rev **67**(4): 593-656.

Nikaido, H. and Vaara, M. (1985). "Molecular basis of bacterial outer membrane permeability." Microbiol Rev **49**(1): 1-32.

Nilsson, C. L., Cooper, H. J., Hakansson, K., Marshall, A. G., Östberg, Y., Lavrinovicha, M. and Bergström, S. (2002). "Characterization of the P13 membrane protein of *Borrelia burgdorferi* by mass spectrometry." J Am Soc Mass Spectrom **13**(4): 295-299.

Noppa, L., Östberg, Y., Lavrinovicha, M. and Bergström, S. (2001). "P13, an integral membrane protein of *Borrelia burgdorferi*, is C-terminally processed and contains surface-exposed domains." Infect Immun **69**(5): 3323-3334.

Orlik, F., Andersen, C. and Benz, R. (2002). "Site-directed mutagenesis of tyrosine 118 within the central constriction site of the LamB (maltoporin) channel of *Escherichia coli*. II. Effect on maltose and maltooligosaccharide binding kinetics." Biophys J **83**(1): 309-321.

Orlik, F., Schiffler, B. and Benz, R. (2005). "Anthrax toxin protective antigen: inhibition of channel function by chloroquine and related compounds and study of binding kinetics using the current noise analysis." Biophys J **88**(3): 1715-1724.

Orloski, K. A., Hayes, E. B., Campbell, G. L. and Dennis, D. T. (2000). "Surveillance for Lyme disease--United States, 1992-1998." MMWR CDC Surveill Summ **49**(3): 1-11.

Östberg, Y., Carroll, J. A., Pinne, M., Krum, J. G., Rosa, P. and Bergstrom, S. (2004). "Pleiotropic effects of inactivating a carboxyl-terminal protease, CtpA, in *Borrelia burgdorferi*." J Bacteriol **186**(7): 2074-2084.

Östberg, Y., Pinne, M., Benz, R., Rosa, P. and Bergström, S. (2002). "Elimination of channel-forming activity by insertional inactivation of the p13 gene in *Borrelia burgdorferi*." J Bacteriol **184**(24): 6811-6819.

Palmieri, F., Indiveri, C., Bisaccia, F. and Kramer, R. (1993). "Functional properties of purified and reconstituted mitochondrial metabolite carriers." J Bioenerg Biomembr **25**(5): 525-535.

Paschen, S. A., Neupert, W. and Rapaport, D. (2005). "Biogenesis of beta-barrel membrane proteins of mitochondria." Trends Biochem Sci **30**(10): 575-582.

Perine, P. L., Krause, D. W., Awoke, S. and McDade, J. E. (1974). "Single-dose doxycycline treatment of louse-borne relapsing fever and epidemic typhus." Lancet **2**(7883): 742-744.

Perkins, D. N., Pappin, D. J., Creasy, D. M. and Cottrell, J. S. (1999). "Probability-based protein identification by searching sequence databases using mass spectrometry data." Electrophoresis **20**(18): 3551-3567.

Pinne, M., Thein, M., Denker, K., Benz, R., Coburn, J. and Bergström, S. (2007). "Elimination of channel-forming activity by insertional inactivation of the p66 gene in *Borrelia burgdorferi*." FEMS Microbiol Lett **266**(2): 241-249.

Probert, W. S., Allsup, K. M. and LeFebvre, R. B. (1995). "Identification and characterization of a surface-exposed, 66-kilodalton protein from *Borrelia burgdorferi*." Infect Immun **63**(5): 1933-1939.

Radolf, J. D., Bourell, K. W., Akins, D. R., Brusca, J. S. and Norgard, M. V. (1994). "Analysis of *Borrelia burgdorferi* membrane architecture by freeze-fracture electron microscopy." J Bacteriol **176**(1): 21-31.

Radolf, J. D., Goldberg, M. S., Bourell, K., Baker, S. I., Jones, J. D. and Norgard, M. V. (1995). "Characterization of outer membranes isolated from *Borrelia burgdorferi*, the Lyme disease spirochete." <u>Infect Immun</u> **63**(6): 2154-2163.

Raoult, D. and Roux, V. (1999). "The body louse as a vector of reemerging human diseases." <u>Clin Infect Dis</u> **29**(4): 888-911.

Rempp, P. (1957). "Contribution a l'étude des solution de molecules en chain a squelette oxigène." <u>J. Chem. Phys.</u> **54**: 432-453.

Reumann, S., Maier, E., Heldt, H. W. and Benz, R. (1998). "Permeability properties of the porin of spinach leaf peroxisomes." <u>Eur J Biochem</u> **251**(1-2): 359-366.

Richter, D., Schlee, D. B., Allgower, R. and Matuschka, F. R. (2004). "Relationships of a novel Lyme disease spirochete, *Borrelia spielmani* sp. nov., with its hosts in Central Europe." <u>Appl Environ Microbiol</u> **70**(11): 6414-6419.

Rosa, P. A., Tilly, K. and Stewart, P. E. (2005). "The burgeoning molecular genetics of the Lyme disease spirochaete." <u>Nat Rev Microbiol</u> **3**(2): 129-143.

Rostovtseva, T. K., Nestorovich, E. M. and Bezrukov, S. M. (2002). "Partitioning of differently sized poly(ethylene glycol)s into OmpF porin." <u>Biophys J</u> **82**(1 Pt 1): 160-169.

Sabirov, R. Z., Krasilnikov, O. V., Ternovsky, V. I. and Merzliak, P. G. (1993). "Relation between ionic channel conductance and conductivity of media containing different nonelectrolytes. A novel method of pore size determination." <u>Gen Physiol Biophys</u> **12**(2): 95-111.

Sabirov, R. Z., Krasilnikov, O. V., Ternovsky, V. I., Merzliak, P. G. and Muratkhodjaev, J. N. (1991). "Influence of some nonelectrolytes on conductivity of bulk solution and conductance of ion channels. Determination of pore radius from electric measurements." <u>Biol. Membr</u> **8**: 280-291.

Sadziene, A., Rosa, P. A., Thompson, P. A., Hogan, D. M. and Barbour, A. G. (1992). "Antibody-resistant mutants of *Borrelia burgdorferi*: in vitro selection and characterization." <u>J Exp Med</u> **176**(3): 799-809.

Saier, M. H., Jr. (2000). "Families of proteins forming transmembrane channels." <u>J Membr Biol</u> **175**(3): 165-180.

Saint Girons, I. and Barbour, A. G. (1991). "Antigenic variation in *Borrelia*." <u>Res Microbiol</u> **142**(6): 711-717.

Sallmann, F. R., Baveye-Descamps, S., Pattus, F., Salmon, V., Branza, N., Spik, G. and Legrand, D. (1999). "Porins OmpC and PhoE of *Escherichia coli* as specific cell-surface targets of human lactoferrin. Binding characteristics and biological effects." <u>J Biol Chem</u> **274**(23): 16107-16114.

Schägger, H. (2006). "Tricine-SDS-PAGE." <u>Nat Protoc</u> **1**(1): 16-22.

Schindler, J., Lewandrowski, U., Sickmann, A. and Friauf, E. (2008). "Aqueous polymer two-phase systems for the proteomic analysis of plasma membranes from minute brain samples." <u>J Proteome Res</u> **7**(1): 432-442.

Schirmer, T. (1998). "General and specific porins from bacterial outer membranes." J Struct Biol **121**(2): 101-109.

Schwan, T. G. (1996). "Ticks and *Borrelia*: model systems for investigating pathogen-arthropod interactions." Infect Agents Dis **5**(3): 167-181.

Schwan, T. G., Burgdorfer, W. and Garon, C. F. (1988). "Changes in infectivity and plasmid profile of the Lyme disease spirochete, *Borrelia burgdorferi*, as a result of in vitro cultivation." Infect Immun **56**(8): 1831-1836.

Schwan, T. G. and Hinnebusch, B. J. (1998). "Bloodstream- versus tick-associated variants of a relapsing fever bacterium." Science **280**(5371): 1938-1940.

Schwan, T. G., Raffel, S. J., Schrumpf, M. E., Policastro, P. F., Rawlings, J. A., Lane, R. S., Breitschwerdt, E. B. and Porcella, S. F. (2005). "Phylogenetic analysis of the spirochetes *Borrelia parkeri* and *Borrelia turicatae* and the potential for tick-borne relapsing fever in Florida." J Clin Microbiol **43**(8): 3851-3859.

Schwan, T. G., Raffel, S. J., Schrumpf, M. E. and Porcella, S. F. (2007). "Diversity and distribution of *Borrelia hermsii*." Emerg Infect Dis **13**(3): 436-442.

Sen, K., Hellman, J. and Nikaido, H. (1988). "Porin channels in intact cells of *Escherichia coli* are not affected by Donnan potentials across the outer membrane." J Biol Chem **263**(3): 1182-1187.

Shang, E. S., Skare, J. T., Exner, M. M., Blanco, D. R., Kagan, B. L., Miller, J. N. and Lovett, M. A. (1998). "Isolation and characterization of the outer membrane of *Borrelia hermsii*." Infect Immun **66**(3): 1082-1091.

Sizonenko, V. L. (1995). "[The role of image charge in ionic-electrostatic interactions of proteins and membranes]." Biofizika **40**(6): 1251-1255.

Skare, J. T., Champion, C. I., Mirzabekov, T. A., Shang, E. S., Blanco, D. R., Erdjument-Bromage, H., Tempst, P., Kagan, B. L., Miller, J. N. and Lovett, M. A. (1996). "Porin activity of the native and recombinant outer membrane protein Oms28 of *Borrelia burgdorferi*." J Bacteriol **178**(16): 4909-4918.

Skare, J. T., Mirzabekov, T. A., Shang, E. S., Blanco, D. R., Erdjument-Bromage, H., Bunikis, J., Bergström, S., Tempst, P., Kagan, B. L., Miller, J. N. and Lovett, M. A. (1997). "The Oms66 (p66) protein is a *Borrelia burgdorferi* porin." Infect Immun **65**(9): 3654-3661.

Skare, J. T., Shang, E. S., Foley, D. M., Blanco, D. R., Champion, C. I., Mirzabekov, T., Sokolov, Y., Kagan, B. L., Miller, J. N. and Lovett, M. A. (1995). "Virulent strain associated outer membrane proteins of *Borrelia burgdorferi*." J Clin Invest **96**(5): 2380-2392.

Sonenshine, D. E. (1997). Biology of Ticks V1, Oxford University Press.

Southern, P. and Sanford, J. (1969). "Relapsing fever: A clinical and microbiological review." Medicine **48**: 129-149.

Steere, A. C., Coburn, J. and Glickstein, L. (2004). "The emergence of Lyme disease." J Clin Invest **113**(8): 1093-1101.

Steere, A. C., Grodzicki, R. L., Kornblatt, A. N., Craft, J. E., Barbour, A. G., Burgdorfer, W., Schmid, G. P., Johnson, E. and Malawista, S. E. (1983). "The spirochetal etiology of Lyme disease." <u>N Engl J Med</u> **308**(13): 733-740.

Stoenner, H. G., Dodd, T. and Larsen, C. (1982). "Antigenic variation of *Borrelia hermsii*." <u>J Exp Med</u> **156**(5): 1297-1311.

Struyve, M., Moons, M. and Tommassen, J. (1991). "Carboxy-terminal phenylalanine is essential for the correct assembly of a bacterial outer membrane protein." <u>J Mol Biol</u> **218**(1): 141-148.

Tabuchi, N., Tomoda, K., Kawaguchi, H., Iwamoto, H. and Fukunaga, M. (2006). "Immunodominant epitope in the C-terminus of a variable major protein in *Borrelia duttonii*, an agent of tick-borne relapsing fever." <u>Microbiol Immunol</u> **50**(4): 293-305.

Takayama, K., Rothenberg, R. J. and Barbour, A. G. (1987). "Absence of lipopolysaccharide in the Lyme disease spirochete, *Borrelia burgdorferi*." <u>Infect Immun</u> **55**(9): 2311-2313.

Ternovsky, V. I., Okada, Y. and Sabirov, R. Z. (2004). "Sizing the pore of the volume-sensitive anion channel by differential polymer partitioning." <u>FEBS Lett</u> **576**(3): 433-436.

Thein, M., Bàrcena-Uribarri, I., Sacher, A., Bunikis, I., Bergström, S. and Benz, R. (2008a). "The P66 porin is present in both Lyme disease and relapsing fever spirochetes: a comparison of the biophysical properties in six species." <u>Manuscript</u>.

Thein, M., Bunikis, I., Denker, K., Larsson, C., Cutler, S., Drancourt, M., Schwan, T. G., Mentele, R., Lottspeich, F., Bergström, S. and Benz, R. (2008b). "Oms38 is the first identified pore-forming protein in the outer membrane of relapsing fever spirochetes." <u>J Bacteriol</u> **190**(21):7035-42.

Thein, M., Bunikis, I., Denker, K., Sickmann, A., Bergström, S. and Benz, R. (2008c). "DipA, a pore-forming protein in the outer membrane of Lyme disease *Borrelia* exhibits specificity for dicarboxylates." <u>Manuscript</u>.

Thomas, V., Anguita, J., Samanta, S., Rosa, P. A., Stewart, P., Barthold, S. W. and Fikrig, E. (2001). "Dissociation of infectivity and pathogenicity in *Borrelia burgdorferi*." <u>Infect Immun</u> **69**(5): 3507-3509.

Tokarz, R., Anderton, J. M., Katona, L. I. and Benach, J. L. (2004). "Combined effects of blood and temperature shift on *Borrelia burgdorferi* gene expression as determined by whole genome DNA array." <u>Infect Immun</u> **72**(9): 5419-5432.

Towbin, H., Staehelin, T. and Gordon, J. (1979). "Electrophoretic transfer of proteins from polyacrylamide gels to nitrocellulose sheets: procedure and some applications." <u>Proc Natl Acad Sci U S A</u> **76**(9): 4350-4354.

van Holten, J., Tiems, J. and Jongen, V. H. (1997). "Neonatal *Borrelia duttoni* infection: a report of three cases." <u>Trop Doct</u> **27**(2): 115-116.

Vial, L., Diatta, G., Tall, A., Ba el, H., Bouganali, H., Durand, P., Sokhna, C., Rogier, C., Renaud, F. and Trape, J. F. (2006). "Incidence of tick-borne relapsing fever in west Africa: longitudinal study." <u>Lancet</u> **368**(9529): 37-43.

Vodyanoy, I. and Bezrukov, S. M. (1992). "Sizing of an ion pore by access resistance measurements." Biophys J **62**(1): 10-11.

Walker, E. M., Borenstein, L. A., Blanco, D. R., Miller, J. N. and Lovett, M. A. (1991). "Analysis of outer membrane ultrastructure of pathogenic *Treponema* and *Borrelia* species by freeze-fracture electron microscopy." J Bacteriol **173**(17): 5585-5588.

Wallich, R., Kramer, M. D. and Simon, M. M. (1996). "The recombinant outer surface protein A (lipOspA) of *Borrelia burgdorferi*: a Lyme disease vaccine." Infection **24**(5): 396-397.

Wang, G., van Dam, A. P., Schwartz, I. and Dankert, J. (1999). "Molecular typing of *Borrelia burgdorferi* sensu lato: taxonomic, epidemiological, and clinical implications." Clin Microbiol Rev **12**(4): 633-653.

Wessel, D. and Flügge, U. I. (1984). "A method for the quantitative recovery of protein in dilute solution in the presence of detergents and lipids." Anal Biochem **138**(1): 141-143.

Wheeler, C. M., Garcia Monco, J. C., Benach, J. L., Golightly, M. G., Habicht, G. S. and Steere, A. C. (1993). "Nonprotein antigens of *Borrelia burgdorferi*." J Infect Dis **167**(3): 665-674.

Wilske, B. (2003). "Diagnosis of lyme borreliosis in europe." Vector Borne Zoonotic Dis **3**(4): 215-227.

Wimley, W. C. (2003). "The versatile beta-barrel membrane protein." Curr Opin Struct Biol **13**(4): 404-411.

Wittig, I., Braun, H. P. and Schägger, H. (2006). "Blue native PAGE." Nat Protoc **1**(1): 418-428.

Woese, C. R. (1987). "Bacterial evolution." Microbiol Rev **51**(2): 221-271.

Wohnsland, F. and Benz, R. (1997). "1/f-Noise of open bacterial porin channels." J Membr Biol **158**(1): 77-85.

Yu, S., Ding, H., Seah, J., Wu, K., Chang, Y., Chang, K. S., Tam, M. F. and Syu, W. (1998). "Characterization of a phage specific to hemorrhagic *Escherichia coli* O157:H7 and disclosure of variations in host outer membrane protein ompC." J Biomed Sci **5**(5): 370-382.

Zhang, J. R., Hardham, J. M., Barbour, A. G. and Norris, S. J. (1997). "Antigenic variation in Lyme disease borreliae by promiscuous recombination of VMP-like sequence cassettes." Cell **89**(2): 275-285.

Zhang, J. R. and Norris, S. J. (1998). "Genetic variation of the *Borrelia burgdorferi* gene vlsE involves cassette-specific, segmental gene conversion." Infect Immun **66**(8): 3698-3704.

7.2. Curriculum vitae

PERSONAL DATA

Dipl. Biol. **Marcus Thein**
born 6th November 1979 in Würzburg
german, unmarried, no children

SCHOOLING

Sept. 1986 – June 1990	Elementary school Lengfeld, Würzburg
Sept. 1990 – June 1999	Secondary school, Riemenschneider-Gymnasium, Würzburg
June 1999	General qualification for university entrance (Abitur)

CIVILIAN SERVICE

Aug. 1999 – May 2000	Alternative civilian service at the Missionsärztliche Klinik, Würzburg

ACADEMICAL CAREER

Oct. 2000 – Oct. 2004 — Study of biology at the Bavarian Julius-Maximilians-University, Würzburg

Major subject: Biotechnology

Minor subjects: molecular plant-physiology and biophysics, microbiology

Sept. 2003 – Feb. 2004 — Erasmus exchange student at the Institute de Pharmacologie et de Biologie Structurale, Toulouse, Frankreich

Nov. 2004 – July 2005 — Diploma thesis: "Study of the outer membrane fraction of *Borrelia duttonii* for porins"

Since Oct. 2005 — PhD student at the Department of Biotechnology of the Bavarian Julius-Maximilians-University, Würzburg

Supervisors: Prof. Dr. Dr. h.c. Roland Benz
Prof. Dr. Sven Bergström (Umeå, Sweden)

Thesis: "Porins of Lyme disease and relapsing fever spirochetes"

May-June 2006, May 2007 and May 2008 — Research stays in the group of Prof. Dr. Sven Bergström at the University Umeå, Sweden

Acknowledgement

The following lines are dedicated to all those people who supported me during the last three years.

I'd like to thank…

… **Prof. Dr. Dr. h. c. Roland Benz** for the possibility to do my doctoral thesis in his group, for combining an experienced, professional, problem-solving and likewise comfortable character during his supervising, for the possibility to visit the Swedish collaboration partners in Umeå several times and for the innumerable dinner invitations.

… **Prof. Dr. Sven Bergström** for being my second supervisor, for his open, encouraging and endless optimistic nature, for the comfortable atmosphere during my research stays in Umeå and for introducing me into the personable and warm Swedish lifestyle, tack så mycket!

… **Iván Bárcena-Uribarri**, the Spanish double master student, bon vivant and *Borrelia* torero, for being such a huge support and pusher in our common projects, for all the Snickers breaks and for being much more a friend than a colleague, ¡muchas gracias!

… my diploma and master students, **Florian Rohleder**, for keeping his humour and positive temper during a despairing project and for being a concert partner and friend beyond all the business and **Anna Sacher** (former: Herreiner) for being an encouraged support during my first PhD months, her Bergkäse supply and her soccer fever and **Maite Salo-Costa** for being a highly motivated student and introducing us into the Catalan snail taste.

… the Swedish collaboration partners **Ignas Bunikis** and **Mari Bonde**, for many exciting experiences during the exchange weeks in Umeå including the surströmming stinky fish test and European song contest party, and **Dr. Christer Larsson** ("der Wurst") for all the help during my first relapsing fever *Borrelia* steps and for enabling the Fjäderegg island weekend.

… the research assistants and practical students in my projects, the "Zausel" **Martin Mau** for support in the P66 story, the Bremen girl **Sabrina Kutschan** for the German contact in Umeå, the motivated and loud-speaking Gijón-girl **María Ochoa-González**, our spanish lab radio **Nathalia Sierra**, the English lady **Catherine Sharpless**, the Egyptian **Dr. Samah Ghanem** for even more international flair and **Meng Zhou** for the Eastern touch in our group.

Big thank you also to…

… all my former colleagues for a wonderful time and a comfortable life in the lab and beyond, such as the Hessian head **Tobias Knaf** for being a close long-time colleague in the basement lab and a number of private highlights (e.g. Barcelona trip, …).

… the FCB-infected, empathetic **Christian Kläckta** for sharing and solving so many common problems during our PhD time and having had some pleasant talks and beers sessions.

…**Dr. Katrin Lokaj** (former: Denker) for introducing me into the *Borrelia* porin field and some further advice, **Dr. Ursula Dörner** for being the heart of the AG Benz basement group for such a long time, **Elke Maier**, the quiet person who supported everyone so much by her experienced competence, **Dr. Christian Andersen** for the many fruitful discussions and advice, **Harry Falk** for demonstrating me how to solve EDV problems by pushing just one button - "määgg" - and **Enrico Barth** for sharing similar problems during the final spurt of the thesis.

… **Christoph Beitzinger** (Chrii, the dry ice artist and hui machine pilot), **Christian Löw**, **Angelika Kronhardt**, **Jennifer Rausch**, **Dr. Lidia Ruiz**, **Bettina Schiffler**, **Verena Krüger, Moritz Ewald, Martin Wirsching** and **Marco Lolicato** for so much fun in the group!!!

…the long-time colleagues **Dr. Michael Leuber** and **Dr. Tobias Neumayer**.

…**Dr. Peter Reichling**, **Nicolas Frank**, **Dr. Johannes Stegmaier** and **Dr. Georg Polleichtner** not only for their stimulatory humour...

… all the other colleagues in the department of Biotechnology for feeling so comfortable during all the years.

And very special thanks to…

… **all my friends** who are not individually listed and heard too many times "Sorry, I don't have time, my thesis…" and the **Handballteams** from Lengfeld and Bergtheim for a necessary balance to my lab work and so many unforgettable and formative parties, adventures and experiences.

… my family, consisting of my **Mom Sigrid**, my **Dad Manfred**, my **brother Dominik** and his wife **Kim** for supporting me whenever possible, respecting my decisions and being the important deep family backbone.

… **Katja**, for infinite mental support and affirmation, for all the (many) wonderful shared years (which should not be seen as a matter of course) and for bringing a deeper sense into my life looking into both past and future.